PART 1 – LITERATURE REVIEW

1.1 Introduction

The annual municipal solid waste (MSW) generation in the U.S. has been on the order of 230 million metric tonnes (Mt) since 2005, with 243 Mt of generation in 2017 (USEPA 2017a). Landfilling constitutes the main means of waste disposal in the U.S. with 127 Mt (52.2% of 243 Mt generated) disposed of in landfills in 2017. Significantly higher rates (on the order of 262 Mt) for landfill disposal also were reported (van Haaren et al. 2010, Powell et al. 2016). For California, the annual MSW disposal amount has been on the order of 35 Mt since 2009, with 37.8 Mt reported for 2017 (CalRecycle 2017). The number of active landfills was reported to be 1,738 in the U.S. (USEPA 2017b) and 133 in California (CalRecycle 2019a).

Landfilling of municipal solid waste (MSW) results in three main byproducts: landfill gas (LFG), leachate, and heat. Landfill gas is a biogas consisting of approximately 45-60% (v/v) methane (CH_4) and 45-60% (v/v) carbon dioxide (CO_2) generated due to anaerobic microbial processes that occur in the landfill (Tchobanoglous et al. 1993). LFG also includes minor amounts of oxygen (0.1 to 1%), hydrogen (0 to 0.2%), and nitrogen (2 to 5%) from the atmosphere, carbon monoxide (0 to 0.2%), sulfides (0 to 1%), and ammonia (0.1 to 1%) as well as a large number of trace components (0.01 to 0.6%), which have been directly volatilized from the waste or generated by biotic or abiotic processes within the landfill (Christensen et al. 1996). More than 200 trace species including alkanes, aromatics, alcohols, aldehydes, reduced S gases, and chlorinated and fluorinated hydrocarbons, with measured concentrations (in gas collection headers) in the range of below detection limit to 57.7 μg/L were reported (Scheutz et al. 2008). Due to the presence of engineered cover and gas extraction systems, concentrations of these trace gas components are much lower in the ambient air as compared to gas collection or passive vent systems. For example, Zou et al. (2003) reported concentrations of 100 NMVOCs in the ambient air at a landfill site, where concentrations across all chemical families ranged from 0.0001 to 1.67 μg/L and are generally higher at the active face of municipal solid waste (MSW) landfills (Saral et al. 2009, Duan et al. 2014). Elevated concentrations of aromatic hydrocarbon hazardous trace gas components have been detected in the vicinity of MSW landfills (Kim et al. 2008).

This literature review provides a summary of landfill gas related processes in landfill environments. Particular emphasis is placed on LFG surface emissions of greenhouse gases and a broad class of organic chemicals. Sections 1.2, 1.3, and 1.4 provide a broad overview of LFG generation, storage within the waste mass, transport mechanisms, collection systems, and emissions. Section 1.5 provides an overview of the specific chemical species and corresponding chemical families included in the current study. Section 1.6 describes the composition of LFG and summarizes the findings from previous studies related to methane, nitrous oxide, and other NMVOC concentrations in landfill gas. Section 1.7 provides concise summaries for results from prior field studies on methane, nitrous oxide, and NMVOC emissions from MSW landfills. Finally, Section 1.8 discusses potential chemical and biological transformation

pathways that may be present both in the waste mass and in the cover systems for the specific chemicals included in this investigation.

1.2 Landfill Gas Generation

The generation of LFG in MSW landfills is affected by various factors, including the quantity, composition and age of the waste materials; pH, moisture content, and temperature of the waste mass; and the ingress of oxygen from the atmosphere as well as site specific landfill design and operational practices (Tchobanoglous et al. 1993, Palmisano and Barlaz 1996, Barlaz et al. 2010). In general, MSW in the U.S. is composed of paper and paperboard (~26%), glass (~4%), metals (~9%), plastics (~13.1%), yard trimmings (~13%), food (~15%), wood (~6%), rubber and leather (~3%), textiles (~6%), and other miscellaneous organic and inorganic wastes (i.e., wastewater sludge, household hazardous wastes, electronic wastes, auto shredder residues, soil, etc.) (USEPA 2017a). These estimates of waste composition are slightly different for California, where the overall waste stream has a high organics composition (37% - mainly food and green waste), followed by inerts and other materials (20% - mainly construction and demolition wastes) and recyclable materials (33% - paper, metals, plastics, glass) (CalRecycle 2017).

The higher quantity and fraction of organic materials in the waste stream reaching MSW landfills, particularly readily biodegradable fractions such as food and green wastes, contribute to greater anaerobic bacterial decomposition and generation of LFG in comparison to national averages. The principal, readily biodegradable components in these wastes are composed of soluble sugars and starches (polysaccharides), cellulose and hemicellulose, whereas the more recalcitrant components include proteins, nucleic acids, lipids, and lignocellulose (lignin present in wood waste does not decompose) (El-Fadel et al. 1997, Barlaz et al. 2010). In addition, the presence of household hazardous wastes such as paints, batteries, or cleaning products leads to volatilization of certain organic chemicals (volatile organic compounds) into LFG (Brosseau and Heitz 1994, Nair et al. 2019). Furthermore, unique chemical or biochemical transformative reactions occurring between different chemicals within the waste mass leads to the generation of various trace gas components (Scheutz and Kjeldsen 2005). In addition to waste composition, age of the waste mass, is a critical factor affecting generation, in which waste that is more recently landfilled (less than 10 years) leads to greater generation of LFG. Peak LFG generation generally ranges from within 5 to 7 years of waste disposal in MSW landfills (Tchobanoglous et al. 1993, Palmisano and Barlaz 1996, Barlaz et al. 2010). Waste age also influences trace gases as reported for F-gases by Yesiller et al. (2018), where the distribution of the F-gases within a landfill varied by historical replacement trends. Newer F-gas species were concentrated in new cells with relatively younger wastes in the landfill with older species uniformly distributed across the entire site.

Landfill gas generation is primarily a biologically mediated process, in which the multifaceted consortium of microorganisms (bacteria) in the waste mass decompose the organic materials in the presence of an electron acceptor (i.e., oxygen, nitrate, etc.), forming new biomass, heat, extracellular byproducts (i.e., polymeric substances), and

biogas (methane and carbon dioxide) (Tchobanoglous et al. 1993, Palmisano and Barlaz 1996). Depending on the presence of oxygen, waste biodegradation can either be classified as an aerobic (with oxygen) or an anaerobic (without oxygen) process. The biological decomposition of MSW has been classified into five successive stages (Tchobanoglous et al. 1993, Palmisano and Barlaz 1996), including an initial adjustment phase (Stage I), a transition phase (Stage II), an anaerobic acid phase (Stage III), an accelerated methane production phase (Stage IV), and a decelerated methane production phase (Stage V) as presented in Figure 1.1. Anaerobic waste decomposition in MSW landfills relies on the symbiotic relationship formed among three primary bacterial groups, all with a specific function, including the hydrolytic/fermentative bacteria, the acetogens, and the methanogens (Barlaz et al. 2010).

Figure 1.1 Stages of Landfill Gas Generation in MSW Landfills (Hofstetter 2014)

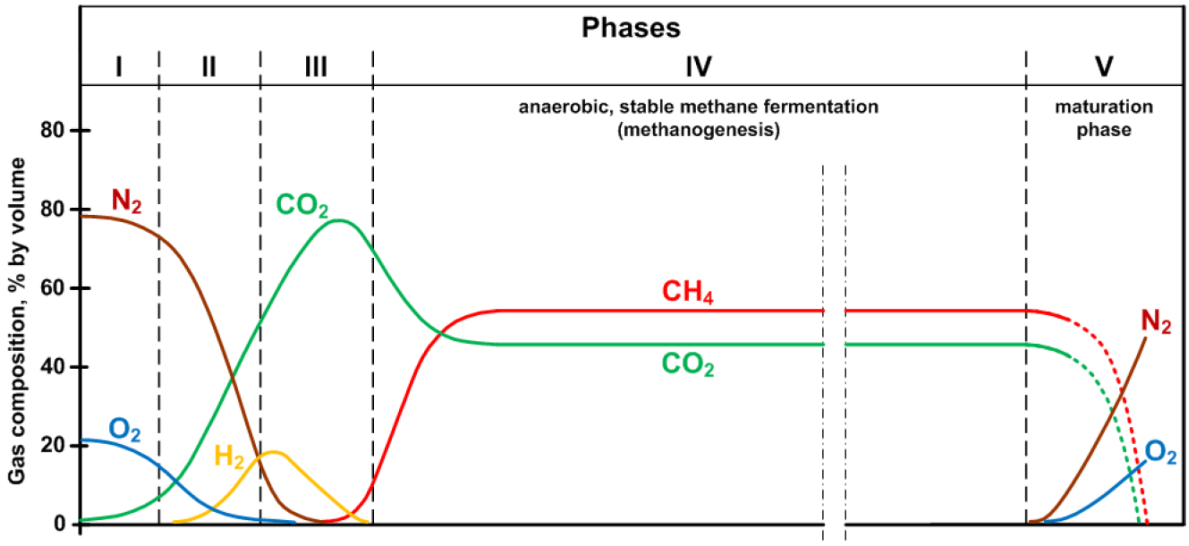

During Stage I of landfill gas generation, oxygen present in voids of the waste mass and in moisture within the waste mass fuels the aerobic decomposition of the organic fraction of MSW. In this phase (lasting on the order of days), both oxygen and nitrate are consumed by aerobic bacteria, along with soluble sugars to form carbon dioxide (100% v/v) (Figure 1.1). The transition phase (Stage II) refers to the time period when oxygen becomes depleted and anaerobic conditions begin to develop. Throughout the early periods of anaerobic decomposition in MSW landfills, complex particulate matter is broken down to proteins, carbohydrates, and lipids, which are then further hydrolyzed to biomonomers such as amino acids, sugars, and high molecular weight fatty acids (El-Fadel et al. 1997). After oxygen is nearly depleted within the waste mass, Stage III (the acidic phase, time frame of months to years) of decomposition begins, where carboxylic acids begin to accumulate as a byproduct of anaerobic soluble sugar fermentation (i.e., organic alcohol production). As more and more acids accumulate, the pH of the waste mass drops considerably (inhibiting methanogenesis, or the production of methane) and due to the fermentative activity, large volumes of carbon dioxide and hydrogen are produced (Palmisano and Barlaz 1996, Barlaz et al. 2010) (Figure 1.1). The fourth stage of decomposition and LFG production denotes the onset of the methane generation

phase, where accumulation of carboxylic acids ceases as they are consumed faster by the acetogens than they are produced by the fermentative and hydrolytic bacteria. At this stage, the pH of the waste mass begins to stabilize (between 6.8 and 8) and acetate, carbon dioxide, and hydrogen produced by the acetogens is consumed anaerobically by the methanogens, thereby producing methane (~60% v/v) and carbon dioxide (~40% v/v) as the primary byproducts. The time period required to reach this stage varies significantly by climate, where peak generation may be reached after only 2 years in a temperate climate, whereas decades may be required in low temperature or arid conditions (Tchobanoglous et al. 1993). Finally, after the onset of methanogenesis, the production of LFG begins to decline as both the available nutrients in the waste mass decline and the substrates that remain in the waste mass are more difficult to biodegrade (Stage V). This phase continues to produce LFG for upwards of 50 years, and LFG will start to include more atmospheric components (i.e., oxygen and nitrogen) as the LFG becomes diluted.

Generation of landfill gas by the microbial populations is highly moisture, pH, and temperature sensitive; therefore, the climate zone in which the landfill resides plays a significant role in LFG generation. The moisture content of fresh waste ranges from 15 to 45% and is generally 20% on a wet weight basis, which is considered low in comparison to optimum conditions for anaerobic microbial decomposition (Farquhar and Rovers 1973, Barlaz et al. 1990). Multiple studies have indicated that moisture content is one of the foremost limiting factors of methane generation, where methane production exhibited an upward trend with increasing moisture content, up to an optimum of 50-60% (w/w, wet basis) (Farquhar and Rovers 1973, Barlaz et al. 1990). Thus, climate zones with high net annual precipitation, and higher probability of infiltration, are favorable for LFG generation. pH is another important factor regulating methanogenesis and LFG generation, where methanogenic bacteria exhibit a narrow range in pH tolerance (6.8 to 7.4) (Tchobanoglous et al. 1993). Even though MSW is typically alkaline in nature (7-8), the fermentative bacteria are largely responsible for lowering the pH and inhibiting LFG generation in the landfill environment. Temperature effects on MSW decomposition is summarized in Yesiller et al. (2015). Biologically mediated decomposition of MSW occurs through two distinct pathways: short-term effects on reaction rates and long-term effects on microbial population balance (Hartz et al. 1982). In general, waste decomposition increases with increasing temperatures up to limiting values. In laboratory studies, optimum temperature ranges for the growth of mesophilic and thermophilic bacteria responsible for waste decomposition were identified to be 35 to 40°C and 50 to 60°C, respectively (Cecchi et al. 1993, Tchobanoglous et al. 1993). Maximum gas production from waste decomposition was identified to occur at temperature ranges between 34 and 41°C based on laboratory analysis representing the landfill environment with a mixture of these two types of microorganisms (Merz and Stone 1964 and Ramaswamy 1970 as reported in DeWalle 1978, Hartz et al. 1982, Mata-Alvarez and Martinez-Viturtia 1986). A temperature range of 40 to 45°C was identified as the optimum range for gas production at a landfill in England (Rees 1980a, b) with highly inhibited and delayed gas generation observed at low waste temperatures (Hanson et al. 2006). Biomass transfer was reported to occur with landfill gas, where the cell counts in the gas were correlated to temperature (Barry 2008). Spatially unique

microbial communities, as influenced by waste temperature among other factors, were reported in landfill environments (Sawamura et al. 2010). Other than climatic factors, the temperature of the waste mass is greatly influenced by heat generation during anaerobic decomposition and other chemical transformations occurring within the waste mass (Yesiller et al. 2005).

As MSW landfills in the U.S. are highly engineered systems, the site-specific landfill design and management of waste materials also influences the generation of landfill gas and subsequent emissions (Section 1.3) from MSW landfills (Tchobanoglous et al. 1993). Regarding landfill design, application of engineered final cover barrier systems affects LFG generation by significantly lowering water and atmospheric air intrusion through the use of the barrier layers with low hydraulic and gas conductivity. Given that the presence of moisture facilitates LFG production, inclusion of a cover system may offset LFG production. However, cover systems also limit oxygen availability in the waste mass, which facilitates biologically mediated anaerobic conversion processes, thereby producing more LFG. Final cover systems range from a thick (~ 1 m) layer of compacted clay overlain by native topsoil to more advanced, composite barrier systems, consisting of a combination of clayey soils, geosynthetic clay liners, or geomembranes ranging up to 1.5 m in thickness (Yesiller and Shackelford 2011). Cover systems typically are equipped with a drainage layer to collect and remove water that collects on the surface of the covers (Yesiller and Shackelford 2011).

Site-specific operational practices, such as the placement and composition of daily and intermediate covers, further affect landfill gas generation and subsequent emissions (Section 1.3) (Tchobanoglous et al. 1993). Daily covers are temporary cover systems used to isolate recently placed waste from the surrounding environment to prevent spread of the waste materials and associated harmful vectors. In the U.S., daily covers are mandated to have a minimum thickness equivalent to the performance of 150 mm of soil, where the composition of materials used in these covers may vary significantly from site to site (USEPA 1993, USEPA 2012). For example, in California, daily covers may consist of soil, wood wastes, green wastes, construction and demolition (C&D) wastes, autofluff, or wastewater biosolids (CalRecycle 2018). The non-soil daily cover materials including natural and synthetic materials are collectively termed alternative daily covers (ADCs). Intermediate covers (also termed interim covers) represent a more permanent barrier system in that they are placed over completed lifts for an extended period of time (ranging from months to a few years). Intermediate cover systems are required to have a minimum thickness equivalent to the performance of 300 mm of soil (USEPA 1993, USEPA 2014). Even though materials similar to ADCs can be used in interim covers, the use of materials other than soils in interim cover systems is generally limited in California (CalRecycle 2018). Similar to final cover systems, the presence of both daily and interim covers limits, to some extent, the ingression of moisture and air into the waste mass, thereby affecting LFG generation. Other operational practices related to placement efficiency of waste materials, such as the degree of compaction and compression of wastes over time, as well as specific waste placement locations and sequence affect LFG production. Higher compaction efforts and compression of the waste mass over time serve to limit atmospheric air intrusion and pore space available

for moisture transport within the waste mass as well as LFG production and transport within the waste mass (Tchobanoglous et al. 1993). Yesiller et al. (2005) reported that waste temperatures increase with increasing waste placement rates and thus lead to rapidly reaching optimum decomposition conditions for landfill gas generation. Winter only placement areas set aside at California landfills contain waste masses at moisture contents above average values and affect LFG generation, potentially increasing gas generation rates due to increased moisture levels.

1.3 LFG Storage, Transport, and Collection

Temporary landfill gas storage within the landfill system has been identified as a significant phenomenon to consider when investigating the complete LFG lifecycle (Bogner and Spokas 1993, Scheutz et al. 2009a). Landfill gas pressures have been observed to vary due to temporal changes in the cover system permeability as a function of precipitation and moisture content. For example, during periods of high precipitation, LFG can be stored temporarily inside the upper portion of waste mass/bottom portion of the soil cover and then subsequently released during follow up dry weather periods. Changes in barometric pressures also can trigger this phenomenon, albeit on much smaller time scales (hours versus days) (Bogner and Spokas, 1993, Scheutz et al. 2009a).

Landfill gas generation throughout the waste mass tends to be heterogenous, producing localized differences in LFG pressure. Therefore, the bulk transport of LFG throughout the waste mass is highly pressure driven (advective) over concentration driven (diffusive), always moving in the direction of least resistance (i.e., areas of higher permeability), across gradients from high to low pressure or concentration (Scheutz et al. 2009a). In addition to advective and diffusive transport, some trace components are highly adsorptive or are likely to partition within different phases of the waste materials. Adsorption entails physico-chemical bonding of a given chemical to a solid present in the waste mass, whereas phase partitioning involves apportionment of a given chemical into another phase (i.e., gas phase dissolving in water, polar versus non-polar) (McCarthy and Zachara 1989). Moreover, many trace components are affected by different chemical and biological reactions while they are transported throughout the waste mass, which either increase or decrease their respective concentrations (Molins et al. 2008). Depending on these differences in local pressures, along with differences in ambient barometric pressure and the physical-chemical nature of the bulk LFG (i.e., molecular weight, densities of different chemicals), LFG is able to migrate in many different directions, including upward, downward, and laterally (Scheutz et al. 2009a). Lateral migration of LFG has been widely reported and is generally enhanced when soil covers are saturated, which drives advective flux of LFG laterally (Christophersen et al. 2001, Christophersen and Kjeldsen 2001).

The installation of passive or active gas extraction wells and a passive or an active gas extraction system are primary measures that help control and stabilize the undesirable migration of LFG. In addition, the presence of a landfill bottom liner and final cover systems both limits the extent of migration of LFG and offsets potential environmental impacts, to some extent. Landfill gas recovery studies with data from Swedish landfills

reported gas collection efficiencies for MSW landfills on the order of 50 to 60% (Borjesson et al. 2007, 2009), where the remaining fraction of LFG escapes into the atmosphere. Studies conducted in the U.S. and France indicated that gas extraction efficiencies can be as high as 97% if state-of-the-art liners, covers, and extraction systems are in place (Spokas et al. 2006). Results reported from a methane mass balance for nine landfill cells at three landfill sites determined that LFG collection efficiencies from the field ranged from 92% to 97% for cover systems incorporating clay covers (Spokas et al. 2006). Recovery results were lower for several cells with geosynthetic covers in place of clay soil covers, ranging from 40.9 to 84% (Spokas et al. 2006). Use of a temporally weighted gas collection efficiency was proposed as an appropriate means for assessing landfill gas recovery over the entire lifetime of a given landfill site (Barlaz et al. 2009). The USEPA has recommended a default value of 75% LFG collection efficiency for performing LandGEM simulations (US EPA 2008).

1.4 Landfill Gas Emissions

Even with engineered protective measures in place, fugitive emissions of LFG through landfill covers remains a significant issue (Bogner et al. 1997a). Similar to the underlying principles governing LFG generation, LFG emissions from landfill covers depend on various interrelated factors. Three general classes of factors affecting LFG migration and subsequent emissions were identified to be meteorological conditions (barometric pressure, precipitation, temperature, wind), soil/cover conditions (cracks, permeability, diffusivity, porosity, moisture content, methane oxidation), and the landfill conditions (LFG production rate, internal barriers, gas vents, extraction system) (Scheutz et al. 2009a). As most single and composite final covers have intrinsically low gas permeability, the primary transport mechanism of bulk LFG from the landfill surface in the presence of final covers is primarily through molecular diffusion, with some contributions from advective transport reported for different cover systems, including highly porous, alternative cover materials (i.e., auto fluff), as well as from wind induced advection (Scheutz et al. 2009a). The pressure differential across the cover systems generated due to the negative pressures (i.e., vacuum) in the waste mass during active gas collection system operation in comparison to the positive outside atmospheric pressure also contributes to potential emissions by creating advective transfer conditions. Pressure gradients between the waste mass and landfill surface can be introduced by wind, variation in barometric pressure, or by pressure build up in the underlying wastes. An increase in barometric pressure often times resulted in reduced advective and/or diffusive transport through landfill covers and frequently ended in a flux reversal (net uptake over net emissions), as reported by several studies (Latham and Young 1993, Kjeldsen and Fisher 1995, Nastev et al. 2001, Christophersen and Kjeldsen 2001, Christophersen et al. 2001, Czepiel et al. 2003, Franzidis et al. 2008, Gebert and Groengroeft 2006). Kjeldsen (1996) and Thorstenson and Pollock (1989) reported that only very low pressure gradients, on the order of 1 Pa/m) are required for LFG transport from advective flux to dominate diffusive flux, where pressure gradients of this magnitude can actually be generated by diffusive processes.

In addition to the meteorological and landfill conditions, the cover conditions, including the degree of LFG (methane, trace gases) oxidation occurring within the cover is a

significant factor influencing LFG emissions. Scheutz et al. (2009a) described methane oxidation as "…a secondary biological treatment process to control methane emissions." Similar to microbial processes occurring within the waste mass, some bacteria (known as the methanotrophs) are responsible for oxidizing (under aerobic conditions only) certain components of LFG (i.e., methane) to produce new biomass, other extracellular byproducts, and biogas (100% carbon dioxide v/v). Most methanotrophic bacterial species are strict aerobes in that they depend on a steady supply of both oxygen and carbon dioxide within the soil cover, confining their distribution to around 15-20 cm below the surface (Scheutz et al. 2009a). Methanotrophs have also been associated with the oxidation of some NMVOC compounds, including F-gases, alkanes, aromatics, and some halogenated hydrocarbons (Kjeldsen et al. 1997, Scheutz and Kjeldsen 2004).

Both methane and NMVOC oxidation are affected by many environmental factors, including soil type, temperature, moisture content, methane/oxygen concentrations, pH, as well as the presence of certain limiting nutrients (i.e., inorganic nitrogen, phosphorus, trace heavy metals, etc.) (Börjesson and Svensson 1997a, Stern et al. 2007, Bogner et al. 1997a). Oxidation of methane, including the relative rates and conversion efficiency, is also affected by the presence of other NMVOC substrates, demonstrating that these methanotrophic communities may show some degree of substrate preference or inhibition through toxicity (Scheutz and Kjeldsen 2004). For example, methane oxidation was demonstrated to be inhibited in the presence of HCFCs, which was likely due to enzyme-substrate competition and accumulation of toxic intermediates during oxidation of the HCFCs (Scheutz and Kjeldsen 2004). Regarding temperature, most methanotrophs cultured in isolation are mesophiles, with optimal temperatures for oxidation in soil environments ranging from 25 to 35°C (oxidation at lower temperatures has been reported for type I methanotrophs at 10°C, albeit at a slower rate) (Hanson and Hanson 1996, Scheutz et al. 2009a).

Soil moisture content is another critical factor affecting oxidation rates, in which the optimal conditions promoting methane oxidation are much more complex than temperature. The soil moisture content must not be too high as to limit diffusion of oxygen or methane into or out of the soil cover, yet not too dry to avoid desiccation of the cells. Reported soil moisture contents that were optimal for methane oxidation ranged from 10 to 20% (w/w), where some studies have reported even higher values (Boeckx et al. 1996, Scheutz et al. 2009a). High air-filled capacity, which defines the share of pores available for gas transport after draining a soil, where the remaining water is bound solely by capillary force, was mentioned as a significant feature of a given cover soil to promote methane oxidation (Scheutz et al. 2009a). Scheutz et al. 2009a identified an air capacity threshold of 50 µm (i.e., 50 x 10^{-6} m) that is necessary for optimal methane oxidation to occur in any cover soil.

Oxygen limitation is another factor that controls methane oxidation. Field studies have reported that oxygen concentrations above 3% are capable of supporting methane oxidation, where lower oxygen mixing ratios have been reported for some methanotrophs in the laboratory setting (0.45%) (Czepiel et al. 2003, Gebert et al.

2003). Oxygen penetration into the soil cover is a factor of both site-specific meteorological conditions, as well as the soil type and geotechnical engineering properties (i.e., particle size distribution, porosity, degree of saturation).

Other important environmental factors affecting methane oxidation include the presence of inorganic nitrogen, production of extracellular polymeric substances, and soil pH (Scheutz et al. 2009a). Several studies have determined that inorganic nitrogen (ammonium/nitrate) may stimulate or inhibit methane oxidation depending on the species of N, the concentration of N, methane concentrations, pH, and the species of methanotrophic bacteria (Boeckx and van Cleemput 1996, Boeckx et al. 1998, Hütsch 1998, Scheutz and Kjeldsen 2004). A majority of studies reviewed have determined that ammonium-based fertilizers stimulate growth and activity of methane oxidizers in landfill cover soils, where the effects of nitrite and nitrate N sources are less understood (Hilger et al. 2000, De Visscher et al. 1999, 2001, De Visscher and van Cleemput 2003, and Bodelier and Laanbroek 2004). Following prolonged exposure to favorable methane oxidizing conditions, the accumulation of EPS as an extracellular byproduct for methanotrophic communities has been shown to decrease the efficiency of methane oxidation. These studies have postulated that EPS either clogs the soil pores, thereby decreasing the gas permeability of the soil or reduces the rate of gaseous diffusive flux of substrate into the bacterial cells (Hilger et al. 1999, Scheutz and Kjeldsen 2003). Optimal soil pH for methanotrophic growth of soils lies between 5.5 and 8.5, which is aligned with expected pH of sandy or loamy soils in the field (4.5-7) (Dunefield et al. 1993, Scheutz and Kjeldsen 2004). Methane and NMVOC oxidation may be significant, however oxidation does not fully attenuate LFG emissions as the conditions in the field typically are not optimal.

Irregularities such as cracks and fissures in landfill cover soils have been reported due to waste settlement or desiccation of the cover soils during dry periods. LFG emissions through these cracks and fissures, termed “hot spots,” can result in high spatial and temporal heterogeneity in LFG emissions. In a study from over two decades earlier more than 50% of the total measured emissions were attributed to less than 5% of the landfill surface with the disproportional emissions indicated to result from hotspots associated with cracks and other heterogeneities in the soil covers Czepiel et al. (1996). As landfill emissions are monitored by landfill owners/operators on a regular basis, such irregularities if present are detected and repaired and do not pose long-term problems. Landfill cover designs have evolved significantly in the last decades with design and analysis used to minimize differential settlement and ascertain structural integrity of the covers. Irregularities are not relevant for conventional final covers as the barrier layers (soil and/or geosynthetics) are placed below ground surface overlain by multiple layers without being exposed to the atmosphere. Geomembranes are not susceptible to cracking and typically have very high tensile strains at break and thus are not susceptible to differential settlement. In general, final covers are placed at areas with old wastes that have completed significant volume change. The PIs during this study or a previous study conducted for CARB, did not observe noticeable cracking on the surface of any of the cover systems installed at the multiple investigated landfills. In the previous study, the void ratio and porosity of the cover soils were determined to be

lower during the dry season indicating shrinkage of the covers. However, cracking was not visually observed and the emissions during the dry season were lower than the emissions in the wet season. The coupled mechanism for the observed behavior is described in detail in Yesiller et al. (2018). High-conductivity, low-fines content, low-cohesion daily and intermediate covers can in themselves constitute hot spots with associated high emissions. The active working face, since there is no cover in place, is also a source of high emissions.

Geotechnical engineering characteristics of cover materials are significant factors for landfill gas emissions. as the particle size of the cover material decreases and soil gradation varies from coarse to fine grained, three distinct phenomena occur: a) the number of pores and amount of pore spaces increase, where the soil pores become more occluded than interconnected; b) tortuosity of the flow paths increases; and c) more water is held (by strong electrochemical forces in addition to gravitational forces and surface tension) and residual state of saturation increases. All three phenomena increase resistance to gas transfer. Yesiller et al. (2018) observed a strong inverse correlation between F-gas emissions and fines content across different soil covers from a landfill site in California. Also, F-gas flux was observed to increase as the degree of saturation of the soil increased, which was attributed to reduced retardation, sorption, and oxidation in cover soils with increasing moisture contents (Yesiller et al. 2018).

Both Bogner et al. (2011) and Yesiller et al. (2018) reported that emissions of methane and F-gases (in Yesiller et al. 2018 only) decreased progressing from daily (thin) to intermediate to final (thick) cover systems, indicating that cover thickness is a significant feature affecting LFG emissions from landfill surfaces. In addition to providing an extra physical barrier to buffer methane or NMVOC emissions (depending of course on the soil properties), extended cover thicknesses also affect the extent and persistence of microbial oxidation of methane or NMVOCs occurring in the cover soils. Cover thickness affects the depth of oxygen penetration and moisture percolation, which highly influences the development, spatial extent, and temporal stability of oxidizing methanotrophic bacterial communities (Scheutz et al. 2009a).

In California and countries with similar climatic attributes, seasonal effects of methane and NMVOC emissions may be less pronounced as compared to the effects of other landfill characteristics such as cover type and site-specific operational practices. For example, mean seasonal fluxes of methane, carbon dioxide, and nitrous oxide rarely exceeded one order of magnitude in difference across a range in daily to intermediate to final covers (Bogner et al. 2011). However, differences between methane fluxes ranged up to four orders of magnitude across daily, intermediate, and final covers at the same landfill sites in California (Bogner et al. 2011). Seasonal differences in LFG emissions can be attributed to the high infiltration of precipitation into the cover soil observed during the winter months, which alters the transport and transformation mechanisms occurring throughout the depth of the soil cover. In some cases, higher moisture contents lead to suboptimal oxidation of methane and other NMVOCs (Scheutz et al. 2009a). During the wet season, higher moisture contents generally reduce the available pore space available for gaseous transport (i.e., volumetric air content), which may have

a stymying effect on transport (Kjeldsen 1996). However, higher soil moisture contents observed in the wet seasons may also facilitate transport of some NMVOCs such as F-gases due to decreased retardation and sorption (Yesiller et al. 2018).

1.5 Chemical Species Included in the Investigation

Information is provided in this section on the potential sources of the chemicals included in the study in the landfill environment, a review of relevant physical-chemical properties affecting fate and transport, and the contribution of these chemicals to air quality on local, to regional, to global scales. The 82 chemical species investigated were categorized into 12 chemical families based on chemical characteristics and atmospheric air impacts. These families include baseline greenhouse gases, reduced sulfur compounds, fluorinated gases (F-gases), halogenated hydrocarbons, organic (alkyl) nitrates, alkanes, alkenes, aldehydes/alkynes aromatic hydrocarbons, monoterpenes, alcohols, and ketones (Table 1.1).

The impact of fugitive LFG emissions emanating from MSW landfills on global climate continues to be a significant issue in both developed and developing countries. In the U.S. and Europe, emissions from MSW landfills constitutes the second largest source of anthropogenic methane emissions, comprising 22 to 23% of the total anthropogenic emissions, respectively (USEPA 2009). In addition to methane, emissions of carbon dioxide, nitrous oxide, and chlorinated and fluorinated gases from MSW landfills have been identified as a direct threat to global climate change. In 2016, the emissions of greenhouse gases (GHGs) including carbon dioxide, methane, nitrous oxide, and F-gases from all global potential sources contributed approximately 72%, 19%, 6%, and 3% of the total global greenhouse gas emissions (49.3 Gt CO_2 equivalents) (Olivier et al. 2017). Emissions from MSW landfills amount to 5% of total global GHG emissions (IPCC 2013).

Table 1.1 – Characteristics of Chemical Species Included in the Investigation

Chemical Family (Abbr.)	Sources	Chemical Species	CAS-#	Chemical Formula	HAP [2]	MIR (g O_3/g species) [3]	FAC (%)[4]	GWP (unitless) [5]	ODP (unitless) [7]
Baseline Greenhouse Gases (GHG)	FW, GW	Methane	74-82-8	CH_4	N	0	0	28	0
		Carbon Dioxide	124-38-9	CO_2	N	0	0	1	0
		Carbon Monoxide	630-08-0	CO	N	0	0	4.4[6]	0
		Nitrous Oxide	10024-97-2	N_2O	N	0	0	265	0
Reduced Sulfur Compounds (RSC)	FW, GW, C&DW	Carbonyl sulfide	463-58-1	COS	Y	0	0	0	0
		Di-methyl sulfide	75-18-3	C_2H_6S	N	0	0	0	0
		Di-methyl disulfide	624-92-0	$C_2H_6S_2$	N	0	0	0	0
		Carbon disulfide	75-15-0	CS_2	Y	0	0	0	0
Fluorinated gases (F-gas)	AppW, C&D, AW	CFC-11	75-69-4	CCl_3F	N	0	0	4660	1
		CFC-12	75-71-8	CCl_2F_2	N	0	0	10200	0.82
		CFC-113	76-13-1	$C_2Cl_3F_3$	N	0	0	5820	0.85
		CFC-114	76-14-2	$C_2Cl_2F_4$	N	0	0	8590	0.58
		HCFC-21	75-43-4	$CHCl_2F$	N	0	0	148	0
		HCFC-22	75-45-6	$CHClF_2$	N	0	0	1760	0.04
		HCFC-141b	1717-00-6	CCl_2FCH_3	N	0	0	782	0.12
		HCFC-142b	75-68-3	$C_2H_3ClF_2$	N	0	0	1980	0.06
		HFC-134a	811-97-2	CH_2FCF_3	N	0	0	1300	0
		HFC-152a	75-37-6	$C_2H_4F_2$	N	0	0	138	0
		HFC-245fa	460-73-1	$CF_3CH_2CHF_2$	N	0	0	858	0
		HFC-365mfc	406-58-6	$C_4H_5F_5$	N	0	0	804	0
		Halon-1211	353-59-3	$CBrClF_2$	N	0	0	1750	7.9
Halogenated Hydrocarbons (HH)	TW, HCW, PW	Chloroform	67-66-3	$CHCl_3$	Y	0.02	0	16	0
		Methyl chloroform	71-55-6	$C_2H_3Cl_3$	Y	0.005	0	160	0.1
		Carbon tetrachloride	56-23-5	CCl_4	Y	0	0	1730	0.82
		Methylene chloride	75-09-2	CH_2Cl_2	Y	0.039	0	9	0
		Trichloroethylene	79-01-6	C_2HCl_3	Y	0.61	0	0	0
		Tetrachloroethylene	127-18-4	C_2Cl_4	Y	0.029	0	0	0
		Methyl chloride	74-87-3	CH_3Cl	Y	0.036	0	12	0.02
		Bromomethane	74-83-9	CH_3Br	Y	0.121	0	0	0.66
		Dibromomethane	74-95-3	CH_2Br_2	N	0	0	0	0
		Bromodichloromethane	75-27-4	$CHBrCl_2$	N	0	0	0	0
		Bromoform	75-25-2	$CHBr_3$	Y	0	0	0	0

Chemical Family (Abbr.)	Sources	Chemical Species	CAS-#	Chemical Formula	HAP [2]	MIR (g O_3/g species) [3]	FAC (%)[4]	GWP (unitless) [5]	ODP (unitless) [7]
		Chloroethane	75-00-3	C_2H_5Cl	N	0.27	0	0	0
		1,2-Dichloroethane	107-06-2	$C_2H_4Cl_2$	Y	1.65	0	0	0
		1,2-Dibromoethane	106-93-04	$C_2H_4Br_2$	Y	0.098	0	0	0
Organic (Alkyl) Nitrates (ON)	OBP	Methyl Nitrate	598-58-3	CH_3NO_3	N	0	0	0	0
		Ethyl Nitrate	625-58-1	$C_2H_5NO_3$	N	0	0	0	0
		Isopropyl nitrate	1712-64-7	$C_3H_7NO_3$	N	0	0	0	0
		N-propyl nitrate	627-13-4	$C_3H_7HO_3$	N	0	0	0	0
		2-butyl nitrate	924-52-7	$C_4H_9NO_3$	N	0	0	0	0
Alkanes (Alk)	PW, HCW, CW, PaW, PapW	Ethane	74-84-0	C_2H_6	N	0.26	0	5.5	0
		Propane	74-98-6	C_3H_8	N	0.46	0	3.3	0
		i-Butane	75-28-5	C_4H_{10}	N	1.17	0	4	0
		n-Butane	106-97-8	C_4H_{10}	N	1.08	0	0	0
		i-Pentane	78-78-4	C_5H_{12}	N	1.36	0	0	0
		n-Pentane	109-66-0	C_5H_{12}	N	1.23	0	0	0
		n-Hexane	110-54-3	C_6H_{14}	Y	1.15	0	0	0
		n-Undecane	1129-21-4	$C_{11}H_{24}$	N	0.55	2.5	0	0
Alkenes (Alke)		Ethene	74-85-1	C_2H_4	N	8.76	0.3	3.7	0
		Propene	115-07-1	C_3H_6	N	11.37	0	1.8	0
		1-Butene	106-98-9	C_4H_8	N	9.42	0	0	0
		i-Butene	115-11-7	C_4H_8	N	6.14	0	0	0
		trans-2-butene	624-64-6	C_4H_8	N	14.79	0	0	0
		cis-2-butene	590-18-1	C_4H_8	N	13.89	0	0	0
		1-Pentene	109-67-1	C_5H_{10}	N	6.97	0	0	0
		Isoprene	78-79-5	C_5H_8	N	10.28	0.6	2.7	0
Aldehydes/Alkynes (Ald/Alky)		Ethyne	74-86-2	C_2H_2	N	0.93	0	0	0
	FW, HCW, CW, PCPW, HSPW, PW, PaW, TW, FuW	Acetaldehyde	75-07-0	C_2H_4O	Y	6.34	0	1.3	0
		Butanal	123-72-8	C_4H_8O	N	5.75	0	0	0
Aromatic Hydrocarbons (Ar)		Benzene	71-43-2	C_6H_6	Y	0.69	2.6	0	0
		Toluene	108-88-3	C_7H_8	Y	3.88	5.4	2.7	0
		Ethylbenzene	100-41-4	C_8H_{10}	Y	2.93	5.4	0	0
		m+p-Xylene	108-38-3/ 106-42-3	C_8H_{10}	Y	7.605	3.15	0	0
		o-Xylene	95-47-6	C_8H_{10}	Y	7.44	5	0	0
		i-Propylbenzene	98-82-8	C_9H_{12}	N	2.43	4	0	0

Chemical Family (Abbr.)	Sources	Chemical Species	CAS-#	Chemical Formula	HAP [2]	MIR (g O_3/g species) [3]	FAC (%)[4]	GWP (unitless) [5]	ODP (unitless) [7]
		n-Propylbenzene	103-65-1	C_9H_{12}	N	1.95	1.6	0	0
		3-Ethyltoluene (M)	620-14-4	C_9H_{12}	N	7.21	6.3	0	0
		4-Ethyltoluene (P)	622-96-8	C_9H_{12}	N	4.32	2.5	0	0
		2-Ethyltoluene (O)	611-14-3	C_9H_{12}	N	5.43	5.6	0	0
		1-3-5-Trimethylbenzene	108-67-8	C_9H_{12}	N	11.44	2.9	0	0
		1,2,3-Trimethylbenzene	526-73-8	C_9H_{12}	N	11.66	3.6	0	0
		1,2,4-Trimethylbenzene	95-63-6	C_9H_{12}	N	8.64	2	0	0
Monoterpenes (Mon)	GW, C&D, HCW, PCPW, HSPW	α-pinene	80-56-8	$C_{10}H_{16}$	N	4.38	30	0	0
		β-pinene	127-91-3	$C_{10}H_{16}$	N	3.38	30	0	0
		Limonene	138-86-3	$C_{10}H_{16}$	N	4.4	0	0	0
Alcohols (Alc)	FW, HCW, PCPW, HSPW	Methanol	67-56-1	CH_4O	Y	0.65	0	2.8	0
		Ethanol	64-17-5	C_2H_6O	N	1.45	0	0	0
		Isopropanol	67-63-0	C_3H_8O	N	0.59	0	0	0
		2-Butanol	78-92-2	$C_4H_{10}O$	N	1.3	0	0	0
Ketones (Ket)		Acetone	67-64-1	C_3H_6O	N	0.35	0	0.5	0
		Butanone	78-93-3	C_4H_8O	N	0.59	0	0	0
		Methylisobutylketone	108-10-1	$C_6H_{12}O$	Y	3.74	0	0	0

[1] Adapted from Nair et al. (2019). FW = food wastes; PapW = paper wastes; GW = green wastes (i.e., yard trimmings); C&D = construction and demolition wastes (e.g., concrete, metal, wood, drywall); AW = auto-wastes; TW = textile wastes (i.e., clothes, carpet); HCW = household cleaning wastes; PW = plastic wastes; OBP = oxidation byproduct of NMVOCs in the landfill environment; CW = cooking wastes (i.e., charcoal, propane fuels); PCPW = personal care product wastes (i.e., shampoo, toothpaste); HSPW = household spray product wastes (i.e., air fresheners); PaW = paint wastes; FuW = furniture wastes; AppW = appliance wastes.
[2]Y(Yes) or N(No) (USEPA 2016b)
[3]Carter (2009)
[4]Grosjean and Seinfeld (1989) and Grosjean (1992)
[5]Indirect GWP values for alkanes, aldehydes, alcohols and ketones obtained from IPCC (2007), all other GWP values obtained from IPCC (2013)
[6]The direct and indirect GWP values based on estimates provided by Daniel and Solomon (1998) (upper range used)
[7]WMO (2014)

Once emitted to the atmosphere, the GHG gases have significant impacts due to their high radiative forcing (RF) and atmospheric lifetimes. RF refers to the relative strength of a given chemical to absorb outgoing thermal (infrared) radiation and thereby alter Earth's energy balance, where larger (positive) values are indicative of a net warming effect on the Earth's average temperature (Scheutz et al. 2009b, IPCC 2013). Chemicals can have both direct and indirect radiative forcing effects on Earth's atmosphere. For example, methane possesses both direct and indirect RF effects as it absorbs outgoing radiation and as the decomposition of methane produces carbon dioxide, water vapor, and ozone, all of which are potent GHGs that affect Earth's energy balance (Scheutz et al. 2009b). The atmospheric lifetime of a given chemical refers to the average time a chemical resides in the atmosphere before being removed or transformed by a chemical reaction or deposition (IPCC 2013). The global warming potential (GWP) is the most widely used metric that integrates both the RF and atmospheric lifetime of a given chemical to measure and compare the net effect of the chemical on global climate change. The mathematical definition of GWP is the time integrated RF resulting from a pulse emission (1 kg) of a given chemical relative to that of carbon dioxide, where a time horizon of 100 years is generally used for calculation (IPCC 2013). Carbon dioxide has a baseline GWP of 1, whereas methane, nitrous oxide, and F-gases have GWP values that range from less than an order to multiple orders of magnitude higher than that of carbon dioxide due to their high infrared absorption properties and atmospheric lifetimes as compared to CO_2. The global warming potentials for the chemical species included in this investigation are presented in Table 1.1.

As compared to impacts on global climate change, the impact of LFG emissions on local to regional atmospheric air quality is a less studied issue. A great majority (95%) of the chemicals included in this investigation are classified as non-methane volatile organic compounds (NMVOCs). NMVOCs constitute a broad class of anthropogenic and biogenic chemical compounds that are chemically distinct, yet have similar fates and transformations once released into the atmosphere (Kansal 2009, Nair et al. 2019). Municipal solid waste landfills represent a small, yet detectable and ongoing source of annual NMVOC emissions in the US. The 2014 USEPA national air emissions inventory (USEPA 2016a) estimated that total landfill NMVOC emissions are 13,741 tonnes per year amounting to 0.024% of the nationwide total. As compared to nationwide results, the California Air Resources Board's (CARB) projected 2015 statewide NMVOC (termed ROG for Reactive Organic Gases) emissions inventory reported estimates of total NMVOCs from MSW landfills of 3,460 tonnes per year, MSW landfill contributions to be an order of magnitude more than national estimates at 0.50% of the statewide total (CARB 2009).

Many NMVOCs are highly reactive compounds, with short to moderate atmospheric half-lives (hours to days), affecting air quality from local to regional scales (Atkinson and Arey 2003). NMVOCs are precursors to tropospheric ozone, photochemical smog, and secondary organic aerosol (SOA) formation in the atmosphere (Kroll and Seinfeld 2008, Ziemann and Atkinson 2012). Due to their active roles in ozone and SOA formation, as well as degradation in the atmosphere, NMVOCs both indirectly and directly contribute

to global climate change (Collins et al. 2002). In addition, some NMVOCs, including benzene and other aromatic or halogenated hydrocarbons, pose acute and/or chronic human health risks, leading to their classification as hazardous air pollutants (HAPs) (Reinhart 1993). Other NMVOC classes, such as reduced sulfur compounds, are olfactory nuisances, presenting aesthetic problems to communities located near emission sources (Ying et al. 2012). Furthermore, in addition to F-gases, some chlorinated and brominated NMVOCs (i.e., chloroform or bromoform) are stratospheric ozone depleting substances (ODSs) (Hodson et al. 2010).

One of the most critical impacts of NMVOC emissions from landfills relates to tropospheric ozone formation. Ozone is a strong chemical oxidant and a GHG, which directly affects human health, environment, and global climate change. The fundamental ozone formation mechanism from NMVOC precursors in the troposphere is as follows: a) OH radicals attack the NMVOCs to produce nitrogen dioxide; b) nitrogen dioxide then dissociates in the presence of sunlight (photolysis) to form nitrogen oxides and oxygen radicals; and c) finally, the oxygen radicals combine with oxygen in the atmosphere forming ozone (Perring et al. 2013). Among many factors, the ozone formation potential ultimately depends on the reactivity of the NMVOC as well as the relative concentrations of NMVOC and nitrogen oxides (NOx) in the atmosphere (Duan et al. 2008, Nair et al. 2019). Depending on these conditions, ozone formation reactions can be either NMVOC or NOx limited, where the former is generally the case in urban environments. Previous field and laboratory studies have determined that aromatics, alkenes, and aldehydes are the main chemical families contributing to tropospheric ozone formation (Duan et al. 2008).

The role of NMVOC emissions in SOA formation also is important, even though this process is more complex and harder to predict in the ambient environment than ozone formation (Hallquist et al. 2009). SOAs are defined as liquid or solid particles suspended in the air that indirectly affect Earth's energy balance through: a) scattering and absorption of incoming solar and outgoing terrestrial radiation, b) influencing cloud formation, and c) being included in chemical reactions that influence the abundance and distribution of atmospheric trace gases (Haywood and Boucher 2000). In addition, SOAs pose a direct threat to human health, where SOA exposure has been linked to damage of respiratory and cardiovascular systems (Harrison and Yin 2000). The fundamental formation of SOA from NMVOC precursors is described as: a) SOA formation is initiated by reaction of NMVOCs with hydroxyl radicals, ozone, or nitrate radicals or via photolysis (the hydroxylation pathway depends on molecular structure of NMVOC and atmospheric conditions); b) the initial oxidation step leads to first generation of polar, fragmented, and oxygenated functional groups (aldehydes, ketones, alcohols, nitrates, carboxylic acids), which either undergo gas to particle transfer, including heterogeneous chemical reactions, condensation, and nucleation (depending on volatility and water solubility), or continue to oxidize to form next generation byproducts in the gas phase; c) the competition between gas-particle transfer and oxidation continues until all fragments have been oxidized to CO_2 or undergo gas-particle transfer (Hallquist et al. 2009). Previous field and laboratory studies have determined that oxygenated compounds, carbonyls, aromatics, alkanes,

and alkenes are the major classes of SOA NMVOC precursors (Ziemann and Atkinson 2012, Guo et al. 2017).

Similar to GWP values used to assess climate change, metrics have been developed to assess and compare the impacts of NMVOC emissions on atmospheric air quality. Common air quality metrics to assess changes in atmospheric air quality used in the current investigation include tropospheric ozone formation, secondary aerosol formation, indirect/direct global warming, and stratospheric ozone depletion potentials. HAP classification can also be used to further evaluate to what extent a chemical emitted from a landfill site impacts human health. The mathematical meaning and calculation of each of these metrics are reviewed in more detail in Section 3.10 of this report.

1.5.1 Baseline Greenhouse Gases

The baseline greenhouse gases included in this investigation consist of the individual chemical species: methane, carbon dioxide, carbon monoxide, and nitrous oxide. Methane, carbon dioxide, and nitrous oxide are well known GHGs that directly affect the radiative forcing of Earth's atmosphere. In addition, carbon monoxide both directly and indirectly affects Earth's radiative forcing through absorption and emission of reflected infrared radiation and by chemically altering the abundances of methane, ozone, and carbon dioxide (Daniel and Solomon 1998). The direct radiative forcing of CO is small (< 1), whereas the indirect forcing is higher at 4.4 (Table 1.1) and results in the production of ozone or oxidation to carbon dioxide as well as the reduction in loss rate of methane (due to a decrease in the hydroxyl mixing ratios) (Daniel and Solomon 1998). Of the baseline GHGs, N_2O has the highest GWP value of 265 (Table 1.1).

The main source of baseline GHGs in the landfill environment is biogenic production during aerobic or anaerobic decomposition of the biodegradable fraction of MSW (Tchobanoglous et al. 1993, Barlaz et al. 2010). Methane is produced during the anaerobic decomposition of waste materials, whereas carbon dioxide and monoxide are both produced during aerobic oxidation and anaerobic decomposition of waste materials. Carbon dioxide and monoxide also are produced as byproducts during methanotrophic oxidation of LFG or oxidation of organic carbon present in soil matter in landfill cover soils (i.e., background soil respiration) (Bogner et al. 1997b). The biological production of CO is not well understood; however, studies have reported that methanogens actively produce CO during exergonic formation of methane from carbon dioxide and hydrogen (Haarstad et al. 2006). Moreover, acetogens and sulfate reducing bacteria also have been observed to produce CO under anaerobic conditions (Haarstad et al. 2006). Aerobic degradation of chlorophyll in leaf waste was identified as another source of CO, which has been observed in composting operations (Haarstad et al. 2006). Depending on the stage of waste decomposition the concentrations of methane, carbon dioxide, and carbon monoxide can vary significantly as described in Section 1.2. While, CO_2 and CO typically are not included in landfill emissions inventories due to the uncertainties in the source of these gases (i.e., waste mass versus cover soils) (USEPA 2008, Henkelman et al. 2016), these gases were measured in this investigation and data and analysis are provided both including and excluding these two gases.

Production of nitrous oxide in the landfill environment is complicated and can be attributed to differences in nitrogen cycling in the waste mass and cover soils. In the waste mass, which is primarily present at anaerobic conditions (depending on the stage of decomposition), denitrification of nitrate producing nitrogen gas releases nitrous oxide as a byproduct through cell leakage (Barton and Atwater 2002). In the top portion of landfill cover soils, which are primarily under aerobic conditions, nitrification of ammonium by resident methanotrophs that co-oxidize methane to nitrate releases nitrous oxide as a byproduct through cell leakage (Mandernack et al. 2000, Barton and Atwater 2002). Moreover, methanotrophs likely compete with indigenous autotrophic and heterotrophic nitrifying bacteria, which naturally oxidize ammonium present in the cover soils and emitted from the waste mass (Mandernack et al. 2000, Barton and Atwater 2002). Emissions of nitrous oxide from landfill leachate is yet another potential nitrous oxide source, as reactive nitrogen tends to dissolve in water percolating through the waste mass (where high total nitrogen concentrations have been reported in the range of 25-1600 mg/L) (Tchobanoglous et al. 1993). Finally, wastewater sludges (biosolids) are another potential source of nitrous oxide emissions (Börjesson and Svensson 1997c). The relative contribution of denitrification and nitrification to nitrous oxide production in MSW landfills depends on MSW age and composition (presence of inorganic and organic nitrogen sources), temperature, pH and moisture content of the waste mass, as well as the presence/absence of oxygen (Barton and Atwater 2002). Similar conditions affect the degree of nitrification in soil covers (i.e. presence of bioavailable ammonium in the soil), soil composition, pH, moisture content, temperature, and presence or absence of oxygen (Barton and Atwater 2002).

Physical and chemical properties of baseline greenhouse gases are presented in Table 1.2. These data are obtained from experimental analysis or predictions compiled in USEPA's CompTox Database (Williams et al. 2017). In this analysis, experimental values are preferred over predicted values. Predicted properties were derived from two quantitative-structure activity modelling suites: TEST and OPERA. Carbon monoxide is the most water-soluble chemical of the baseline GHGs, whereas methane is the least water soluble (Table 1.2). The high vapor pressures, Henry's constants and very low boiling points of all baseline GHG species indicate that these chemicals most likely will be present in the gaseous phase in the landfill environment. Based on octanol-air partition coefficients, nitrous oxide is the most likely to sorb to organic matter in the waste mass or present in cover materials (no experimental or predicted values available for carbon monoxide).

Table 1.2 – Physical and Chemical Properties of Baseline GHGs

Chemical Species	Mol. Weight (g/mol)	Boiling Point (°C)	Log_{10} (Vapor Pressure)	Log_{10} (Octanol-Air)	Log_{10} (Dim. Henry's Constant)	Water Solubility (mg/L)	Log_{10} (Octanol-Water)
Methane	16.04	-163	5.67	-0.38	-0.91	21.97	0.63
Carbon Dioxide	44.01	-78.2	4.68	1.57	-2.88	14699	0.83
Carbon Monoxide	28.01	-192	3.53	-	-1.78	238645	0.07

Chemical Species	Mol. Weight (g/mol)	Boiling Point (°C)	Log_{10} (Vapor Pressure)	Log_{10} (Octanol-Air)	Log_{10} (Dim. Henry's Constant)	Water Solubility (mg/L)	Log_{10} (Octanol-Water)
Nitrous Oxide	44.013	-88.3	4.59	4.13	-3.79	8759	1.38

1.5.2 Reduced Sulfur Compounds

The reduced sulfur compounds included in this investigation consist of the individual chemical species: carbonyl sulfide, dimethyl sulfide, dimethyl disulfide, and carbon disulfide. These chemicals do not affect climate change or impact atmospheric air quality, based on data presented in Table 1.1. However, two of these chemicals, carbon disulfide and carbonyl sulfide are hazardous air pollutants (USEPA 2016b). In addition, these chemical species are largely responsible for olfactory nuisances that have adverse effects on the surrounding communities (Kim 2006, Kim et al. 2006).

The chemical species included under the reduced sulfur compound chemical family are primarily produced from anaerobic biological decomposition of food (dairy and meat products), green wastes, paper, and wastewater sludge materials (Table 1.1) in MSW landfills (Ko et al. 2015). In general, sulfate reducing bacteria are responsible for the generation of the reduced sulfur compounds that use the organic sulfur (sulfate) present in the food or green wastes as terminal electron acceptors (Ko et al. 2015). Amino acids containing sulfur (which are derived from proteins in food/green wastes, including cysteine and methionine) are the principal sources of reduced sulfur compounds in MSW landfills. However, C&D materials containing gypsum (composed of calcium sulfate and water) are also significant sources of sulfate in MSW landfills in the U.S. (Lee et al. 2006).

Physical and chemical properties of reduced sulfur compounds are presented in Table 1.3. The volatility is highest for carbonyl sulfide and lowest for dimethyl disulfide based on the reported median values of vapor pressure and boiling point (in contrast to trends in the dimensionless Henry's Constant). Sorption of carbonyl sulfide to organic matter either in the waste mass or cover soil is least likely for carbonyl sulfide based on octanol-air partition coefficients. Water solubility is highest for carbonyl sulfide and lowest for carbon disulfide, based on data for water solubilities and octanol-water partition coefficients (Table 1.3).

Table 1.3 – Physical and Chemical Properties of Reduced Sulfur Compounds

Chemical Species	Mol. Weight (g/mol)	Boiling Point (°C)	Log_{10} (Vapor Pressure)	Log_{10} (Octanol-Air)	Log_{10} (Dim. Henry's Constant)	Water Solubility (mg/L)	Log_{10} (Octanol-Water)
Carbonyl Sulfide	60.07	-50	3.97	2.18	-4.14	100918	0.39
Dimethyl Sulfide	62.13	38	2.70	2.26	-2.50	20814	1.09
Dimethyl Disulfide	94.19	109	1.46	3.35	-2.62	2995	1.77
Carbon Disulfide	76.131	46	2.56	2.28	-1.55	1180	1.94

1.5.3 Fluorinated Gases (F-gases)

The fluorinated gases included in this investigation consist of chlorofluorocarbons (CFCs), hydrochlorofluorocarbons (HCFCs), hydrofluorocarbons (HFCs), and halons. The CFCs investigated are CFC-11, CFC-12, CFC-113, and CFC-114 The HCFCs investigated are HCFC-21. HCFC-22, HCFC-141b, and HCFC-142b. The HFCs investigated are HFC-134a, HFC-152a, HFC-245fa, and HFC-365mfc. A single species, H-1211, is selected for analysis within the halon category of F-gas chemicals. All chemical species within the F-gas chemical family are high GWP gases, where GWP values are generally highest for the CFCs followed by the HCFCs and HFCs (Table 1.1). The CFCs and HCFCs also are ozone depleting substances, where ODP values are higher for the CFCs than the HCFCs (Table 1.1). H-1211 has the highest ODP value of all species within the F-gas chemical family (Table 1.1).

F-gases are commonly used as blowing agents applied to improve the insulation properties of foam materials as they can absorb large amounts of heat upon vaporization (Kjeldsen and Jensen 2001). The fluorinated gases are alkanes (long groups of single bonded carbon atoms) where all of the hydrogen atoms are replaced by fluorine and chlorine atoms (Vollhardt and Schore 1999). Common sources of the fluorinated gases in the landfill environment include rigid foam insulation materials used in domestic, commercial, and industrial appliances (Fredenslund et al. 2005). Other significant sources of F-gases in the landfill environment include insulation materials used in buildings (C&D wastes) and automobiles (automotive shredder residues) (Scheutz et al. 2010). Due to their negative effects on stratospheric ozone concentrations, CFCs were banned by the Montreal protocol in 1993. After replacement of CFCs with HCFCs (smaller ODP values), HCFCs were eventually phased out by HFCs, which are the latest replacement species (Powell 2002). Halons are commonly used in fire suppressant applications, such as fire extinguishers in residential and commercial settings (McCulloch 1992).

Physical and chemical properties of the CFCs, HCFCs, HFCs, and the halon species are presented in Table 1.4. Due to their relatively low boiling points (in the range of <0 to 100°C) and high vapor pressures and Henry's Constants, CFCs, HCFCs, HFCs, and halon fall within the general classification of NMVOCs. Molecular weights of the CFCs, HCFCs, and HFCs are relatively low, with the lowest values associated with HCFC-22 and HFC-152a (Table 1.4). On average, the HFCs have higher volatility (higher vapor pressure, lower boiling point) and relatively moderate solubility in water as compared to CFCs and HCFCs (HCFCs had the highest water solubility, CFCs the lowest) (Table 1.4). HFCs have the lowest octanol-water and octanol-air partition coefficients, indicating that they are more likely to remain in the water or air phase over organic phases present in the landfill environment (Table 1.4). The CFCs (especially CFC-113 and 114) are most likely to partition to organic phases present in the landfill environment. H-1211 has moderate volatility and moderate-high partitioning potential to the organic matter in the landfill environment.

Table 1.4 – Physical and Chemical Properties of the Fluorinated Gases

Chemical Species	Mol. Weight (g/mol)	Boiling Point (°C)	Log_{10} (Vapor Pressure)	Log_{10} (Octanol-Air)	Log_{10} (Dim. Henry's Constant)	Water Solubility (mg/L)	Log_{10} (Octanol-Water)
CFC-11	137.37	23.8	2.90	2.19	-0.72	1100	2.53
CFC-12	120.91	-29.8	3.69	1.31	-0.17	281	2.16
CFC-113	187.375	47.8	2.56	2.82	-0.79	170	3.16
CFC-114	170.92	3.64	3.30	2.19	0.21	130	2.82
HCFC-21	102.923	8.9	3.13	2.02	-1.46	18835	1.55
HCFC-22	86.47	-40.8	3.86	0.56	-1.10	2767	1.08
HCFC-141b	116.95	32	2.78	2.22	-2.70	420	1.99
HCFC-142b	100.495	-9.52	3.40	1.30	-0.94	1397	1.57
HFC-134a	102.03	-26.5	3.70	0.04	-1.01	2530	1.18
HFC-152a	66.05	-24.9	3.66	0.47	-1.40	3203	0.75
HFC-245fa	134.05	40	3.05	0.44	-0.84	1249	1.43
HFC-365mfc	148	40	3.29	0.97	-0.89	445	2.06
H-1211	165.36	-2.8	3.31	1.78	-0.25	678	2.13

1.5.4 Halogenated Hydrocarbons

The halogenated hydrocarbons included in this investigation consist of the individual chemical species: chloroform, methyl chloroform, carbon tetrachloride, methylene chloride, trichloroethylene, tetrachloroethylene, methyl chloride, bromomethane, dibromomethane, bromodichloromethane, bromoform, chloroethane, 1,2-dichloroethane, and 1,2-dibromoethane. Eleven of the fourteen halogenated hydrocarbons with the exceptions of dibromomethane, bromodichloromethane, and chloroethane are designated as hazardous air pollutants (USEPA 2016b), indicating that the emissions of these chemical species may significantly affect human health. Several of the halogenated hydrocarbon chemical species contribute to tropospheric ozone formation including from most to least active, based on reported MIR values: trichloroethylene, bromomethane, methylene chloride, methyl chloride, tetrachloroethylene, chloroform, and methyl chloroform (Table 1.1). Indirect GWP values are highest for carbon tetrachloride along with methyl chloroform and methyl chloride, indicating that emissions of halogenated hydrocarbons may affect climate change in addition to the well-known GHGs (Table 1.1). Carbon tetrachloride, bromomethane, methyl chloroform, and methyl chloride also are ozone depleting substances, where ODP values are generally less than 1 (Table 1.1).

In this report, halogenated compounds are classified as hydrocarbons (linear or branched, composed of C and H atoms) composed of one or more halogen atoms (i.e., F, Cl, Br, I). Hydrocarbons can be either unsaturated (single bonded) or saturated (double or triple bonded) (Vollhardt and Schore 1999). In this particular inventory of target chemicals, the most common halogen atoms are chlorine and bromine and a majority of chemicals are saturated (i.e., chloroform, bromomethane) as opposed to unsaturated species(methylene chloride, trichloroethylene). Nair et al. (2019) indicated

that halogenated hydrocarbons in the landfill environment are mostly directly volatilized (abiotically) from a variety of waste household consumer products, mainly including cleaning and fragrance-containing products (Table 1.1). Additional sources of halogenated hydrocarbons in the landfill environment are more difficult to define. Methyl chloride has been used as a refrigerant and in the production of synthetic rubber materials. Methylene chloride and chloroform are both commonly used industrial solvents. Carbon tetrachloride and tetrachloroethylene have been used extensively as dry-cleaning solvents, while carbon tetrachloride also has been used in fire extinguishers (Vogel et al. 1987).

Given that there is a general lack of consistent and reliable information on the origin of halogenated hydrocarbons in the landfill environment, CPCat (Chemical/Product Categories) database (Dionisio et al. 2015, 2018) was used to search for specific product use categories for each target chemical. CPCat database contains information on over 75,000 chemical species and 15,000 consumer products which mapped to over 800 terms categorizing their use or function, (Dionisio et al. 2015, Isaacs et al. 2016). Even though this database is not fully representative of the materials that are disposed of in MSW landfills, it provides a general indication of the sources of these chemicals from consumer related products.

For the halogenated hydrocarbons included in this investigation, 175 unique functional use categories were obtained from this database. The fifteen most significant overall categories for this chemical family were determined by summing the number of products linked to each functional use category and then sorting the results in descending order. The relative contribution of each chemical species to products contained within a given functional use category is presented in Table 1.5. This analysis provided several significant functional uses of the halogenated hydrocarbons that have not been identified in the literature including: pesticides (home or lawn/backyard care), adhesives, automotive products, metal, plastic, rubber manufacturing, paints, and other personal care products (i.e., makeup, fragrances, shampoos) (Table 1.5).

The relative contribution of each chemical to different functional uses is also reviewed. Bromomethane is identified as a chemical species present in a large number of products associated with household or commercial pesticide applications. Carbon tetrachloride, methylene chloride, trichloroethylene, and tetrachloroethylene are identified as common chemical ingredients present in products associated with solvent, adhesive, cleaning, and painting applications. Most chemical species were equally distributed among products associated with automotive and personal care products (Table 1.5). Of all chemical species within the halogenated hydrocarbon family, dibromomethane and chloroethane are not associated with any products from the top fifteen functional use categories identified (Table 1.5). The 1,2 dichloro/dibromo ethanes are used in manufacturing chemicals, plastics, and other raw materials intended for a variety of industries.

Physical and chemical properties of the halogenated hydrocarbons are presented in Table 1.6. Of the halogenated hydrocarbons included in this investigation, methyl

chloride and bromoform are the most and least volatile, based on the low and high boiling points and high and low vapor pressures, respectively (Table 1.6). Both of these chemical species are also relatively soluble in water, based on water solubility and octanol-water partition coefficients. Based on Henry's Constant, water solubility, and octanol-water partition coefficients, dibromomethane is the most water-soluble halogenated hydrocarbon included in this study. Tetrachloroethylene and bromoform have high likelihood to partition into organic phases in the landfill environment (based on high octanol-air and octanol-water partition coefficients).

Table 1.5 – Fifteen Most Common Functional Use Categories for Halogenated Hydrocarbons

CPCat Functional Use Category	Definition	Relative Contribution to Each Functional Use Category (%)												
		Chloroform	Methyl Chloroform	Carbon Tetrachloride	Methylene Chloride	Trichloroethylene	Tetrachloroethylene	Methyl Chloride	Bromomethane	Dibromomethane	Bromodichloromethane	Chloroethane	1,2-DCE	1,2-DBE
pesticide	Substances used for preventing, destroying or mitigating pests	5.56	3.33	8.89	1.11	1.11	1.11	1.11	54.4	0	1.11	0	0	6.67
solvent	Paint/graffiti removers, general solvents	17.6	8.82	2.94	26.5	17.6	20.6	0	0	0	0	0	0	5.88
adhesive	General adhesive/binding agents	9.09	6.06	21.2	21.2	24.2	12.1	6.06	0	0	0	0	0	0
manufacturing:chemical	Manufacturing of a given chemical	12.5	0	9.38	12.5	12.5	12.5	15.6	3.13	0	0	0	15.6	6.25
automotive	Related to automobiles or their manufacture	14.3	14.3	14.3	14.3	14.3	14.3	0	14.3	0	0	0	0	0
cleaning_washing	Related to all forms of cleaning/washing including detergents, soaps, de-greasers, spot removers	3.85	15.4	0	23.1	26.9	30.8	0	0	0	0	0	0	0
manufacturing:metals	Manufacturing of metals	0	4.17	12.5	29.2	33.3	20.8	0	0	0	0	0	0	0
chemical:laboratory	Chemical use designated in laboratory	31.8	0	18.2	31.8	9.09	4.55	0	0	0	0	0	0	4.55

CPCat Functional Use Category	Definition	Relative Contribution to Each Functional Use Category (%)												
		Chloroform	Methyl Chloroform	Carbon Tetrachloride	Methylene Chloride	Trichloroethylene	Tetrachloroethylene	Methyl Chloride	Bromomethane	Dibromomethane	Bromodichloromethane	Chloroethane	1,2-DCE	1,2-DBE
personal_care:cosmetics:prohibited_ASEAN	Personal care products: fragrances, shampoos, makeup (banned in ASEAN countries)	10	0	10	10	10	10	10	10	0	0	0	10	10
paint	Various types of paint for various uses	0	0	44.4	38.9	16.7	0	0	0	0	0	0	0	0
manufacturing:machines	Manufacturing of machinery related to production of different products	0	11.8	17.6	35.3	29.4	5.88	0	0	0	0	0	0	0
manufacturing:plastics	Manufacturing of plastics (plastic additives)	0	11.8	17.6	29.4	17.6	17.6	0	0	0	0	0	0	5.88
manufacturing:raw_material	Raw materials used in manufacturing of a variety of products in different industries	5.88	0	17.6	5.88	5.88	5.88	17.6	5.88	5.88	0	0	17.6	11.8
manufacturing:rubber	Manufacturing of rubbers (rubber additives)	0	6.67	26.7	13.3	26.7	26.7	0	0	0	0	0	0	0
pesticide:inert_ingredient	Inert ingredient in a pesticide	7.69	30.8	7.69	7.69	7.69	7.69	7.69	7.69	0	0	0	7.69	7.69

Table 1.6 – Physical and Chemical Properties for the Halogenated Hydrocarbons

Chemical Species	Mol. Weight (g/mol)	Boiling Point (°C)	Log_{10} (Vapor Pressure)	Log_{10} (Octanol-Air)	Log_{10} (Dim. Henry's Constant)	Water Solubility (mg/L)	Log_{10} (Octanol-Water)
Chloroform	119.4	61.2	2.29	2.80	-2.14	7951	1.97
Methyl Chloroform	133.4	96.7	2.09	2.70	-1.47	1494	2.49
Carbon Tetrachloride	153.8	76.8	2.06	2.79	-1.27	794	2.83
Methylene Chloride	84.9	39.8	2.64	2.27	-2.19	12994	1.25
Trichloroethylene	131.4	87	1.84	2.99	-1.71	1100	2.42
Tetrachloroethylene	165.8	121	1.27	3.48	-1.46	201	3.40
Methyl Chloride	50.45	-24.2	3.63	1.39	-1.76	5301	0.91
Bromomethane	109.0	3.6	3.21	2.00	-1.84	17435	1.19
Dibromomethane	173.8	97.3	1.65	3.07	-2.79	11905	1.70
Bromodichloromethane	163.8	88.7	1.97	2.81	-2.38	3031	2.00
Bromoform	252.7	149	0.73	3.98	-2.98	3488	2.40
Chloroethane	64.5	12.3	3.00	2.19	-1.66	5677	1.43
1,2-Dichloroethane	99.0	83	1.90	2.78	-2.63	8520	1.48
1,2-Dibromoethane	187.9	132	1.05	3.65	-2.89	4152	1.96

1.5.5 Organic Alkyl Nitrates

The organic alkyl nitrates included in this investigation consist of the individual chemical species: methyl nitrate, ethyl nitrate, isopropyl nitrate, n-propyl nitrate, and 2-butyl nitrate. These chemical species are relatively reactive, non-hazardous chemicals with moderate-long atmospheric lifetimes compared to other NMVOCs (Muthuramu et al. 1994). Even though the organic alkyl nitrates have not been assigned MIR or FAC values, several studies have identified these species as affecting ozone production/depletion and species involved in SOA formation in the troposphere (Atkinson et al. 1982, Muthuramu et al. 1994, Perring et al. 2015). While these species do not directly affect global climate change, they may have indirect effects by disturbing the balance of ozone in the troposphere (Table 1.1).

The production, fate, and emissions of organic alkyl nitrates in the landfill environment has received little attention in the scientific literature. Alkyl nitrates consist of a nitrate group (negatively charged) bonded to a hydrocarbon chain. Even though the alkyl nitrates in this study are classified as organic, these trace gases generally are not produced as a biogas through aerobic or anaerobic decomposition of waste materials. In contrast, these chemicals are likely produced abiotically through similar transformation pathways as demonstrated in the troposphere involving organic reactants. Perring et al. (2015) summarized two primary pathways for the production of alkyl nitrates in the atmosphere including: 1) hydroxyl radical initiated oxidation of hydrocarbons (alkanes) in the presence of nitrogen oxides (likely occurs in the presence of sunlight), and 2) nitrate radical initiated oxidation of alkenes (occurs in the absence of sunlight). The alkyl nitrate production pathways in the atmosphere may constitute surrogates for the formation of organic alkyl nitrates in the landfill environment. For pathway 1, it is likely that availability of sufficient oxygen is required for transformation reactions to be carried out. In the landfill environment, these reactions may take place and organic alkyl nitrates may be generated in the upper portion of the soil cover where oxygen and radicals are available for the chemical reactions. The second transformation pathway is likely more dominant, as sunlight does not penetrate far into the cover soils or underlying waste layers, and thus alkenes may be precursors for organic alkyl nitrate production in the landfill environment. The sources of alkene precursors are described in Section 1.5.7.

Physical and chemical properties of the halogenated hydrocarbons are presented in Table 1.7. As observed in Table 1.7, as the number of carbons comprising an alkyl nitrate increases, the molecular weights and boiling points also increase. Vapor pressures (and corresponding volatility) are generally higher for methyl nitrate and decrease with increasing number of carbon atoms comprising each chemical species. Both octanol air and octanol water coefficients also increase with an increasing number of carbon atoms, as the chemical species become more non-polar in nature. Thus, 2-butyl nitrate is more likely to partition into organic phases in the landfill environment as compared to all other alkyl nitrates. Water solubility for all alkyl nitrates is generally high (highest for 2-butyl nitrate, which has a relatively low Henry's constant).

Table 1.7 – Physical and Chemical Properties of the Organic Alkyl Nitrates

Chemical Species	Mol. Weight (g/mol)	Boiling Point (°C)	Log_{10} (Vapor Pressure)	Log_{10} (Octanol-Air)	Log_{10} (Dim. Henry's Constant)	Water Solubility (mg/L)	Log_{10} (Octanol-Water)
Methyl Nitrate	77.0	64.6	1.94	2.18	-2.88	150226	0.45
Ethyl Nitrate	91.1	87.2	1.81	2.32	-2.49	34332	0.71
Isopropyl Nitrate	105.1	40	2.29	2.14	-4.59	31318	1.14
N-propyl Nitrate	105.1	110	1.37	2.78	-2.60	3289	1.38
2-butyl Nitrate	119.1	124.3	1.19	3.20	-2.53	1330000	1.97

1.5.6 Alkanes

The alkanes included in this investigation consist of the individual chemical species: ethane, propane, iso-butane, n-butane, iso-pentane, n-pentane, n-hexane, and n-undecane. Most of the alkanes are involved in ozone formation, where reactivity (in terms of ozone production) is generally higher for the pentane isomers and lowest for ethane/n-undecane. Excluding n-undecane, the remaining alkanes are not actively involved in SOA formation (Table 1.1). Indirect GWPs have been reported for ethane and propane. n-hexane is the only alkane that has been identified as a hazardous air pollutant by the USEPA (Table 1.1).

The alkanes are generally straight chain hydrocarbons (composed of carbon and hydrogen) that are saturated (composed of single bonds only) and vary according to the number of carbon atoms comprising each chain (Vollhardt and Schore 1999). Structural isomers (i.e., i/n) of butane and pentane were investigated in this study, where structural isomers refer to the configuration of these molecules in three-dimensional space (iso-variants are branched and not straight-chained). Abiotic sources of alkanes in the landfill environment include household spray products and paints (Nair et al. 2019). Food packaging, cooking oils and fuels (charcoal or vegetable oils), and paper also are indicated as potential sources of alkanes in the landfill environment (Duan et al. 2014). In addition, alkanes are produced during anaerobic decomposition of waste materials (Xie et al. 2013). Although not documented in landfills, methanogens can generate low molecular weight alkanes in the presence of ethylene (i.e., ethylene reduction) (Xie et al. 2013). A similar production and transformation mechanism was suggested by Ikeguchi and Watanabe (1991), where ethane production from ethene was postulated. Ethene can be synthesized by microorganisms in aerobic, upper portions of soil (Primrose 1979), that Ikeguchi and Watanabe (1991) identified as a potential mechanism in landfill cover soils. The biogenic production of longer chain alkanes is possible, but not yet documented in the landfill environment.

Analysis of the top fifteen functional use categories based on the CPCat database indicated more categories related to personal use items for the alkanes as compared to the halogenated hydrocarbons (Table 1.8). Personal care products associated with shaving creams, hair styling, hair spray and deodorant contain alkane chemicals. Paints, lubricants, insecticides, cleaning products, and products associated with automotive care are likely to contain the alkane chemical species included in this report. For personal care products, i-pentane, i-butane, i-butane, and i-butane are the chemical species most likely present in shaving creams, hair-style products, hair sprays, and

deodorants, respectively. Propane and n-butane are most likely present in the paint products identified in Table 1.8. Within the top 15 functional use categories, n-undecane is only present in lubricant products. The functional use categories for ethane are significantly different than the overall functional use categories for the alkane chemical family (Table 1.9). Ethane is present in cooking and camping fuels and also in some paint and lubricant-related products. Household cleaning related products are more likely contain propane, n-butane, i-butane, n-pentane, and n-hexane as compared to the remaining three alkane chemical species included in this investigation (Table 1.8).

Table 1.8 – Fifteen Most Common Functional Use Categories for Alkanes

CPCat Functional Use Category	Definition	Relative Contribution to Each Functional Use Category (%)							
		Ethane	Propane	i-Butane	n-Butane	i-Pentane	n-Pentane	n-Hexane	n-Undecane
personal care: shaving cream	-	0	9.45	23.6	2.55	64	0.36	0	0
personal care: hair styling	-	0	35.5	43.2	19.4	1.47	0.37	0	0
home maintenance: paint	-	0	51	0	49	0	0	0	0
manufacturing:metals	Manufacturing of metals	0	23.3	21.9	23.3	2.74	13.7	15.1	0
pesticides: insecticide	-	0	40.8	33.8	25.4	0	0	0	0
paint	Various types of paint for various uses, modifiers included when more information is known	2.99	23.9	17.9	23.9	4.48	5.97	20.9	0
lubricant	Generic lubricants, lubricants for engines, brake fluids, oils, etc. (does not include personal care lubricants)	3.03	24.2	15.2	22.7	1.52	13.6	15.2	4.55
manufacturing:machines	Manufacturing of machinery related to production of different products	0	26.2	15.4	26.2	1.54	16.9	13.8	0
personal care: hair spray	-	0	22.6	41.9	24.2	3.23	8.06	0	0
surface_treatment	Surface treatments for metals, hardening agents, corrosion inhibitors, polishing agents, rust inhibitors, water repellants, etc. (surfaces to be applied to often not indicated in source description)	0	31.1	18	32.8	0	8.2	9.84	0
auto products: auto paint	-	0	50	0	50	0	0	0	0
cleaning_washing	Related to all forms of cleaning/washing including detergents, soaps, de-greasers, spot removers	0	25	19.6	23.2	1.79	14.3	16.1	0
arts and crafts: arts and crafts paint	-	0	50	0	50	0	0	0	0
personal care: deodorant	-	0	22.4	44.9	30.6	2.04	0	0	0
automotive_care	Related to the maintenance and repair of automobiles, products for cleaning and caring for automobiles (auto shampoo, polish/wax, undercarriage treatment, brake grease)	0	22.9	18.8	20.8	4.17	16.7	16.7	0

Physical and chemical properties of the alkanes are presented in Table 1.9. As molecular weight increase, the boiling points and vapor pressures of the alkanes increase and decrease, respectively with ethane identified as the most and n-undecane as the least volatile species. As the carbon chain length increases, the likelihood of partitioning into organic phases in the landfill environment increases significantly. Water solubility generally decreases from small to long chain lengths, which can be expected as these chemicals become more non-polar and hydrophobic with ethane identified as the most and n-undecane as the least soluble species.

Table 1.9 – Physical and Chemical Properties of the Alkanes

Chemical Species	Mol. Weight (g/mol)	Boiling Point (°C)	Log_{10} (Vapor Pressure)	Log_{10} (Octanol-Air)	Log_{10} (Dim. Henry's Constant)	Water Solubility (mg/L)	Log_{10} (Octanol-Water)
Ethane	30.1	-88.5	4.50	0.42	-0.16	60	1.81
Propane	44.1	-42.2	3.85	0.97	-0.12	63	2.36
i-Butane	58.1	-11.7	3.42	2.00	-0.06	49	2.76
n-Butane	58.1	-2.19	3.26	1.53	-0.04	61	2.89
i-Pentane	72.2	28.6	2.84	2.26	0.06	49	2.99
n-Pentane	72.2	35.9	2.71	1.96	0.39	38	3.39
n-Hexane	86.2	68.6	2.18	2.40	-0.02	9	3.90
n-Undecane	156.3	196	-0.39	5.01	-0.54	0.004	6.06

1.5.7 Alkenes

The alkenes included in this investigation consist of the individual chemical species: ethene, propene, 1-butene, i-butene, trans-2-butene, cis-2-butene, 1-pentene, and isoprene. Comparison of the MIR values indicated that the alkenes are more active in ozone production than the alkanes, in which some chemical species also actively participate in SOA formation (ethene and isoprene) (Table 1.1). Similar to the alkanes, due to their active roles in ozone formation, several alkenes indirectly affect climate change, including ethene, propene, and isoprene. None of the alkenes are recognized hazardous air pollutants as determined by the USEPA (Table 1.1).

The alkenes included in this investigation are acyclic compounds (straight chain and branched) with at least one double bond (unsaturated with respect to hydrogen atoms) (Vollhardt and Schore 1999). For butene, several structural isomers are included and differentiated as iso, trans and cis species. The iso-butene structural isomer has a branched molecular structure, whereas the 1-butene configuration is a straight chain. In the trans isomer, the functional groups reside on opposite sides of the double bond (vertically) and in the cis isomer, the functional groups reside on the same sides of the double bond (vertically) (Vollhardt and Schore 1999). As alkenes are hydrocarbons, major sources identified by Duan et al. (2014) for alkanes also are relevant for the alkene chemical family and include food packaging materials, cooking oils and fuels, as well as paper materials. As presented in the previous section, ethene production in soils (by aerobic bacteria) and from vegetation is a well-known phenomenon and has been postulated to occur in landfill cover soils (Ikeguchi and Watanabe 1991). Production of isobutene and isoprene from bacteria in aerobic environments has also been

documented in the scientific literature (Wilson et al. 2018). Therefore, it is likely that both abiotic and biotic production of alkenes occur in landfill systems.

Analysis of the top fifteen functional use categories based on the CPCat database indicated few categories related to personal use items for the alkenes (Table 1.10). Pesticides, lubricants, adhesives, and paints are the significant functional use categories identified for the alkenes. Fuels, plastics, and food packaging related functional use categories also apply to alkenes. Alkenes also are present in products used in the manufacturing of chemicals, oils, raw materials, and rubber. Ethene and iso-butene are the chemical species that are associated with the greatest number of products under the top fifteen functional use categories (Table 1.10). Ethene is present in products under the lubricants, consumer use products, fuels/fuel additives, plastics and filler functional use categories. Iso-butene is present in rubber manufacturing, pesticides, plastics, and food packaging functional use categories. The cis and trans butene isomers, and 1-pentene are not associated with products under many of the functional use categories prioritized in Table 1.10. Propene is present in products related to lubrication and isoprene in products related to the manufacturing of plastic materials.

Table 1.10 – Fifteen Most Common Functional Use Categories for Alkenes

CPCat Functional Use Category	Definition	Relative Contribution to Each Functional Use Category (%)							
		Ethene	Propene	1-Butene	i-Butene	trans-2-Butene	cis-2-Butene	1-Pentene	Isoprene
pesticide	Substances used for preventing, destroying or mitigating pests	11.1	16.7	16.7	33.3	11.1	11.1	0	0
fuel	General fuels, fuel additives, motor/automotive fuels	35.3	17.6	17.6	11.8	0	0	0	17.6
manufacturing:chemical	Manufacturing of a given chemical	11.8	17.6	17.6	23.5	11.8	5.88	0	11.8
manufacturing:oil	Manufacturing of crude oil, crude petroleum, refined oil products, fuel oils, drilling oils	18.2	18.2	9.09	18.2	18.2	0	9.09	9.09
consumer_use	Consumer product, unspecific	45.5	9.09	9.09	18.2	0	0	0	18.2
manufacturing:plastics	Manufacturing of plastic materials	30	0	10	30	0	0	0	30
adhesive	General adhesive/binding agents	20	30	20	10	10	10	0	0
chemical:laboratory	Chemical use designated in laboratory	10	20	20	10	10	10	0	20
manufacturing:raw_material	Raw materials used in manufacturing of a variety of products in different industries	30	10	10	20	0	10	0	20
manufacturing:rubber	Manufacturing of rubbers (rubber additives)	11.1	11.1	11.1	66.7	0	0	0	0
lubricant	Generic lubricants, lubricants for engines, brake fluids, oils, etc. (does not include personal care lubricants)	66.7	33.3	0	0	0	0	0	0
paint	Various types of paint for various uses, modifiers included when more information is known	25	25	25	12.5	0	0	0	12.5
plastics	Plastic products, industry for plastics, manufacturing of plastics, plastic additives (modifiers included when known)	28.6	14.3	0	28.6	0	0	0	28.6
filler	Fillers for paints, textiles, plastics, etc.	28.6	14.3	14.3	14.3	0	0	14.3	14.3
food_contact	Includes food packaging, paper plates, cutlery, small appliances such as roasters, etc.; does not include facilities that manufacture food	11.1	16.7	16.7	33.3	11.1	11.1	0	0

Physical and chemical properties of the alkenes are presented in Table 1.11. Similar to the alkanes, as the number of carbons in the hydrocarbon chain increases, the boiling point and the vapor pressure increases with ethane identified as the most and isoprene as the least volatile species. Both the octanol-air and octanol-water partition coefficients increase as the chain length increases, indicating that alkene species containing more carbon atoms are more likely to partition into the organic phases in the landfill environment. Differences in water solubility are counterintuitive and with increasing solubility from shorter chain to longer chain alkene chemical species. Solubility may be altered due to different structural conformations, where at least four different structural isomers are included for butene. The low dimensionless Henry's Constants of similar order of magnitude among the alkene species indicate high affinity for the air phase over the aqueous phase for all of the alkene chemical species (Table 1.11).

Table 1.11 – Physical and Chemical Properties of the Alkenes

Chemical Species	Mol. Weight (g/mol)	Boiling Point (°C)	Log_{10} (Vapor Pressure)	Log_{10} (Octanol-Air)	Log_{10} (Dim. Henry's Constant)	Water Solubility (mg/L)	Log_{10} (Octanol-Water)
Ethene	28.05	-104	4.72	0.28	-0.35	131	1.13
Propene	42.08	-47.9	3.94	1.60	-0.41	200	1.77
1-Butene	56.11	-6.3	3.35	2.28	-0.34	221	2.40
i-Butene	56.11	-6.93	3.36	2.28	-0.37	263	2.34
trans-2-butene	56.11	1.42	3.16	2.29	-0.35	578	2.33
cis-2-butene	56.11	2.98	3.17	2.29	-0.35	578	2.33
1-Pentene	70.13	30.2	2.80	1.93	-0.39	148	2.82
Isoprene	68.12	34.3	2.74	2.06	-0.71	636	2.42

1.5.8 Aldehydes/Alkynes

The aldehydes/alkynes included in this investigation consist of the individual chemical species: ethyne, acetaldehyde, and butanal. The aldehydes including acetaldehyde and butanal are significant precursors in tropospheric ozone formation and have high reported MIR values (Table 1.1). An indirect GWP value has been reported for acetaldehyde, indicating potential effects of acetaldehyde on atmospheric chemistry. While aldehydes and alkynes potentially participate as precursors in SOA formation, a FAC value has not been commonly reported for these chemicals. In addition, acetaldehyde has been designated as a hazardous air pollutant by the USEPA (Table 1.1).

Aldehydes are formed from a centralized carbonyl group (carbon atom double bounded to an oxygen atom) that is singly bonded to a hydrogen atom on one side and a variable hydrocarbon chain or functional group on the opposing side. Alkynes are generally straight or branched chain hydrocarbons in which one carbon to carbon bond consists of a triple bond. The potential sources of aldehydes and alkynes in the landfill environment are both abiotically and biotically generated. Potential sources of acetaldehydes in landfills are furniture, cooking charcoals, and textiles, with no chemical sources identified for the alkyne chemical family (Nair et al. 2019). Most oxygenated compounds, including the aldehydes, were indicated to be derived from anaerobic decomposition of food or green wastes in the landfill environment (Duan et al. 2014).

During acidogenesis (the acid phase of LFG production), volatile fatty acids (including carboxylic acids) are produced by fermentative bacteria. Under similar environmental conditions, these volatile fatty acids are building blocks for the anaerobic bacterial synthesis of various organic compounds including aldehydes (Eggeman and Verser, 2005, Singhania et al. 2013). Bacteria also form aldehydes via the oxidation of aliphatic (alkane) hydrocarbons at the methylene carbon alpha to the methyl group (McKenna et al. 1965, Forney and Markovetz 1971, Klug and Markov 1971). Biogenic sources of aldehydes also include emissions from vegetation including plants growing on the cover surface or from decaying green waste materials used as covers or disposed of in a landfill.

Analysis of the top fifteen functional use categories based on the CPCat database indicated that aldehyde containing products are generated in manufacturing operations for chemicals, metals, machines, plastics, raw materials, paints, and paper (Table 1.12). Products related to printing (inks), drugs, and food related additives also are potential sources of the aldehydes. Among the three species within this chemical family, acetaldehyde is present in most of the functional use categories including paints, adhesives, food additives, manufacturing of plastics, printing, and automotive related products. Ethyne is classified as an alkyne with different functional use categories from the aldehydes including metal manufacturing, drugs, plastics, and raw materials (Table 1.12). Butanal is commonly present in paint and the manufacturing of raw materials.

Table 1.12 – Fifteen Most Common Functional Use Categories for Aldehydes/Alkynes

CPCat Functional Use Category	Definition	Relative Contribution to Each Functional Use Category (%)		
		Ethyne	Acetaldehyde	Butanal
manufacturing:chemical	Manufacturing of chemicals	18.8	43.8	37.5
manufacturing:metals	Manufacturing of metals	37.5	25	37.5
paint	Various types of paint for various uses, modifiers included when more information is known	0	53.8	46.2
manufacturing:food	Manufacturing of food for human consumption, does not include food additives (see food_additive)	0	100	0
manufacturing:machines	Manufacturing of machinery related to production of different products	20	40	40
adhesive	General adhesive/binding agents	0	77.8	22.2
food_additive:flavor	Includes spices, extracts, colorings, flavors, etc. added to food for human consumption	0	66.7	33.3
manufacturing:plastics	Manufacturing of plastic materials	14.3	71.4	14.3

CPCat Functional Use Category	Definition	Relative Contribution to Each Functional Use Category (%)		
		Ethyne	Acetaldehyde	Butanal
manufacturing:raw_material	Raw materials used in manufacturing of a variety of products in different industries	14.3	42.9	42.9
printing	Related to the process of printing (newspapers, books media, etc.), printing inks, toners, etc.	0	100	0
building_construction	Related to the building or construction process for buildings or boats (includes activities such as plumbing and electrical work, bricklaying, etc.)	0	80	20
drug	Drug product, or related to the manufacturing of drugs; modified by veterinary, animal, or pet if indicated by source	20	80	0
manufacturing:paint	Manufacturing of paint materials	0	80	20
manufacturing:paper	Manufacturing of paper materials	20	80	0
automotive	Related to automobiles or their manufacture	0	100	0

Physical and chemical properties of the aldehydes/alkynes are presented in Table 1.13. Ethyne and butanal have the lowest and highest molecular weights, respectively. Boiling points and vapor pressures follow the trends in molecular weights, where ethyne and butanal are the most and least volatile chemical species, respectively. Acetaldehyde has the highest water solubility, followed by ethyne and butanal. Butanal is the chemical species most likely to partition into organic phases in the landfill environment due to the high octanol-air and octanol-water coefficients (Table 1.13).

Table 1.13 – Physical and Chemical Properties of the Aldehydes/Alkynes

Chemical Species	Mol. Weight (g/mol)	Boiling Point (°C)	Log_{10} (Vapor Pressure)	Log_{10} (Octanol-Air)	Log_{10} (Dim. Henry's Constant)	Water Solubility (mg/L)	Log_{10} (Octanol-Water)
Ethyne	26.0	-84.3	4.56	0.44	-2.27	1200	0.37
Acetaldehyde	44.1	20.5	2.96	1.79	-3.88	999935	-0.34
Butanal	72.1	75.1	2.05	3.39	-3.65	71028	0.88

1.5.9 Aromatic Hydrocarbons

The aromatic hydrocarbons included in this investigation consist of the individual chemical species: benzene, toluene, ethylbenzne, m/p/o-Xylene, i/n-propylbenzene, 2/3/4-ethyltoluene, as well as 1,3,5-, 1,2,3-, and 1,2,4-trimethylbenzene. Aromatics contribute to tropospheric ozone and secondary aerosol formation (Table 1.1). For ozone formation, trimethyl benzenes are the most reactive compounds with MIR values up to 11.66 g O_3/g VOC. Secondary aerosol formation potentials based on the FAC are highest for the ethyltoluenes (M and O). Benzene, toluene, ethylbenzene, and the

Xylene isomers (collectively termed BTEX) are known human carcinogens that are acutely toxic and are designated as hazardous air pollutants by the USEPA. Toluene is the only species in this chemical family with atmospheric impacts (indirect GWP of 2.7). While the reactivities of other benzene derivatives indicate potential atmospheric effects, GWP values have not been reported for these chemicals (Table 1.1).

Aromatic compounds are unsaturated (alternating single/double bonds) chemical compounds in which the carbon atoms (6) are joined in a hexagonal ring arrangement. The ring-like structure provides chemical stability. These species are not easily broken down or transformed due to physical, chemical, or biological reactions occurring in the landfill environment (Vollhardt and Schore 1999). Benzene is the most commonly used aromatic. Benzene derivatives are formed through substitution or attachment of different functional groups located at various positions of the ring structure. For example, the Xylene isomers differ in the arrangement of the methyl groups attached to the ring structure. Similarly, for ethylbenzene, different isomers vary in the arrangement of the ethyl groups attached to the ring structure.

Similar to the halogenated hydrocarbons, the aromatic hydrocarbons are often termed xenobiotic compounds in that they originate from abiotic sources in the landfill environment. Potential sources of aromatics include household cleaning solvents, personal care products, household spray applications, paints, textiles, cooking fuels, and furniture Nair et al. (2019). Additional potential sources are food packaging and containers and paints (Liu et al. 2016). The ratios of BTEX concentrations (benzene and toluene specifically) in landfill gas have been compared to concentrations in the atmosphere of urban environments to identify different emission sources (Liu et al. 2016). Ratio of benzene to toluene of approximately 0.5 indicate vehicular emissions in the urban environment, with lower values reported for the landfill environment (Liu et al. 2016).

Analysis of the top fifteen functional use categories based on the CPCat database indicate that household and automotive paint products are a potential source of the aromatic hydrocarbons in the landfill environment, (Table 1.14). Solvents, adhesives, manufacturing of plastics, cleaning/washing, and building/construction related materials also are functional use categories for the aromatic hydrocarbons. Toluene, ethylbenzene, and benzene are the three species present in the highest number of products (Table 1.14). Toluene and ethylbenzene are mostly in paint product functional use categories, whereas benzene is in cleaning and washing products and products used in manufacturing of metals and machinery. Trimethyl benzene derivatives are mainly present in paint materials, solvents, and building/construction materials. The remaining chemical species (xylene isomers, propylbenzene, and ethylbenzene derivatives) are present to a lesser extent in products under the top fifteen functional use categories (Table 1.14).

Table 1.14 – Fifteen Most Common Functional Use Categories for Aromatic Hydrocarbons

CPCat Functional Use Category	Definition	Relative Contribution to Each Functional Use Category (%)													
		Benzene	Toluene	Ethylbenzene	m-Xylene	p-Xylene	o-Xylene	i-Propylbenzene	n-Propylbenzene	3-Ethyltoluene	4-Ethyltoluene	2-Ethyltoluene	1,3,5-Trimethylbenzene	1,2,3-Trimethylbenzene	1,2,4-Trimethylbenzene
home maintenance: paint	-	0	44	44	0.5	0	0	0	0	0	0	0	0	0	11
paint	Various types of paint	10	17	15	4.2	4.2	5.5	6.7	9.1	0	1.8	0	12	1.8	12
manufacturing:metal	Manufacturing of metals	21	18	8	1.5	1.5	2.2	8.1	8.1	0	0	0	11	2.2	8.8
manufacturing:mach.	Manufacturing of machinery related to production of different products	23	18	16	1.9	1.9	6.5	7.5	5.6	0	0	0	9.4	0	10
arts and crafts: arts and crafts paint	-	0	26	51	0.9	0	0	0	0	0	0	0	0	0	22
surface treatment	Surface treatments for metals, corrosion inhibitors, etc.	16	20	16	4	0	5.1	5.1	7.1	0	0	0	12	3	11
adhesive	Adhesive/ binding agents	19	25	17	1.3	2.7	5.3	9.3	2.7	0	0	0	8	1.3	8

CPCat Functional Use Category	Definition	Relative Contribution to Each Functional Use Category (%)													
		Benzene	Toluene	Ethylbenzene	m-Xylene	p-Xylene	o-Xylene	i-Propylbenzene	n-Propylbenzene	3-Ethyltoluene	4-Ethyltoluene	2-Ethyltoluene	1,3,5-Trimethylbenzene	1,2,3-Trimethylbenzene	1,2,4-Trimethylbenzene
solvent	Paint/graffiti removers, general solvents	13	16	13	2.8	2.8	5.6	9.9	9.9	0	0	0	13	2.8	13
paint:volatile_ organic	-	10	15	13	0	0	4.4	12	12	0	0	0	15	4.4	15
auto products: auto paint	-	2	48	42	0	0	0	0	0	0	0	0	0	0	7.8
manufacturing: plastics	Manufacturing plastic materials	17	25	19	0	1.6	3.1	11	6.3	0	0	0	7.8	0	9.4
building construction	Related to the building or construction process for buildings or boats	16	15	13	6.5	6.5	6.5	8.1	9.7	0	0	0	9.7	0	9.7
manufacturing: chemical	Manufacturing of chemicals	17	22	12	5.1	5.1	5.1	5.1	3.4	0	1.7	0	8.5	3.4	12

CPCat Functional Use Category	Definition	Relative Contribution to Each Functional Use Category (%)													
		Benzene	Toluene	Ethylbenzene	m-Xylene	p-Xylene	o-Xylene	i-Propylbenzene	n-Propylbenzene	3-Ethyltoluene	4-Ethyltoluene	2-Ethyltoluene	1,3,5-Trimethylbenzene	1,2,3-Trimethylbenzene	1,2,4-Trimethylbenzene
cleaning_ washing	Related to all forms of cleaning/washing including detergents, soaps, de-greasers, spot removers	20	18	14	1.8	3.6	3.6	8.9	7.1	0	0	0	11	0	13
fuel	General fuels, fuel additives, motor/automotive fuels	16	18	13	1.8	1.8	5.4	8.9	5.4	0	0	0	11	3.6	16

Physical and chemical properties of the aromatic compounds are presented in Table 1.15. Benzene has the lowest molecular weight and thee benzene derivatives and isomers have similar molecular weights. The boiling points and vapor pressures increase and decrease, respectively as the number of substituted carbon/hydrogen functional groups increase (Table 1.15). For example, benzene has the lowest boiling point and the highest vapor pressure, whereas the trimethylbenzene groups (with 3 additional functional groups) have higher boiling points and lower vapor pressures. The hydrophobicity, as indicated by the water solubility and octanol-water partition coefficients, increase from benzene to derivatives with increasing carbon/hydrogen atom contents. Thus, the trimethyl benzenes and ethyltoluene derivatives are more likely than benzene and toluene to partition into organic phases in the landfill environment.

Table 1.15 – Physical and Chemical Properties of the Aromatic Hydrocarbons

Chemical Species	Mol. Weight (g/mol)	Boiling Point (°C)	Log_{10} (Vapor Pressure)	Log_{10} (Octanol-Air)	Log_{10} (Dim. Henry's Constant)	Water Solubility (mg/L)	Log_{10} (Octanol-Water)
Benzene	78.1	80	1.98	2.78	-1.96	1789	2.13
Toluene	92.1	111	1.45	3.31	-1.88	526	2.73
Ethylbenzene	106.2	136	0.98	3.74	-1.81	169	3.15
m-Xylene	106.2	139	0.92	3.78	-1.85	161	3.20
p-Xylene	106.2	138	0.95	3.79	-1.87	162	3.15
o-Xylene	106.2	144	0.82	3.91	-1.99	178	3.12
i-Propylbenzene	120.2	152	0.65	3.98	-1.65	61	3.66
n-Propylbenzene	120.2	159	0.53	4.09	-1.68	52	3.71
3-Ethyltoluene	120.2	160	0.48	4.56	-1.79	81	3.98
4-Ethyltoluene	120.2	162	0.48	4.56	-1.78	95	3.63
2-Ethyltoluene	120.2	165	0.42	4.56	-1.81	75	3.53
1,3,5-Trimethylbenzene	120.2	164	0.39	4.54	-1.76	48	3.42
1,2,3-Trimethylbenzene	120.2	176	0.23	4.54	-2.07	75	3.66
1,2,4-Trimethylbenzene	120.2	169	0.32	4.54	-1.92	57	3.63

1.5.10 Monoterpenes

The monoterpenes included in this investigation consist of the individual chemical species: alpha-pinene, beta-pinene, and limonene. The monoterpenes contribute to both ozone and secondary aerosol formation. These chemicals have very short atmospheric lifetimes (on the order of minutes) compared to the other NMVOC chemical families included in this study (Kesselmeier and Staudt 1999). Alpha- and beta-pinene have the highest SOA formation potentials of all of the chemicals included in this investigation (Table 1.1). The monoterpenes are not considered hazardous air pollutants. GWP values have not been assigned to these chemicals, even though the species indirectly contribute to ozone, carbon monoxide, and methane formation in the atmosphere (Perring et al. 2013).

Both isoprene (included under alkenes) and monoterpenes are isoprenoids (terpenoids) with carbon skeletons composed of 5 carbon atoms (termed a unit) that can be arranged in an acyclic, mono-, bi-, or tri- cyclic molecular structure (Kesselmeier and Staudt 1999). The number of carbon units allows terpenes to be classified as either monoterpenes (one unit), di (two units), tri (three units), tetra (four units), or even poly terpenes (> four units), in which the monoterpenes are generally the most volatile out of the existing terpene chemicals. Terpenes generally have strong smells, are not highly water soluble, and ubiquitous in plants, animals, and microorganisms (Kesselmeier and Staudt 1999). Monoterpenes are generated biogenically by plant matter including trees and vegetation. A summary of specific vegetative release characteristics for monoterpenes is provided in Kesselmeier and Staudt (1999).

Monoterpenes also are present in a variety of household consumer products and thus can be released abiotically in the landfill environment. Potential monoterpene sources are household cleaning solvents, personal care products (body wash/air fresheners), and household spray products (Nair et al. 2019). Limonene can be emitted during decomposition of MSW, specifically associated with food wastes (Duan et al. 2014) and may appear as an intermediate byproduct during aerobic oxidation of various compounds (Eitzer 1995, Duan et al. 2014). High concentrations of limonene were reported for LFG in Chinese landfills and attributed to fragrant household detergent and air freshener sources over volatilization from green wastes or emissions from aerobic or anaerobic waste degradation (Duan et al. 2014).

Analysis of the top fifteen functional use categories based on the CPCat database indicate that many of the potential abiotic sources of monoterpenes in the landfill environment are associated with personal hair products (shampoos and conditioners), fragrances, hair styling, air fresheners, deodorants, moisturizers, lotions, hair sprays and color products (Table 1.16). Of the monoterpenes included in this investigation, limonene is present in the highest number of products across all of the functional use categories, with nearly 100% contributions to the functional use categories related to hair styling, shampoos, conditioners, lotions, and moisturizers. Both alpha- and beta-pinene have less presence in the top fifteen functional use categories with presence in cleaning/washing, industrial cleaning/washing, paints, and air fresheners (Table 1.16).

Table 1.16 – Fifteen Most Common Functional Use Categories for Monoterpenes

CPCat Functional Use Category	Definition	Relative Contribution to Each Functional Use Category (%)		
		alpha-Pinene	beta-Pinene	Limonene
personal care: fragrance	-	0	2.22	97.8
personal care: hair styling	-	0	0	100
personal care: shampoo	-	0	0	100

CPCat Functional Use Category	Definition	Relative Contribution to Each Functional Use Category (%)		
		alpha-Pinene	beta-Pinene	Limonene
personal care: hair conditioner	-	0	0	100
inside the home: air freshener	-	0	26	74
personal care: deodorant	-	0	0	100
personal care: face cream/moisturizer	-	0	0	100
personal care: hand/body lotion	-	0	0	100
personal care: hair color	-	0	0	100
cleaning_washing	Related to all consumer forms of cleaning/washing including detergents, soaps, de-greasers, spot removers	25.8	25.8	48.4
personal care: hair spray	-	0	0	100
personal care: hair conditioning treatment	-	0	0	100
industrial:cleaning_washing	Related to all industrial forms of cleaning/washing including detergents, soaps, de-greasers, spot removers	34.8	30.4	34.8
paint	Various types of paint	27.3	13.6	59.1
personal care: body wash	-	0	0	100

Physical and chemical properties of the monoterpenes are presented in Table 1.17. The monoterpenes generally have high volatility (high vapor pressures) and low water solubilities. Alpha-pinene has the highest volatility and the lowest water solubility. All three chemicals in this chemical family are likely to partition into the organic phase in the landfill environment.

Table 1.17 – Physical and Chemical Properties of the Monoterpenes

Chemical Species	Mol. Weight (g/mol)	Boiling Point (°C)	Log_{10} (Vapor Pressure)	Log_{10} (Octanol-Air)	Log_{10} (Dim. Henry's Constant)	Water Solubility (mg/L)	Log_{10} (Octanol-Water)
alpha-Pinene	136.2	155	0.68	4.44	-0.58	2	4.83
beta-Pinene	136.2	165	0.47	4.48	-0.72	8	4.16
Limonene	136.2	175	0.19	4.31	-1.21	11	4.57

1.5.11 Alcohols

The alcohols included in this investigation consist of the individual chemical species: methanol, ethanol, isopropanol, and 2-butanol. The alcohols are relatively reactive compounds in the troposphere, based on the MIR values presented in Table 1.1.

However, these chemical species do not contribute to SOA formation and FAC values have not been reported in the literature. Within this chemical family, only methanol has an assigned GWP. The remaining alcohols are expected to have adverse climate change impacts due to their effects in various atmospheric reactions. However, GWP values have not been reported for these chemicals at the present time. Methanol is considered a hazardous air pollutant by the USEPA.

Alcohols are hydrocarbons (composed of carbon and hydrogen atoms) attached to one or more hydroxyl (OH) groups, where the number of carbon atoms and placement of the hydroxyl group varies with the chemical species (Vollhardt and Schore 1999). Alcohols can be generated both abiotically and biotically in the landfill environment from various sources. Alcohols, similar to monoterpenes, are emitted naturally by vegetation, where emissions likely vary from live plants on the cover soil to green wastes used as covers or disposed of within the waste mass (Kesselmeier and Staudt 1999). Similar to the aldehydes, alcohols are also formed indirectly from carboxylic acids that are produced during acidogenesis (the acid phase) in the anaerobic portions of the waste mass (Barlaz et al. 2010). Some alcohols (including ethanol) are direct products of anaerobic fermentation that occurs during the acid phase of anaerobic waste decomposition (Barlaz et al. 2010). Bacteria also form alcohols via the oxidation of aliphatic (alkane) hydrocarbons by directing their attack between the methylene carbon alpha to the methyl group (McKenna et al. 1965, Forney and Markovetz 1971, Klug and Markov 1971). With these biogenic generation pathways, which occur during preliminary stages of anaerobic waste decomposition, alcohols are associated with fresh as opposed to old waste materials (Allen et al. 1997).

Potential abiotic sources of alcohols in the landfill environment include household cleaning solvents, personal care products, and household spray products (Nair et al. 2019). Analysis of the top fifteen functional use categories based on the CPCat database indicate that many alcohols are present in personal care products such as fragrances, nail polish, hair spray, hair color, shampoo/conditioner, hair styling products, sunscreen, moisturizers, and air fresheners (Table 1.18). Alcohols also are present in laundry detergents, paints, pesticides, and cleaning/washing solvents (Table 1.18). Of the alcohols included in this investigation, ethanol and isopropanol are present in the highest number of products across the functional use categories. Fragrances, hair sprays, hair styling products, hair conditioners, moisturizers, sunscreen, laundry detergents, and air fresheners contain ethanol. Isopropanol is present in nail polish, hair coloring, surface treatments, paints, cleaning/washing materials, and hair conditioners (Table 1.18). The remaining species, methanol and 2-butanol, are least represented under the top 15 functional use categories, where methanol is present in products related to metal manufacturing, surface treatments and paint, whereas 2-butanol is present in paints and cleaning/washing solvent materials.

Table 1.18 – Fifteen Most Common Functional Use Categories for Alcohols

CPCat Functional Use Category	Definition	Relative Contribution to Each Functional Use Category (%)			
		Methanol	Ethanol	Isopropanol	2-Butanol
personal care: fragrance	-	0	99.5	0.48	0
personal care: nail polish	-	0	16.5	83.5	0
personal care: hair spray	-	0	99	0.98	0
personal care: hair color	-	0	6.88	93.1	0
personal care: hair styling	-	0	92.3	7.74	0
inside the home: laundry detergent	-	0	99	1.01	0
manufacturing:metals	Manufacturing of metals	30.1	30.1	33.3	6.45
surface_treatment	Surface treatments for metals, corrosion inhibitors, etc.	29.9	24.1	39.1	6.9
paint	Various types of paint	26.5	27.7	28.9	16.9
personal care: sunscreen	-	0	100	0	0
personal care: face cream/moisturizer	-	0	96.1	3.95	0
pesticide	Substances used for preventing, destroying or mitigating pests	11.1	45.8	41.7	1.39
inside the home: air freshener	-	0	77.5	22.5	0
cleaning_washing	Related to all consumer forms of cleaning/washing including detergents, soaps, de-greasers, spot removers	24.3	30	34.3	11.4
personal care: hair conditioner	-	0	40.3	59.7	0

Physical and chemical properties of the alcohols are presented in Table 1.19. As molecular weights increase from methanol to 2-butanol with increasing number of carbon atoms, the boiling point increases and corresponding vapor pressure decreases. Methanol and 2-butanol are the most and least, respectively volatile alcohols included in this study. Water solubility is relatively similar among the four alcohol species. The likelihood to partition into organic phases in the landfill environment is higher for 2-butanol, which is the most hydrophobic alcohol species based on the high octanol-air and octanol-water partition coefficients.

Table 1.19 – Summary of Relevant Physical and Chemical Properties for the Alcohols

Chemical Species	Mol. Weight (g/mol)	Boiling Point (°C)	Log_{10} (Vapor Pressure)	Log_{10} (Octanol-Air)	Log_{10} (Dim. Henry's Constant)	Water Solubility (mg/L)	Log_{10} (Octanol-Water)
Methanol	32.0	64.5	2.10	2.88	-5.05	999648	-0.77
Ethanol	46.1	78.4	1.77	3.25	-5.01	999719	-0.31
Isopropanol	60.1	82.5	1.66	3.41	-4.80	997660	0.05
2-Butanol	74.1	99.2	1.26	3.85	-4.75	180853	0.61

1.5.12 Ketones

The ketones included in this investigation consist of the individual chemical species: acetone, butanone, and methylisobutylketone. Similar to the aldehydes, the ketones are relatively reactive oxygenated chemical species that readily produce ozone in the troposphere. Among ketones, methylisobutylketone has the highest contribution to ozone production in the troposphere. Ketones are not identified to contribute to SOA formation. However, previous studies indicate potential implications in SOA formation (Perring et al. 2013). Ketones are expected to have adverse climate change impacts due to their effects in various atmospheric reactions. However, GWP values have not been reported for these chemicals at the present time. Methylisobutylketone is considered a hazardous air pollutant by the USEPA (Table 1.1).

Ketones are formed from a centralized carbonyl group (carbon atom double bonded to an oxygen atom) that is singly bonded to a variable hydrocarbon chain or functional group on both sides of the carbonyl group (Vollhardt and Schore 1999). Ketones range from straight chained to branched in configuration (acyclic) with high variation in the functional groups or number of carbons contained in each hydrocarbon chain. Similar to the aldehyde and alcohol chemical families, ketones are generated abiotically and biotically in the landfill environment. Biogenic sources of ketones include emissions from vegetation (similar to monoterpenes aldehydes/alkynes and alcohols) including plants growing on the cover surface or from decaying green waste materials used as covers or disposed of in a landfill. Additional biogenic sources of ketones in the landfill environment include generation from carboxylic and other volatile fatty acids during the acidogenesis phase of anaerobic waste decomposition (Barlaz et al. 2010). Ketones are also potentially produced by fungi through decarboxylation of beta-keto fatty acids and in similarity to alcohols and aldehydes, bacteria also form ketones through oxidation of aliphatic (alkane) hydrocarbons at the methylene carbon alpha to the methyl group (Leadbetter and Foster 1959, Forney and Markovetz 1971). For example, acetone is produced by butyric acid bacteria as a product of butyl alcohol fermentation and further decarboxylation of acetoacetate (Forney and Markovetz 1971). Even though these particular biogenic pathways have not been documented in the landfill environment, these processes are likely for the synthesis of ketones under aerobic and anaerobic conditions present in MSW landfills.

Abiotic production of ketones in the landfill environment is based on volatilization of chemical materials present in the MSW. Potential chemical sources of ketones in the landfill environment are household spray products (Nair et al. 2019). Analysis of the top

fifteen functional use categories based on the CPCat database indicates that ketones are present in paints, adhesives, cleaning/washing materials, and solvents. In addition, ketones are present in products associated with manufacturing of chemicals, plastics, and machinery as well as building/construction functional use categories (Table 1.20). Acetone is the chemical species that is present in the highest number of products within the top 15 functional use categories, followed by butanone and methylisobutylketone. Acetone is common in paints (auto and home), surface treatment products, and nail polish removers. Butanone is present in paints, products used in manufacturing of metal and plastic materials, and cleaning/washing solvents. Methylisobutylketone is present in solvents, paints, products used in manufacturing applications, and building/construction materials (Table 1.20).

Table 1.20 – Fifteen Most Common Functional Use Categories for Ketones

CPCat Functional Use Category	Definition	Relative Contribution to Each Functional Use Category (%)		
		Acetone	Butanone	Methylisobutylketone
home maintenance: paint	-	70.5	13.5	16
auto products: auto paint	-	67.2	23	9.84
paint	Various types of paint	32.8	36.2	31
arts and crafts: arts and crafts paint	-	49.1	23.6	27.3
manufacturing:metals	Manufacturing of metals	32.7	36.5	30.8
adhesive	Adhesive/binding agents	37.5	37.5	25
manufacturing:machines	Manufacturing of machinery related to production of different products	34	36.2	29.8
surface_treatment	Surface treatments for metals, corrosion inhibitors, etc.	50	27.8	22.2
manufacturing:plastics	Manufacturing of plastic materials	33.3	45.5	21.2
cleaning_washing	Related to all consumer forms of cleaning/washing including detergents, soaps, de-greasers, spot removers	36.7	40	23.3
solvent	Paint/graffiti removers, general solvents	33.3	33.3	33.3
manufacturing:chemical	Manufacturing of chemicals	34.5	34.5	31
personal care: nail polish remover	-	100	0	0
paint:volatile_organic	-	35.7	32.1	32.1

CPCat Functional Use Category	Definition	Relative Contribution to Each Functional Use Category (%)		
		Acetone	Butanone	Methylisobutylketone
building_construction	Related to the building or construction process for buildings or boats	36	36	28

Physical and chemical properties of the ketones are presented in Table 1.21. Methylisobutylketone and acetone have the highest and lowest molecular weights, respectively, associated with the lowest and highest volatilities, respectively (based on boiling points and vapor pressures summarized in Table 1.21). Acetone is the ketone with the highest water solubility, whereas methylisobutylketone is the most hydrophobic chemical species. Similarly, methylisobutylketone is most likely to partition into the organic phase in the landfill environment based on the high octanol-air and octanol-water partition coefficients.

Table 1.21 – Physical and Chemical Properties of the Ketones

Chemical Species	Mol. Weight (g/mol)	Boiling Point (°C)	Log_{10} (Vapor Pressure)	Log_{10} (Octanol-Air)	Log_{10} (Dim. Henry's Constant)	Water Solubility (mg/L)	Log_{10} (Octanol-Water)
Acetone	58.1	56	2.37	2.31	-4.16	998976	-0.24
Butanone	70.1	79.7	1.96	2.71	-3.95	216578	0.29
Methylisobutyl-ketone	100.2	117	1.30	3.58	-0.43	19030	1.31

1.6 Landfill Gas Composition

Landfill gas is collected directly from the waste mass and directly represents the gas generated and/or transformed in the waste mass. The source gas composition can provide insight into attenuation processes occurring within the cover systems. A comprehensive review of LFG concentrations of methane, carbon dioxide, nitrous oxide, carbon monoxide, and the trace NMVOCs included in this investigation is provided based on a total of 34, 26, 2, 1, and 33 previously reported studies, respectively. Overall, data from a total of 1109, 497, 59, 8 and 9350 individual summa canister measurements were reviewed herein for methane, carbon dioxide, nitrous oxide, carbon monoxide, and NMVOCs, respectively. The complete summary for the reviewed studies is presented in Table A1 in Appendix A. The studies included were from a wide range of countries, climate zones, and landfill environments. Grab sampling via Summa canister

was used in a majority of the studies. Samples were analyzed by GC-MS typically with low analytical detection limits reported. Samples were taken either from gas headers, wells, or from custom built gas sampling ports that extended beneath the covers to some depth within the wastes. The geographic locations of the LFG composition studies were across multiple continents and included landfill sites in U.S., France, Finland, UK, Japan, Germany, Turkey, South Korea, Spain, Italy, China, and Australia. Four sites were reviewed in California, including Marina landfill, Scholl Canyon landfill, Potrero Hills landfill, and Yolo County landfill (Bogner et al. 2011, Saquing et al. 2014, Sohn 2016, Yesiller et al. 2018).

A summary of the LFG concentrations from literature for the gases included in the investigation is presented in Figure 1.2, organized by chemical family. Overall means and standard deviations for these distributions in LFG concentrations were calculated using the group contribution statistical method (Burton 2016). Methane, carbon dioxide, nitrous oxide, and carbon monoxide are plotted separately for comparison purposes. The diamonds indicate the mean of each distribution, the boxes indicate the 95% confidence intervals surrounding the mean values (assuming normal distributions). The whiskers indicate the maximum and minimum reported values of LFG concentration for each chemical family.

Figure 1.2 LFG Concentrations of Gas Chemical Families Obtained from the Literature

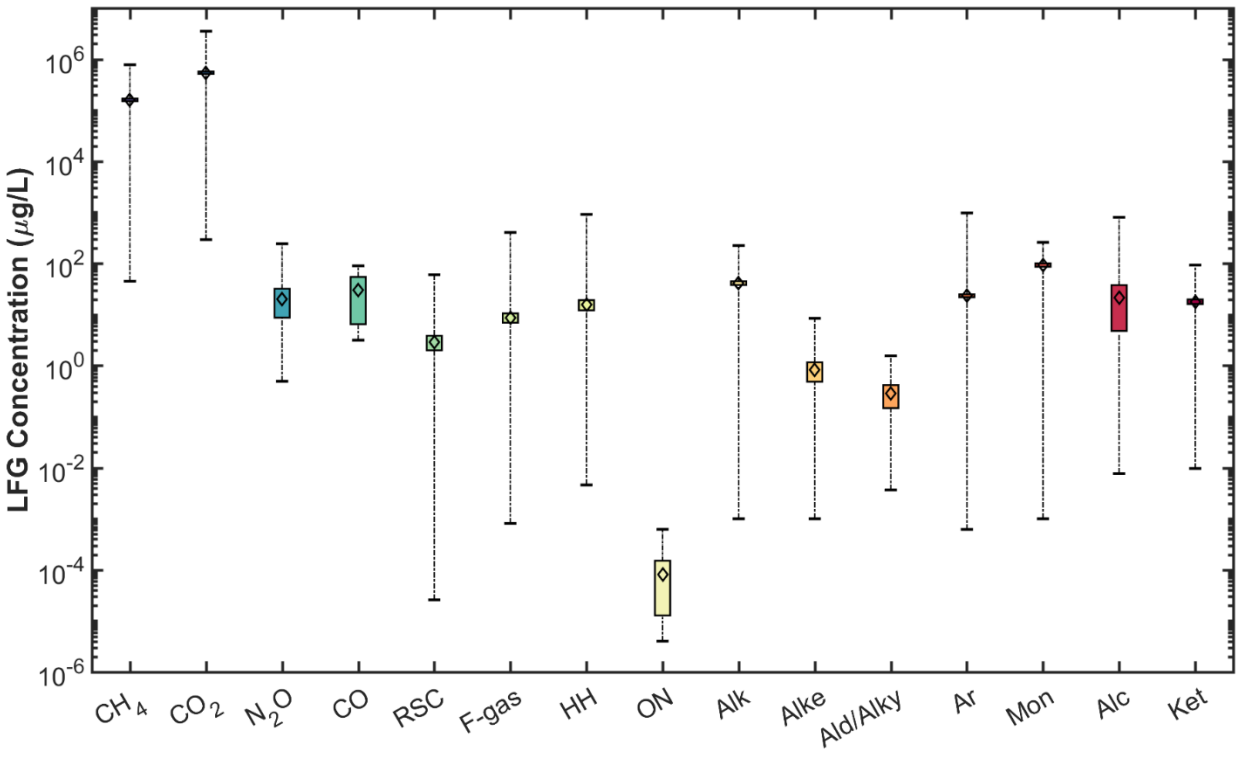

Methane and carbon dioxide were the dominant constituents of LFG across the studies summarized, where the mean values were slightly higher for carbon dioxide

concentrations (on the order of $1x10^6$ μg/L). Concentrations of methane and carbon dioxide in LFG ranged from $1x10^2$ to $1x10^6$ μg/L, or 4 orders of magnitude difference across the landfill sites investigated (Figure 1.2). Mean concentrations of nitrous oxide and carbon monoxide were somewhat higher than all NMVOC chemical families, where the variation was generally higher for carbon monoxide (based on the wide extent of the 95% confidence intervals). For NMVOCs, the monoterpene concentrations were the greatest out of all chemical families included in the analysis (Figure 1.2). Within this family, limonene had the greatest mean LFG concentration of approximately $1.60x10^2$ μg/L. The organic alkyl nitrates demonstrated the smallest mean LFG concentration of approximately $8.2x10^{-5}$ μg/L, while still being detected by GC-MS (Figure 1.2). The alkanes and the aromatics were the chemical families that ranked second and third behind the monoterpenes, with mean LFG concentrations of $4.14x10^1$ and $2.34x10^1$ μg/L, respectively. Within the alkane and aromatic chemical families, ethane and toluene were the individual chemical species that had the highest mean LFG concentrations. The variations in LFG concentrations, as indicated by the width of the boxplots, were generally higher for the alcohol chemical family. Most of the NMVOCs were distributed within a relatively broad range of LFG concentrations (8 orders of magnitude, ranging between $4x10^{-6}$ to $9.71x10^2$ μg/L). In comparison, the baseline GHG LFG concentrations were distributed over 7 orders of magnitude, ranging between $4.92x10^{-1}$ to $3.52x10^6$ μg/L. For a given chemical family, the highest variation in concentrations was 5 orders of magnitude (alcohol family) and the lowest variation was 1 order of magnitude (organic alkyl nitrate family).

1.7 Landfill Gas Surface Flux

An in-depth literature review was conducted on surface flux of the gas species included in this investigation. Data and analysis from studies conducted with the static flux chamber method were included in line with the methodology used in the current investigation. MSW landfill sites included in the review varied from open dumping sites (Malaysia, India) to properly engineered sanitary landfills (U.S., China, Europe). A comprehensive review of surface fluxes of methane, carbon dioxide, nitrous oxide, carbon monoxide, and the trace NMVOCs included in this investigation is provided based on a total of 91, 37, 18, 1, and 14 previously reported studies, respectively. Overall data from a total of 16193, 15613, 2444, 1, 5667 experimental measurements of landfill surface flux were reviewed herein for methane, carbon dioxide, nitrous oxide, carbon monoxide, and NMVOCs, respectively. The complete summary for the reviewed studies is presented in Table A2 in Appendix A. Data provided in Table A2 includes (when available) the location, climate zone, season, waste age, cover material soil index properties, presence of a gas extraction system, cover thickness, cover moisture content and temperature, estimated waste in place, cover category (daily, intermediate, final), air temperature, barometric pressure, and an overview of the waste composition with special emphasis placed on the fraction of organic wastes reported. Table A3 summarizes the overall distributions of methane, carbon dioxide, nitrous oxide, and NMVOC landfill gas surface fluxes from the studies reviewed.

High flux measurements were reported for landfills in Spain, U.S., Italy, China, and Germany. Analysis of the climate zone data indicated that the Csa (29%), Bwk (20.5%),

Cfa (10.5%), Cfb (9.8%), and Dfb (9.1%) zones (based on Koppen-Geiger climate system, Peel at al. (2007)) were dominant in the studies reviewed from the literature. The Csa climate zone was also investigated in the current study. Approximately half of the landfills studied (48%) did not have active gas extraction systems. Presence or absence of extraction systems were not identified in several studies. The types of cover systems tested (daily, intermediate, or final) were not identified in nearly half of the studies (47%) available in the literature. When identified, data were most commonly reported for final cover systems followed by intermediate covers with very limited data provided for daily covers. A large majority of these studies (>99%) were conducted using relatively small static flux chambers with smaller than 1 m^2 in areal coverage.

A summary of the LFG surface fluxes from literature for the gases included in the investigation is presented in Figures 1.3 and 1.4, organized by chemical family and cover category, respectively. Similar to Figure 1.2, overall means and standard deviations for these distributions in LFG concentrations were calculated using the group contribution statistical method (Burton 2016). Methane, carbon dioxide, nitrous oxide, and carbon monoxide are plotted separately for comparison purposes. The diamonds indicate the mean of each distribution, the boxes indicate the 95% confidence intervals surrounding the mean values (assuming normal distributions). The whiskers indicate the maximum and minimum reported values of LFG surface flux for each chemical family.

Figure 1.3 LFG Surface Fluxes of Gas Chemical Families Obtained from the Literature

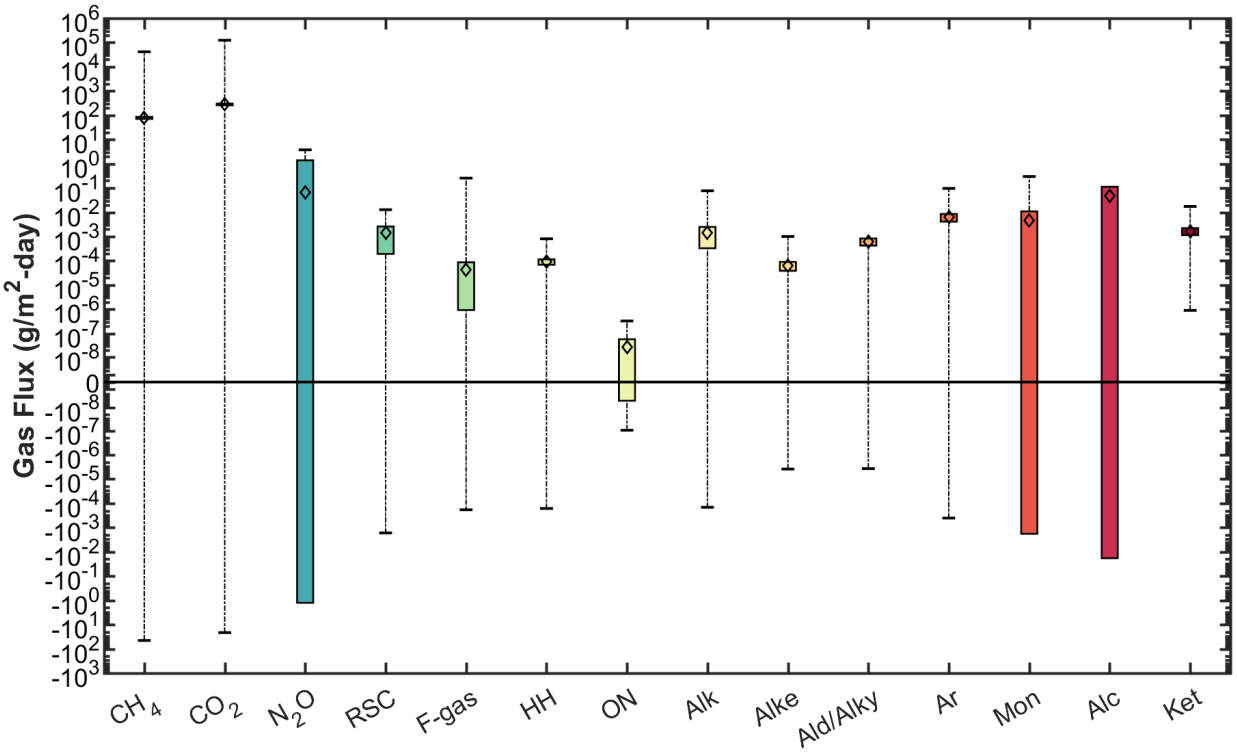

Carbon dioxide fluxes were the greatest among the gases investigated and also had the largest reported range -2.14x10^1 to 1.24x10^5 g/m^2-day (Table A3). Methane fluxes

ranged from -4.50x10^{1} to 4.15x10^{4}. Nitrous oxide emissions were generally greater than the NMVOCs (based on the mean values presented) with high variability (based on the width of the boxplots) and reported net negative emissions, ranging from -2.54x10^{-3} to 3.76x10^{0} g/m^{2}-day. The range in NMVOC emissions obtained from the literature was -1.66x10^{-3} to 3.00x10^{-1} g/m^{2}-day (Table A3). Of the NMVOCs evaluated in this review, the alcohol chemical family was associated with the greatest flux values followed by the aromatics, monoterpenes, and ketones. Within these chemical families, ethanol, m-xylene, alpha-pinene, and acetone were the chemical species associated with the greatest flux measurements. The relative flux values for the NMVOCs were different than the relative concentrations of the same NMVOCs in source landfill gas, which indicated that the monoterpenes (specifically limonene) were the most dominant constituents in raw LFG. As indicated in previous studies, concentrations in LFG do not provide direct indication for flux for a given species and are not recommended to be used as surrogates (Yesiller et al. 2018, Saquing et al. 2014). For a given chemical family, the highest variation in reported flux was observed for the alcohol chemical family, ranging from -1.90x10^{-5} to 5.20x10^{-1} g/m^{2}-day and the lowest variation was observed for the organic alkyl nitrate chemical family, ranging from -9.54x10^{-8} to 3.29x10^{-7} g/m^{2}-day.

Figure 1.4 LFG Surface Fluxes as a Function of Cover Category as Observed from the Literature

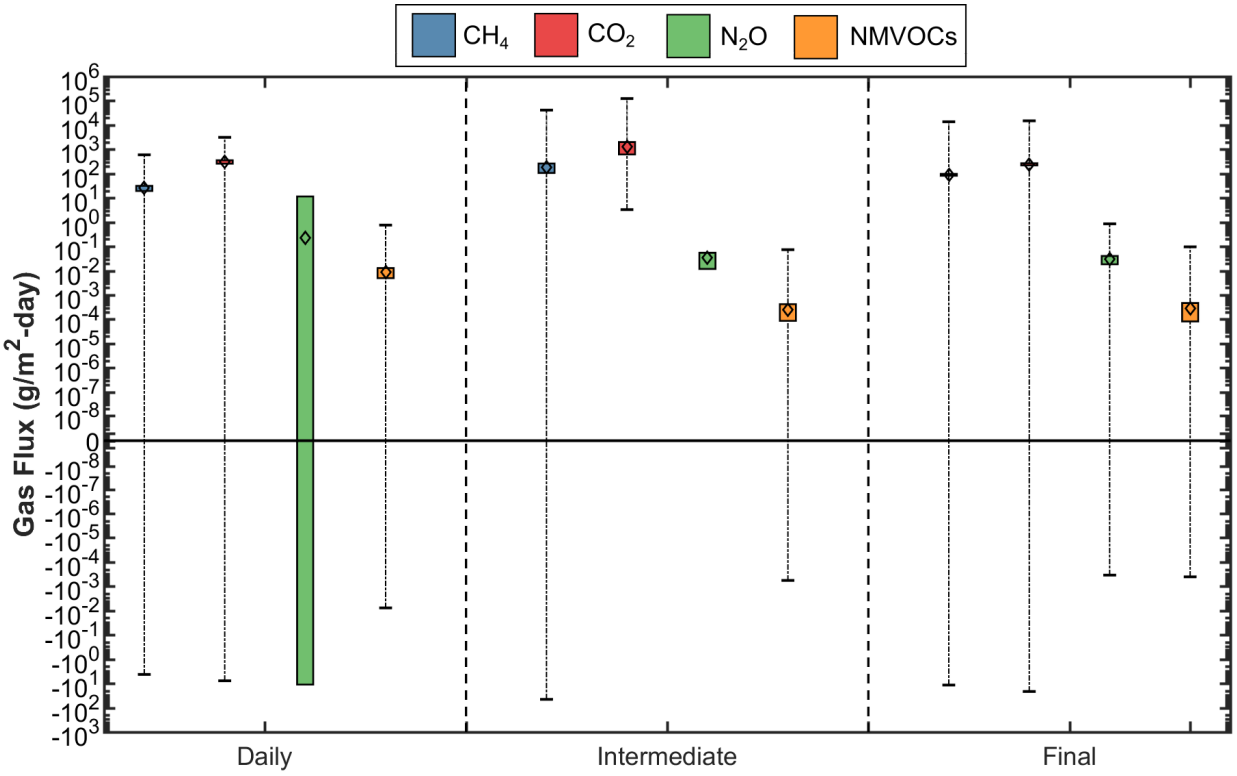

As a function of overall cover category, both methane and carbon dioxide fluxes were observed to increase progressing from daily to intermediate categories. Contrary to what was expected initially, the reported range in methane and carbon dioxide fluxes

were relatively similar between daily and final cover categories. Nitrous oxide fluxes were highly variable for daily cover categories, where the variation tended to decrease progressing to intermediate cover categories (Figure 1.4). The mean and variation in NMVOC fluxes obtained from the literature were relatively similar for the NMVOCs, but tended to decrease slightly progressing from daily, to intermediate, to final cover categories. The overall similarities observed in the central tendencies of the flux distributions obtained from the literature are most likely associated with the wide range and variety of cover types investigated within a given category in addition to the wide international coverage of site specific landfill operational practices and climatic conditions.

1.8 California Specific Inventory of Methane and NMVOC Fluxes and Emissions

California specific methane emissions were obtained from the scientific literature to provide a direct basis for comparison of methane emissions measured in this study. Results from studies conducted using direct (i.e., static flux chambers) and indirect (vertical radial plume mapping, VRPM, and aerial surveys) were summarized in Table 1.22. Data were presented for closed and currently active landfill sites. The WIP at the sites ranged from 6,225,912 to 124,963,317 tons. The reported methane fluxes ranged from -7.77×10^{-4} to 86.3 g/m^2-day, whereas emissions ranged from 355 to 37,600 Mg/year across approximately 50 different landfill sites (Pieschl et al. 2013, Krautwurst et al. 2017, Duren et al. 2019, Thompson et al. 2019, Cusworth et al. 2020). Of all the sites included in the literature review, Puente Hills and Monterey Peninsula Landfills had the highest reported annual net methane emissions and flux, respectively (Table 1.22). Puente Hills had the largest total WIP. The high flux reported from the Monterey Peninsula Landfill was attributed to an interim cover area with sub optimal conditions for methane oxidation (Bogner et al. 2011). Emissions from the active face of Potrero Hills landfill were estimated using remote sensing (Cusworth et al. 2020), where emissions ranged from 1,130 to 1,533 Mg/year which was significantly lower than whole-site emissions reported from larger landfill sites (Table 1.22).

Table 1.22 – Methane Fluxes and Emissions from California Landfills

Reference	Landfill	WIP (tons) (2010 data)	Measurement Methodology	CH_4 Flux (g/m^2-day)	Annual Emissions (Mg/yr)
Spokas et al. (2011), Goldsmith Jr. et al. (2012)	Tri-Cities Recycling and Disposal Facility	10,103,797	Flux Chamber, VRPM	5.6 to 7.1	N/A
Goldsmith Jr. et al. (2012), Green et al. (2009)	Altamont Landfill and Resource Recovery Facility	44,281,078	Flux Chamber, VRPM, CRDS	0.079 to 14.3	N/A
Goldsmith Jr. et al. (2012), Green et al. (2009)	Redwood Landfill	14,143,215	Flux Chamber, VRPM, CRDS	0.018 to 17	N/A
Bogner et al. (2011)	Scholl Canyon Landfill	29,409,357	Flux Chamber	-7.77×10^{-4} to 1.17×10^{-2}	N/A

Reference	Landfill	WIP (tons) (2010 data)	Measurement Methodology	CH_4 Flux (g/m^2-day)	Annual Emissions (Mg/yr)
Spokas et al. (2011)	Lancaster Landfill and Recycling Center	6,225,912	Flux Chamber	0.08 to 2.43	N/A
Pieschl et al. (2013), Shan et al. (2013), Goldsmith Jr. et al. (2012)	Puente Hills Landfill	124,963,317	Aircraft[2], VRPM, Flux Chamber	0.88 to 38.4	36,000 to 37,600
Shan et al. (2013)	Calabasas Landfill	23,441,895	Flux Chamber	0.05	N/A
Bogner et al. (2011)	Monterey Peninsula Landfill	8.388,784	Flux Chamber	0.003 to 86.3[3]	N/A
Pieschl et al. (2013), Shan et al. (2013), Krautwurst et al. (2017)	Olinda Alpha Landfill	52,017,040	Aircraft, VRPM, Flux Chamber	4.3 to 20	9,500 to 24,300
Spokas et al. (2011), Goldsmith Jr. et al. (2012)	Kirby Canyon Recycling and Disposal Facility	7,312,751	Flux Chamber	0.07 to 20.9	N/A
Duren et al. (2019)	28 Different Landfill Facilities	Varies	Aircraft[1]	N/A	355 to 26,359
Thompson et al. (2019)	17 Different Landfill Facilities	Varies	Aircraft[2]	N/A	619 to 28,034
Cusworth et al. (2020)	Portrero Hills LF	11,798,655	Aircraft[1]	19 to 39.2[4]	1,130 to 1,533

N/A Not reported by the study
[1] Anayzed by airborne visible/infrared imaging spectrometer
[2] Analyzed by Picaro cavity ring down spectrometer
[3] A max/min was not given so a range in the mean estimates is provided across different cover categories
[4] Estimated for the active face portion of this landfill only

In addition to methane, California specific emissions estimates of nitrous oxide were obtained from the scientific literature. Nitrous oxide fluxes obtained using static flux chambers were reported in two studies with results summarized in Table 1.23. Data were obtained from daily, intermediate, and final cover systems. The landfills investigated included a large, now closed site (Olinda Alpha Landfill) with high WIP and medium and small landfills with significantly lower WIP (Monterey Peninsula and San Joaquin Landfills). Bogner et al. (2011) conducted flux measurements in both wet and dry seasons. Overall nitrous oxide fluxes ranged from 0.0 (non-detect) to 2.5×10^{-1} g/m^2-day. The range in flux values reported by Bogner et al. (2011) were average flux ranges across daily, intermediate, and final cover categories, whereas the flux values reported by Mandernack et al. (2000) were minimum and maximum ranges for a specific cover category. Annual nitrous oxide emission estimates were not reported for California landfills in the literature.

Table 1.23 – Nitrous Oxide Fluxes from California's Landfills

Reference	Landfill	WIP (tons) (2010 data)	Measurement Methodology	N_2O Flux (g/m^2-day)
Mandernack et al. (2000)	Olinda Alpha Landfill	52,017,040	Flux Chamber	0.0 to $7.9x10^{-3}$
	UCI Landfill	N/A	Flux Chamber	$4x10^{-4}$ to $4.5x10^{-3}$
	San Joaquin Landfill	N/A	Flux Chamber	$4x10^{-4}$ to $4.0x10^{-3}$
Bogner et al. (2011)	Scholl Canyon Landfill	29,409,357	Flux Chamber	$2.3x10^{-3}$ to $2.5x10^{-1}$
	Monterey Peninsula Landfill	8.388,784	Flux Chamber	$1.28x10^{-2}$ to $9.15x10^{-2}$

Yesiller et al. (2017) was the only study in the literature that reported a large number of NMVOC surface fluxes from a landfill in California (Table 1.24). In this study, NMVOC fluxes from Potrero Hills Landfill were measured for daily (soil, green waste, autofluff), intermediate (soil), and final (conventional compacted clay) cover categories over the wet and dry seasons. Static flux chambers were used to measure NMVOC fluxes of halogenated hydrocarbon, alkane, alkene, aldehyde/alkyne, monoterpene, aromatic, reduced sulfur compound, alcohol, ketone, and F-gas chemical families. A total of 53 chemical species within the 10 chemical families identified above were quantified in this investigation. The overall NMVOC fluxes from Potrero Hills landfill ranged from $-7.71x10^{-3}$ to $7.64x10^{-1}$ g/m^2-day across both wet and dry seasons as well as the variety of cover categories investigated. Annual emissions of NMVOCs were not reported by this study.

Table 1.24 – NMVOC Fluxes and Emissions from California's Landfills

Reference	Landfill	WIP (tons) (2010 data)	Measurement Methodology	NMVOC Flux (g/m^2-day)	Annual Emissions (Mg/yr)
Yesiller et al. (2017)	Potrero Hills Landfill	11,798,655	Flux Chamber	$-7.71x10^{-3}$ to $-7.64x10^{-1}$	N/A

1.9 Landfill Gas Transformation Pathways

Once landfill gas is generated in and transported throughout the landfill environment, the gas goes through several potential transformation pathways before being emitted to the atmosphere. In general, transformation pathways can be categorized as biological or physical/chemical in that biological pathways are mediated by microorganisms, whereas physical/chemical pathways are mediated by physical/chemical conditions in the landfill environment (Table 1.22). Transformation can occur within the waste mass as well as through the soil or alternative covers. The processes can take place in the solid, liquid, or gas phases in the wastes or cover materials. Biological transformation pathways can include both aerobic oxidation and anaerobic decomposition in the waste mass or cover materials. Physical/chemical transformation pathways primarily include,

but are not limited to, dissolution of gas into landfill leachate or moisture present in the waste mass/cover materials; phase partitioning of a given gas into organic phases present in the waste mass or organic matter present in the cover materials; and chemical sorption or physical attachment of the gases to solid matter in the waste mass or in the cover materials (Kjeldsen and Christensen 2001, Lowry et al. 2008).

Deipser and Stegmann (1997) studied the anaerobic transformation of select trace NMVOCs simulating conditions in the waste mass. Landfill lysimeters were set up with MSW sampled from the field (in different stages of waste decomposition) and combined with digester sludge and compost. In general, reductive dichlorination of the halogenated hydrocarbons was observed. For example, carbon tetrachloride was degraded to tri/di/chloromethane under the anaerobic conditions studied. Tetrachloroethylene was reduced to trichloroethylene (TCE), 1-1-dichloroethylene (1,1-DCE), cis and trans-1,2-dichloroethylene (1,2-DCE), and vinyl chloride. Methyl chloroform was reduced to chloroethane, whereas methylene chloride was reduced to methyl chloroform (Deipser and Stegmann 1997). HCFC-21 and HCFC-22 are were reported to be significant products of transformation of CFC-11 and CFC-12, respectively in the waste mass (Scheutz et al. 2007). HFCs were reported not to degrade within wastes based on laboratory tests (Scheutz et al. 2007).

For biological transformation pathways, studies were conducted on attenuation of different trace gas constituents in landfill cover soils (Table 1.22) (Kjeldsen et al. 1997, Scheutz and Kjeldsen 2003, Scheutz and Kjeldsen 2004, Scheutz and Kjeldsen 2005, Scheutz et al. 2007). These studies included assessment of landfill cover soils. The soils were sampled from several locations at a landfill and laboratory tests were conducted to assess the biological attenuation of the NMVOCs through these soils. Three modes of testing were used: batch testing, where target gases were added to a container, along with cover soils with bacteria present (in the presence/absence of

Table 1.25 – Summary of Landfill Gas Transformation Pathways

Classification	Transformation Pathway	Location	Chemical Species/Family	Transformed	Documented in Landfill	Reference	Notes
Biological	Aerobic Oxidation	Cover Soil, Waste Mass	Benzene	Yes	Yes	Kjeldsen et al. 1997, Scheutz and Kjeldsen 2003, Scheutz and Kjeldsen 2004, Scheutz and Kjeldsen 2005, Scheutz et al. 2007,	Oxidation byproducts not monitored or reported
			Toluene	Yes	Yes		
			Ethylbenzene	Yes	Yes		
			Xylene	Yes	Yes		
			Trichloroethylene	Yes	Yes		
			Tetrachloroethylene	No	No		
			Carbon tetrachloride	No	No		
			Chloroform	Yes	Yes		
			Methyl chloroform	Yes	Yes		
			Methylene chloride	No	No		
			CFC-11	No	No		
			CFC-12	No	No		
			CFC-113	No	No		
			HCFC-141b	No	No		
			HCFC-142b	-	-		
			HCFC-21	Yes	Yes		
			HCFC-22	Yes	Yes		
			HFC-134a	No	No		
			HFC-245fa	No	No		
			Alkanes	Yes	Yes	Tassi et al. 2009	Alkanes and aromatics oxidized=>ketones, aldehydes produced
			Alkenes	-	-		
			Aldehydes/Alkynes	No	No		
			Monoterpenes	-	-		
			Alcohols	-	-		
			Ketones	No	No		
	Anaerobic Decomposition	Cover soil, Waste mass	Benzene	Yes	Yes	Deipser and Stegmann 1997, Kjeldsen et al. 1997, Balsiger et al. 2002, Scheutz and Kjeldsen 2003, Scheutz	Oxidation byproducts monitored for F-gases only
			Toluene	Yes	Yes		
			Ethylbenzene	-	-		
			Xylene	-	-		
			Trichloroethylene	Yes	Yes		
			Tetrachloroethylene	-	-		
			Carbon tetrachloride	Yes	Yes		

Classification	Transformation Pathway	Location	Chemical Species/Family	Transformed	Documented in Landfill	Reference	Notes
			Chloroform	Yes	Yes	et al. 2004, Scheutz and Kjeldsen 2005, Scheutz et al. 2007, Grossi et al. 2008. Musat 2015	
			Methyl chloroform	-	-		
			Methylene chloride	No	No		
			CFC-11	Yes	Yes		
			CFC-12	Yes	Yes		
			CFC-113	Yes	Yes		
			HCFC-141b	No	No		
			HCFC-142b	No	No		
			HCFC-21	Yes	Yes		
			HCFC-22	Yes	Yes		
			HFC-134a	No	No		
			HFC-245fa	-	-		
			Alkanes	Yes	Yes		
			Alkenes	Yes	Yes		
			Aldehydes/Alkynes	-	-		
			Monoterpenes	-	-		
			Alcohols	-	-		
			Ketones	-	-		
			Benzene	-	-		
Physical-Chemical	Dissolution	Cover Soil	Alcohols, aldehydes, ketones	Yes	Yes	-	-
	Phase Partitioning		Aromatics, long chain alkanes, monoterpenes	Yes	Yes	-	-
	Chemical Sorption		Alcohols, aldehydes, ketones	Yes	Yes	-	-

oxygen), and the headspace monitored over time; soil column testing, where landfill soils were packed in a column and artificial landfill gas was passed through the system and the concentrations at inlet/outlet monitored over time; and a more complex counter gradient system where both oxygen and artificial LFG were injected at opposing sides of the column and the inlet/outlet monitored over time. Similar transformations reported for the waste mass for the CFCs were observed in the cover soil experiments. Many CFCs and highly chlorinated organics (i.e., carbon tetrachloride, tetrachloroethylene) were not aerobically oxidized, whereas some of the HCFCs (21/22) and most of the aromatics (benzene/ toluene/ethylbenzene/xylene) were rapidly oxidized. Some of the more chlorinated organics, such as trichloroethylene and methyl chloroform, were only co-oxidized in the presence of methane by the methanotrophic populations present in the cover soils (and not oxidized alone in batch experiments) (Kjeldsen et al. 1997). In the absence of oxygen, the CFCs and HCFCs (21 and 22) were readily biodegraded in the simulated cover soil environments (Scheutz and Kjeldsen 2003, Scheutz and Kjeldsen 2005, Schuetz et al. 2007). Carbon tetrachloride, which was not biodegraded during the oxygenated experiments, was observed to be degraded in the anaerobic experiments (Table 1.22). HCFC 141b, HCFC-142b, HFC-134a, and HFC-245fa were recalcitrant to biodegradation in all experiments performed, whether aerobic or anaerobic in nature. Balsiger et al. (2002) and Scheutz et al. (2007) identified the degradation byproducts of CFC-11, CFC-12, and CFC-113 under anaerobic conditions. CFC-11 was transformed to HCFC-21 and the further transformed to HCFC-31. CFC-12 was degraded to HCFC-22 and then further degraded to HFC-32 or HFC-41. Finally, CFC-113 was degraded to HCFC-123a, then further degraded to HCFC-133b or HCFC-133.

A single study was identified in the literature (Tassi et al. 009) on oxidation of NMVOCs in a soil cover directly in the field. In this study, soil gas probes were installed and monitored in a final cover system of a closed landfill over an extended time period. Tassi et al. (2009) reported that the C_2-C_{15} alkanes (ethane, propane, butane, undecane) and aromatics were oxidized by resident methanotrophs in the cover soils, where the alkanes were reduced from 11.6% total composition at the deepest measurement location in the cover to 0.45% in the shallowest depth monitored. The ketones, esters, aldehydes, and organic acids were observed to be the most stable and common byproducts of oxidation reactions involving the aromatics or alkanes out of all chemical families in the cover system studied (enriched close to the air-soil surface). Relatively little biotransformation of the halogenated hydrocarbons was observed. Results of this study demonstrated that biological transformations of NMVOCs within the cover soil can be significant factors affecting emissions.

Dissolution, phase partitioning, and sorption, among many competing factors are the main potential physical and chemical transformation reactions for NMVOCs. Dissolution depends on the relative affinity for a chemical species for the aqueous phase. Such affinity depends on the physico-chemical characteristics of the chemical, including water solubility and volatility properties. NMVOC chemicals with low boiling points, high vapor pressures, high Henry’s constants and low water solubilities are more likely to remain in the gaseous phase in wastes and covers within the landfill

environment. Based on these criteria, the physical and chemical properties of the gases included in the investigation were ranked from most to least soluble using the following parameters (in order of most to least significant): water solubility (high values desired), vapor pressure (low values desired), boiling point (high values desired), and Henry's constant (low values desired). The analysis indicated that the alcohols (i.e., methanol), aldehydes, ketones, and some monoterpenes were most likely to dissolve into the aqueous phase in the landfill environment. These gases are oxygenated species (leading to potential hydrogen bonds) and small in molecular weight (limited number of carbon atoms) supporting the high potential for dissolution in the liquid phase (Table 1.22).

A similar exercise was conducted to assess the extent of organic partitioning in the landfill environment for the target gases included in this study. NMVOC chemicals were ranked from most to least likely to partition based on the octanol-air (most significant) and octanol-water partition coefficients (least significant), where higher values of each parameter were desired. Using the above criteria and ranking schemes, many of the chemicals included in the aromatics, long-chain alkanes, monoterpenes, and some baseline GHGs (carbon monoxide/nitrous oxide) were likely to partition into the organic phases present in the landfill environment. Both aromatic compounds and long-chain alkanes or alkenes are generally more hydrophobic than hydrophilic (and lipophilic) and tend to partition into non-polar solvents (Table 1.22).

Data and analysis on sorption of target gases for chemical or physical attachment to waste materials or soil particles present in the landfill environment have not been studied in great detail. In general, various attachment mechanisms are present for chemicals in the environment. The most predominant type of interaction is that based on charge differences. The relative charge of a given chemical depends on its polarity and ionization potential, where more polar compounds (that exert greater differences in electronegativity through dipole moments) and those with a greater number of ionizable functional groups (at the pH range expected in the landfill environment) are more likely to sorb and interact chemically with different materials present (Vollhardt and Schore 2004). Due to the presence of oxygen and hydroxyl functional groups, the aldehydes, alcohols, and ketones are relatively polar compounds among the target gases included in the investigation and may be more inclined to chemically attach to cover soil particles and organic or inorganic materials present in the waste mass.

PART 2 – LANDFILL CLASSIFICATION

2.1 Introduction

The initial step of the investigation consisted of development of a scheme for classifying landfill sites in California and selecting representative sites for aerial emissions measurements and ground-based static flux chamber tests. The main factors and associated expected variations in the main factors used for categorization of the sites are listed in Table 2.1. The categorization scheme was used for active landfill sites in California.

Table 2.1 – General California Landfill Classification Scheme

Main Factor		Variation
Facility Size	Waste in place	Amount of waste disposed at the site
	Disposal area	Permitted waste footprint area
	Waste column height	Average depth of waste at the site
	Permitted throughput	Annual waste intake
Climate		Classification designation by Köppen Geiger System
Oil and Gas Operations		Oil and gas operation sites in California and proximity of the landfill to these sites
Fault Lines		California quaternary faults and proximity of the landfill to the faults
Population Density		Urban and rural areas
Gas System		Yes, no
Tire Disposal		Yes, no

The classification scheme identified in Table 2.1 was used for all of the active landfill sites in California. Further detailed analysis was conducted for finalizing the sites selected for the experimental program by incorporating additional criteria. The detailed classification scheme used in the investigation is provided in Table 2.2. Categories from Table 2.1 are included in Table 2.2 for completeness of the analysis.

Table 2.2 – Detailed California Landfill Classification Scheme

Main Factor		Variation
Facility Size	Waste in place	Amount of waste disposed at the site
	Disposal area	Permitted waste footprint area
	Waste column height	Average depth of waste at the site
	Permitted throughput	Annual waste intake
Climate		Classification designation by Köppen Geiger System
Oil and Gas Operations		Oil and gas operation sites in California and proximity of the landfill to these sites
Fault Lines		California quaternary faults and proximity of the landfill to the faults
Population Density		Urban and rural areas
Gas System		Yes, no

Main Factor		Variation
Tire Disposal		Yes, no
Cover Conditions	Daily	Conventional-soil type and thickness Alternative daily covers (ADCs) including green waste, construction & demolition, biosolids, tarp, spray-on products, other
	Intermediate	Soil type and thickness
	Final	Presence of final cover: Yes, no Type and thickness of final cover - Traditional: single covers [compacted clay (CCL), geosynthetic clay liner (GCL), geomembrane (GM)]; composite covers [GM-CCL, GM-GCL] - Alternative: monolithic or capillary break
Relative Fraction of Cover Categories		Relative areas of daily, intermediate, and final covers (% of waste footprint)
Working Face		Size of active waste disposal area
Range for Age of Waste		Age of wastes
Landfill Configuration		Canyon, area
Operational Conditions		Particularly in relation to N_2O emissions including leachate recirculation, biosolids disposal, etc.

2.2 California Landfill Site Characteristics

The active landfill sites in California were first categorized using the criteria in Table 2.1. The information used for the categorization mainly was obtained from the SWIS database (CalRecycle 2017, data from July 2017) and Landfill Data Compilation provided by Walker (2010). A total of 133 active landfill sites was identified for inclusion in the analysis. A summary of data for all 133 active landfills is presented in Appendix B1. The geographical distribution of these sites is presented in Figure 2.1.

The facility size analysis included waste in place, disposal area, waste column height, and permitted throughput categories. The waste in place (WIP) data were obtained from the SWIS database by calculating the difference between the reported “capacity” and “remaining capacity” data. These data were reported in volume units. In addition, waste in place was calculated by using data obtained from ARB in relation to methane reporting requirements. These data were provided in mass units and converted to volume using a waste density of 1300 lbs/yd^3 (771 kg/m^3) provided by ARB. The WIP data obtained using the two approaches are compared in Figure 2.2 and were determined to be in good agreement. The volumetric WIP data obtained from the SWIS database were selected to be used herein as the data directly represent the amount of waste disposed of at a landfill i) due to no conversions required using assumed parameters (i.e., density) and ii) as the loss in mass due to decomposition/degradation of older wastes is accounted for with periodic surveys that provide the volumetric data.

Figure 2.1 Active California Landfill Sites

Figure 2.2 Waste in Place Determined Using Two Approaches

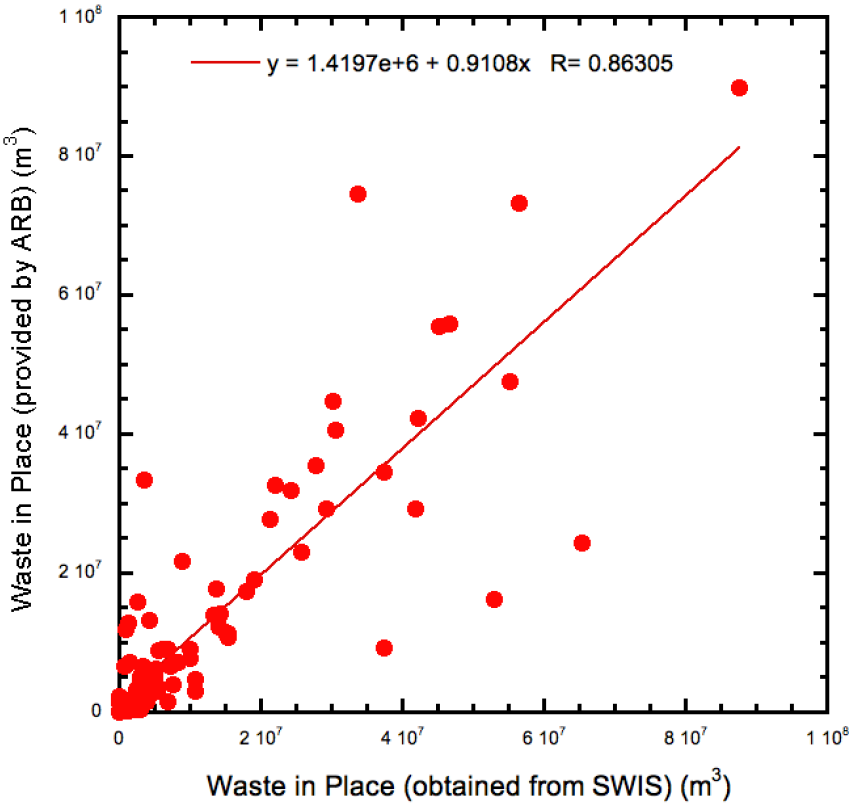

The variation of waste in place with number of landfills is presented in Figure 2.3. The landfills were categorized as small, medium, and large using major breaks in WIP data (analysis performed on large graphical representations of the data) and also presented in Figure 2.3. The limiting WIP values for the cutoffs between the categories were 4,000,000 m^3 and 40,000,000 m^3 based on large breaks in the histogram data. This approach was used for all of the histograms in Part 2. All histograms in Part 2 were presented without and with limiting thresholds to clearly present overall data and delineate categories identified in this investigation. The disposal area was obtained from the "Disposal Acreage" category in the SWIS database. The variation of disposal area with number of landfills is presented in Figure 2.4. The landfills were categorized into small, medium, and large sites using large breaks in area data (analysis performed on large graphical representations of the data) and also presented in Figure 2.4. The limiting disposal area values for the cutoffs between the categories were 1,000,000 m^2 and 2,000,000 m^2. The average waste column height was determined by dividing the WIP with disposal area. The variation of waste column height with number of landfills is presented in Figure 2.5. The landfills were categorized into short, moderate, and tall landfills using large breaks in waste column height data as presented in Figure 2.5. The limiting waste height values for the cutoffs between the categories were 14 m and 30 m. The variation of waste throughput with number of landfills is presented in Figure 2.6. The data were obtained from the SWIS database. The landfills were categorized into low, medium, and large landfills using large breaks in throughput data with limiting values for the cutoffs between the categories as 1500 tons/day and 7000 tons/day.

Figure 2.3 Variation of Waste in Place with Number of Landfills

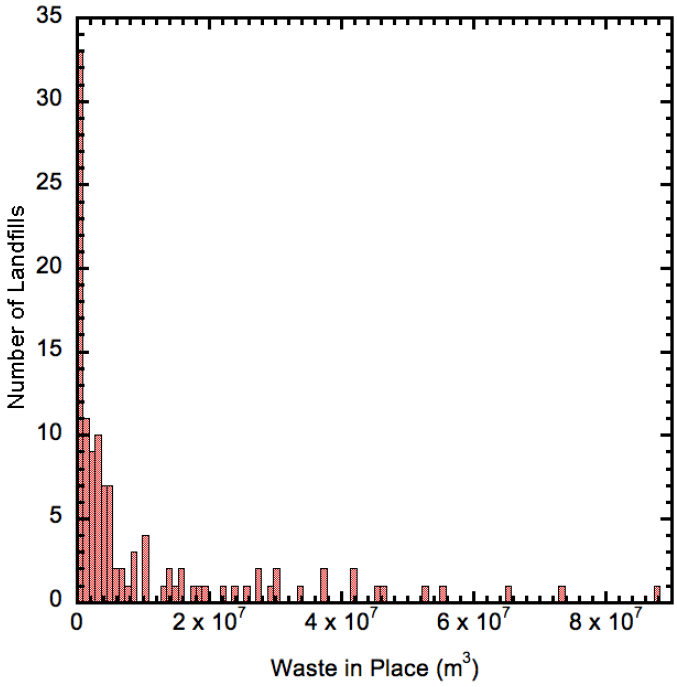

a) Distribution without Thresholds

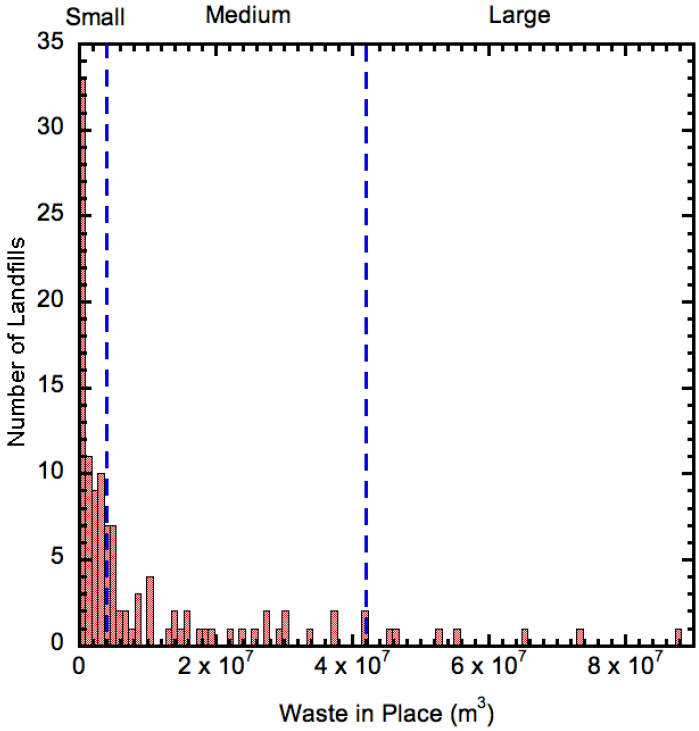

b) Distribution with Thresholds

Figure 2.4 Variation of Disposal Area with Number of Landfills

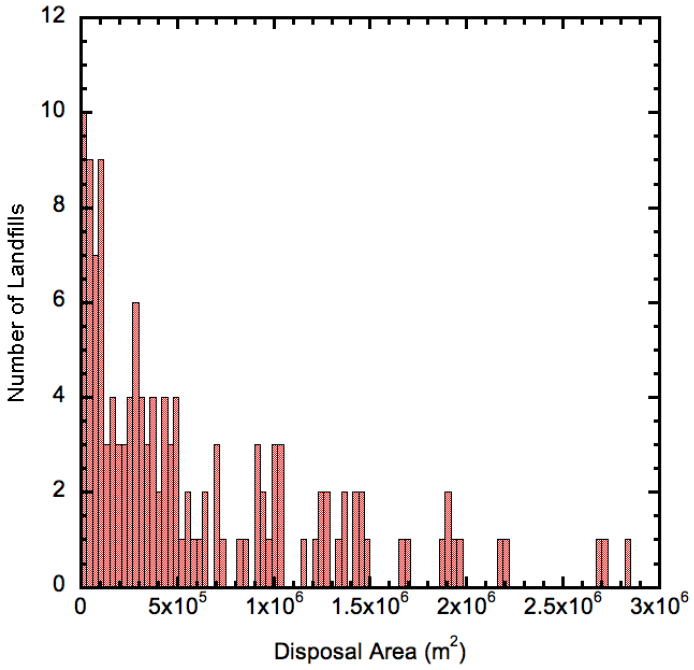

a) Distribution without Thresholds

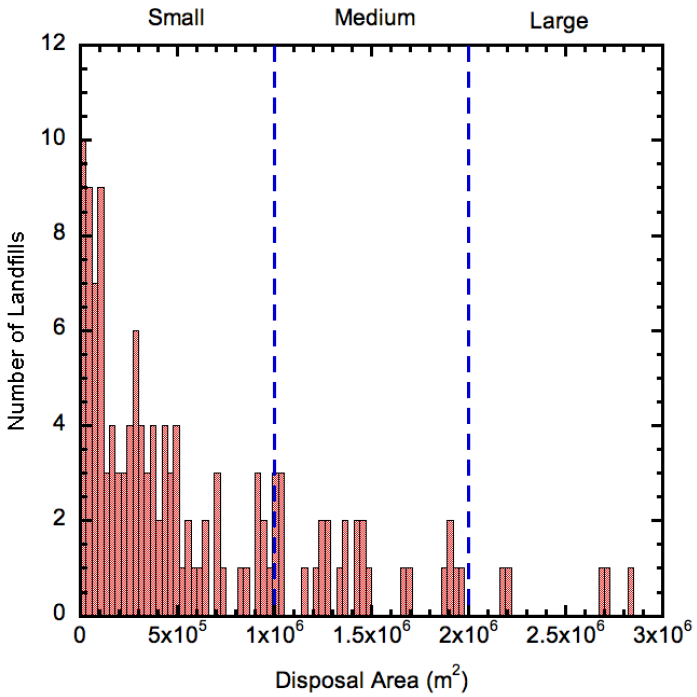

b) Distribution with Thresholds

Figure 2.5 Variation of Average Waste Column Height with Number of Landfills

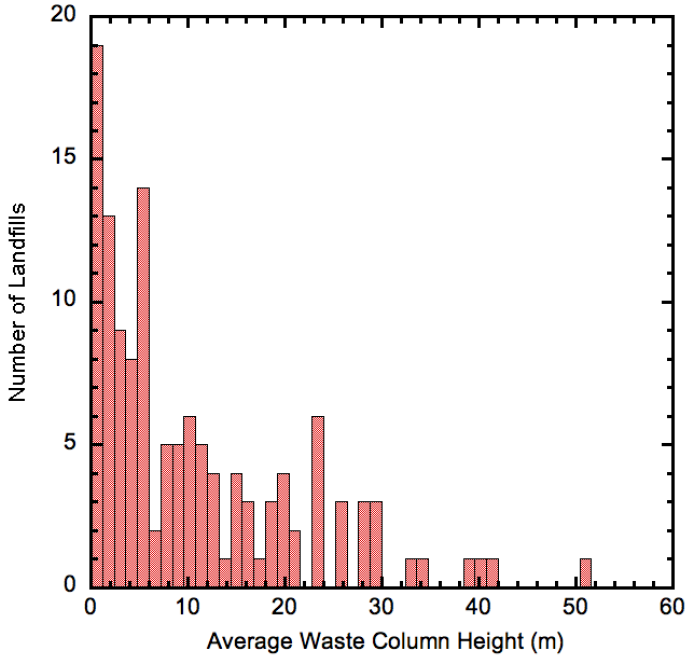

a) Distribution without Thresholds

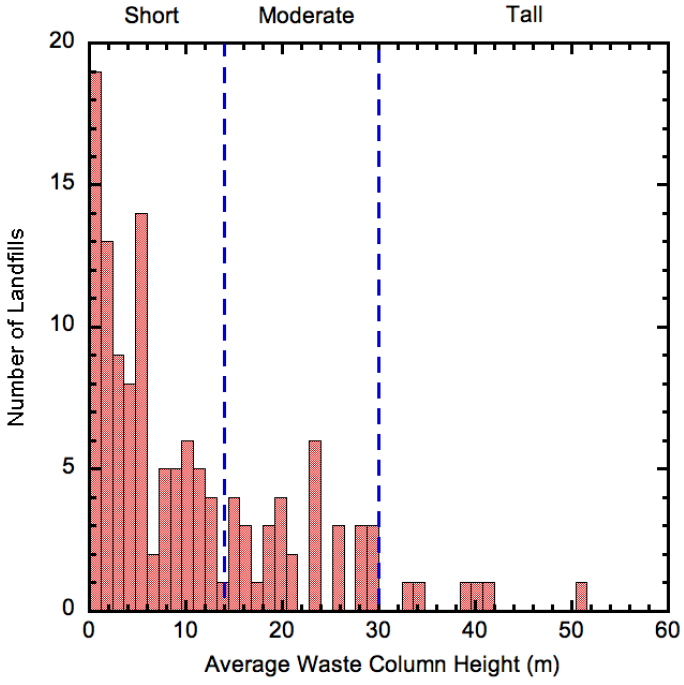

b) Distribution with Thresholds

Figure 2.6 Variation of Waste Throughput with Number of Landfills

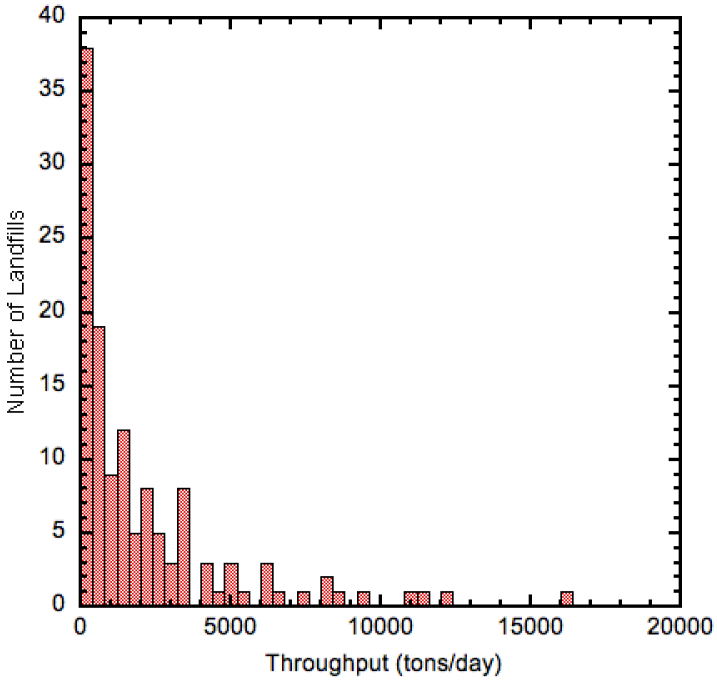

a) Distribution without Thresholds

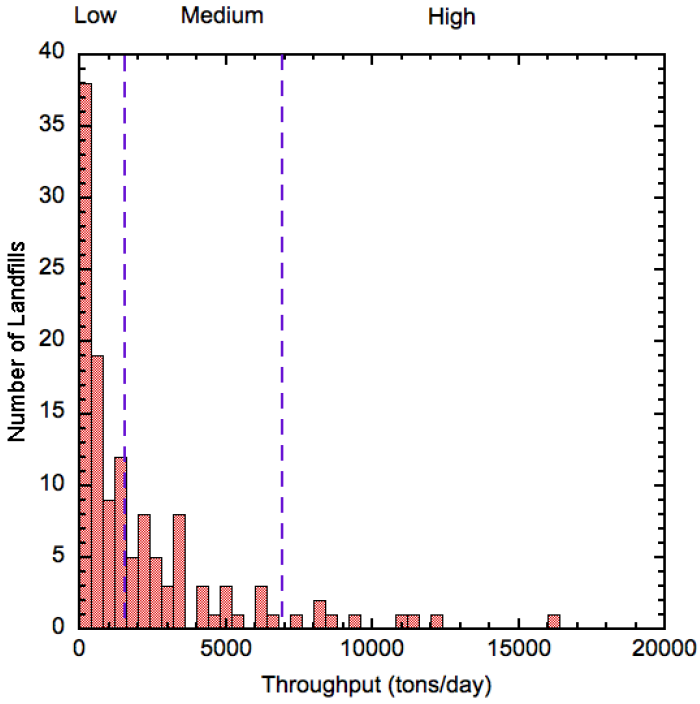

b) Distribution with Thresholds

Positive correlations between waste in place and annual landfill gas recovery were demonstrated for California landfills with increasing gas recovery with increasing WIP (Spokas et al. 2015). Therefore, landfill facility size quantified using the waste in place parameter was identified to be a significant factor for the current emissions study and further analysis was conducted using the waste in place data. Relative distribution of WIP in small, medium, and large landfills is presented in Figure 2.7 for the total WIP amount of 1,237,674,433 m^3 in California. While the highest number of landfills (80) was in the small landfill category (Figure 2.3), the relative amount of WIP in these landfills amounted to only 8.2% (99,347,605 m^3) of the total WIP in California. The majority of the WIP, 50.9% (627,991,773 m^3), was in the 44 medium landfills. With only 9 facilities, the WIP in large landfills was significant at 40.8% of total WIP and equaled to 510,335,055 m^3 of waste.

Figure 2.7 Relative Distribution of Waste in Place in California Landfills

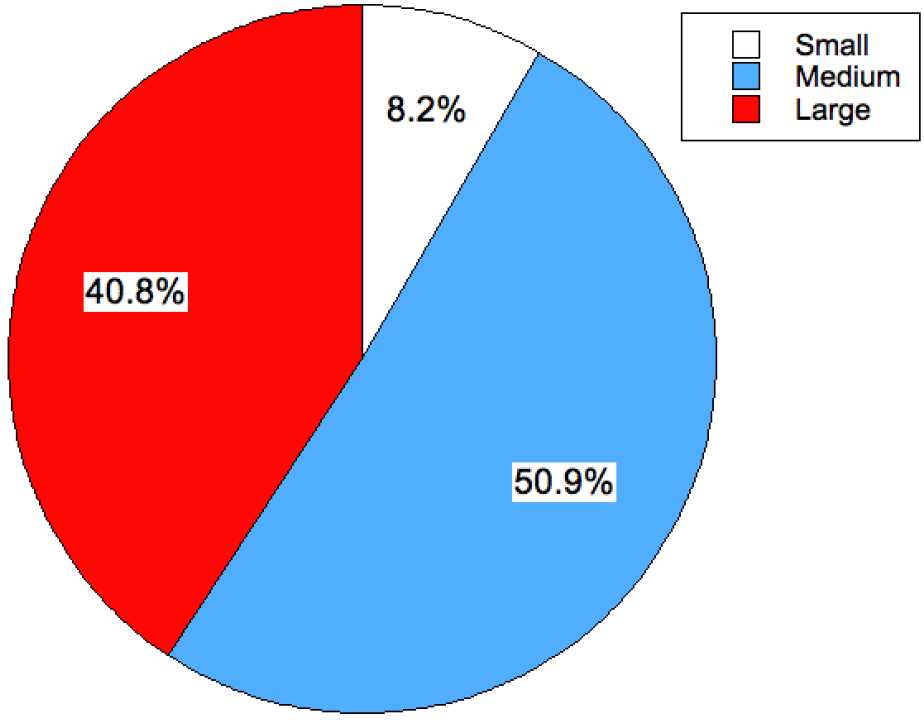

Waste in place data was added to the location data and active California landfills by WIP amount are presented in Figure 2.8. The six main climatic zones in California (Figure 2.9) according to the Köppen Geiger System (Peel et al. 2007) were added to the data in Figure 2.8 and a composite plot of landfill location, size, and climatic zone is presented in Figure 2.10. The majority of California landfills (77 landfills) were located in the Csb (temperate, dry summer, warm summer) climate zone (Figure 2.11). The relative fraction of these 77 facilities was 57.9% (Figure 2.12). The number of landfills in the Csa (temperate, dry summer, hot summer) and BSk (arid, steppe, cold) climate zones were similar and equal to 20 and 22, respectively (Figure 2.11. The majority of the WIP in California was also located in the Csb climate zone (Figure 2.13), which amounted to 77.5% of the total WIP in the state (Figure 2.14). This was

followed by 14% and 7.3% WIP present at the landfills in Csa and BSk climate zones, respectively (Figure 2.14. No landfills were located in the Dsc (cold, dry summer, cold summer) climate zone; only small landfills were located in the BWh (arid, desert, hot) climate zone, and a total of only two landfills (one small, one medium) were located in the BWk (arid, desert, cold) climate zone (Figures 2.11 and 2.13). The WIP in these three climate zones was minimal (Figure 2.14).

Figure 2.8 Active California Landfills with Waste in Place Data

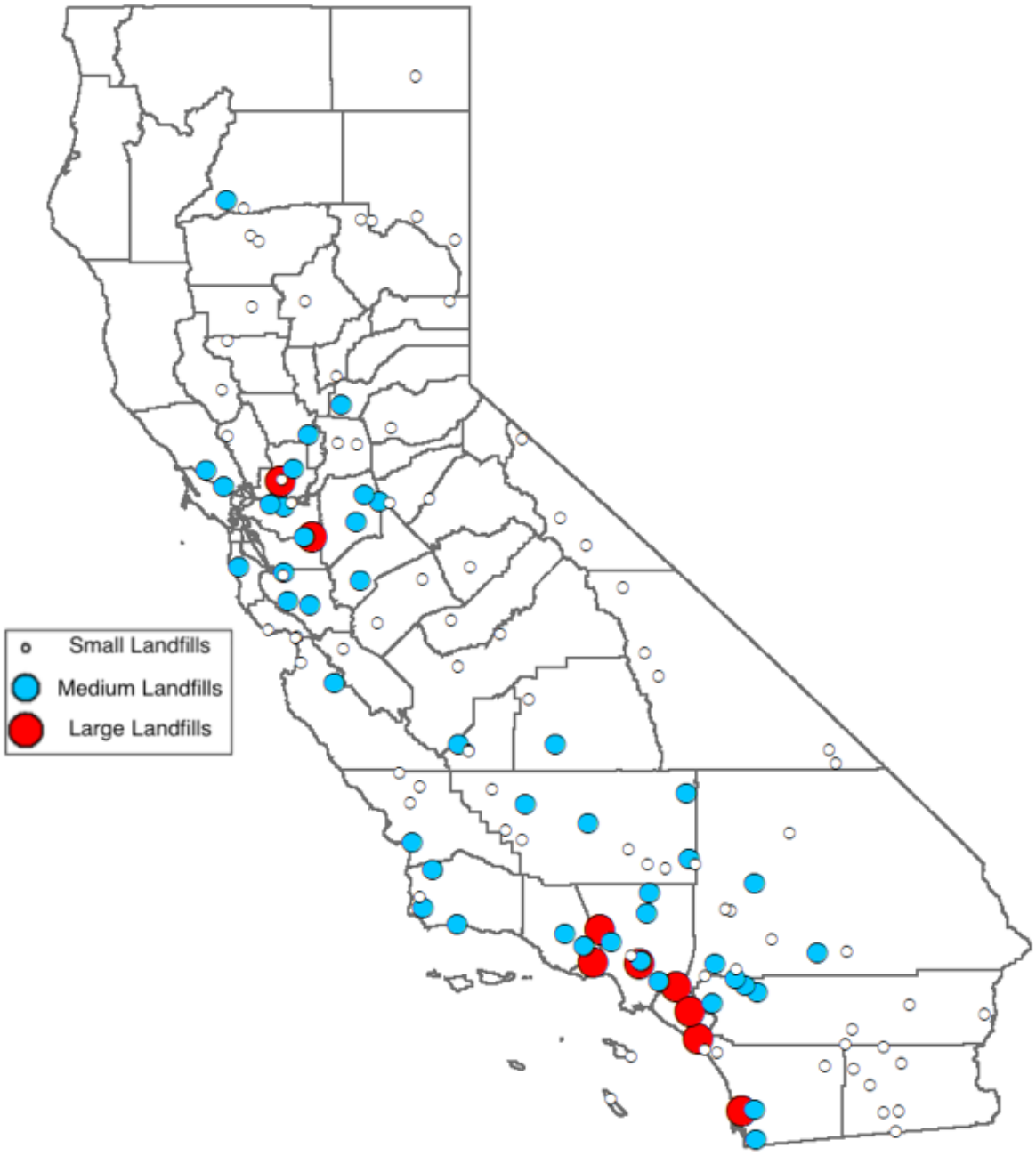

Figure 2.9 Main Climate Zones in California

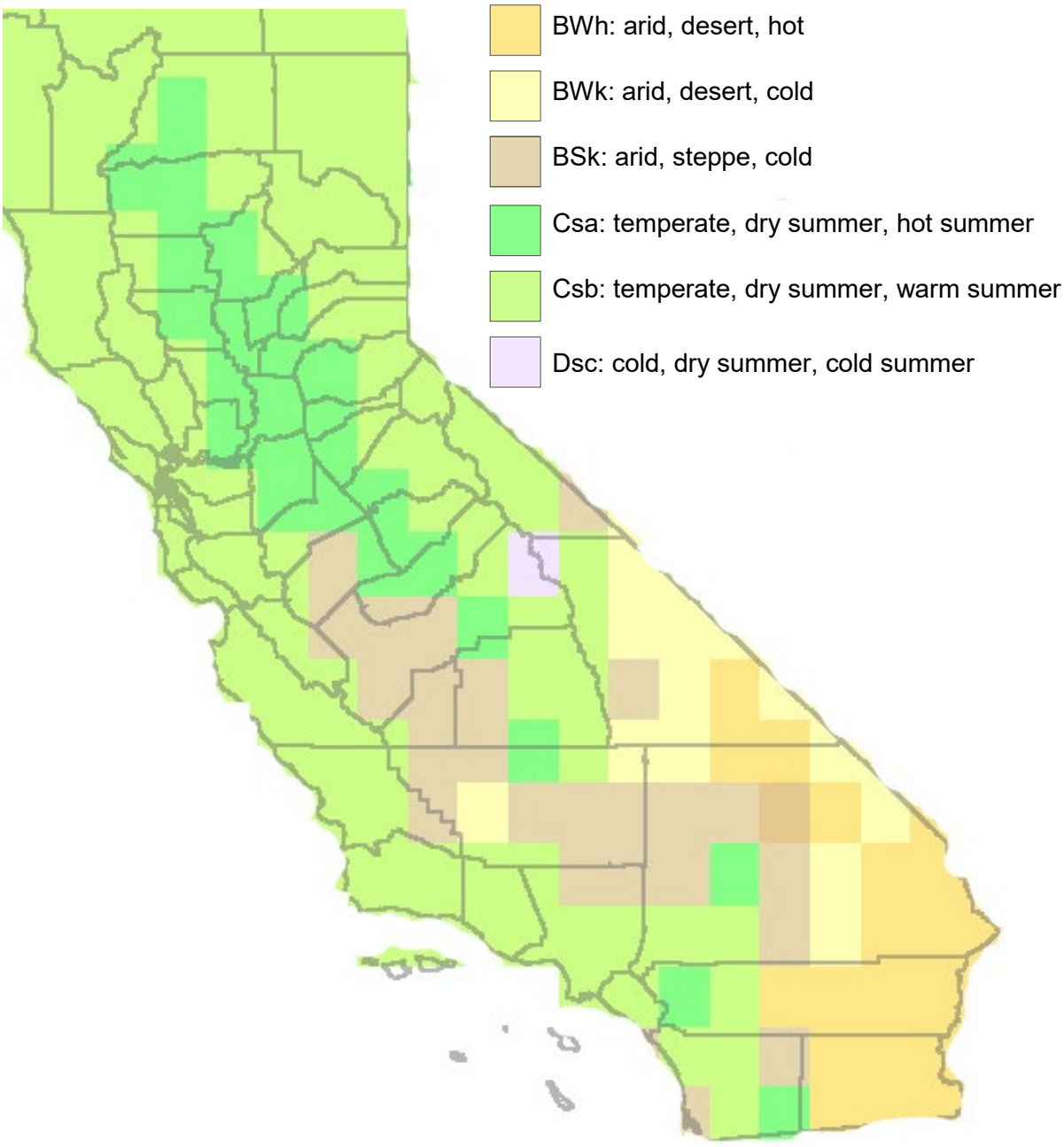

Figure 2.10 Active California Landfills with Waste in Place Data Across Climate Zones

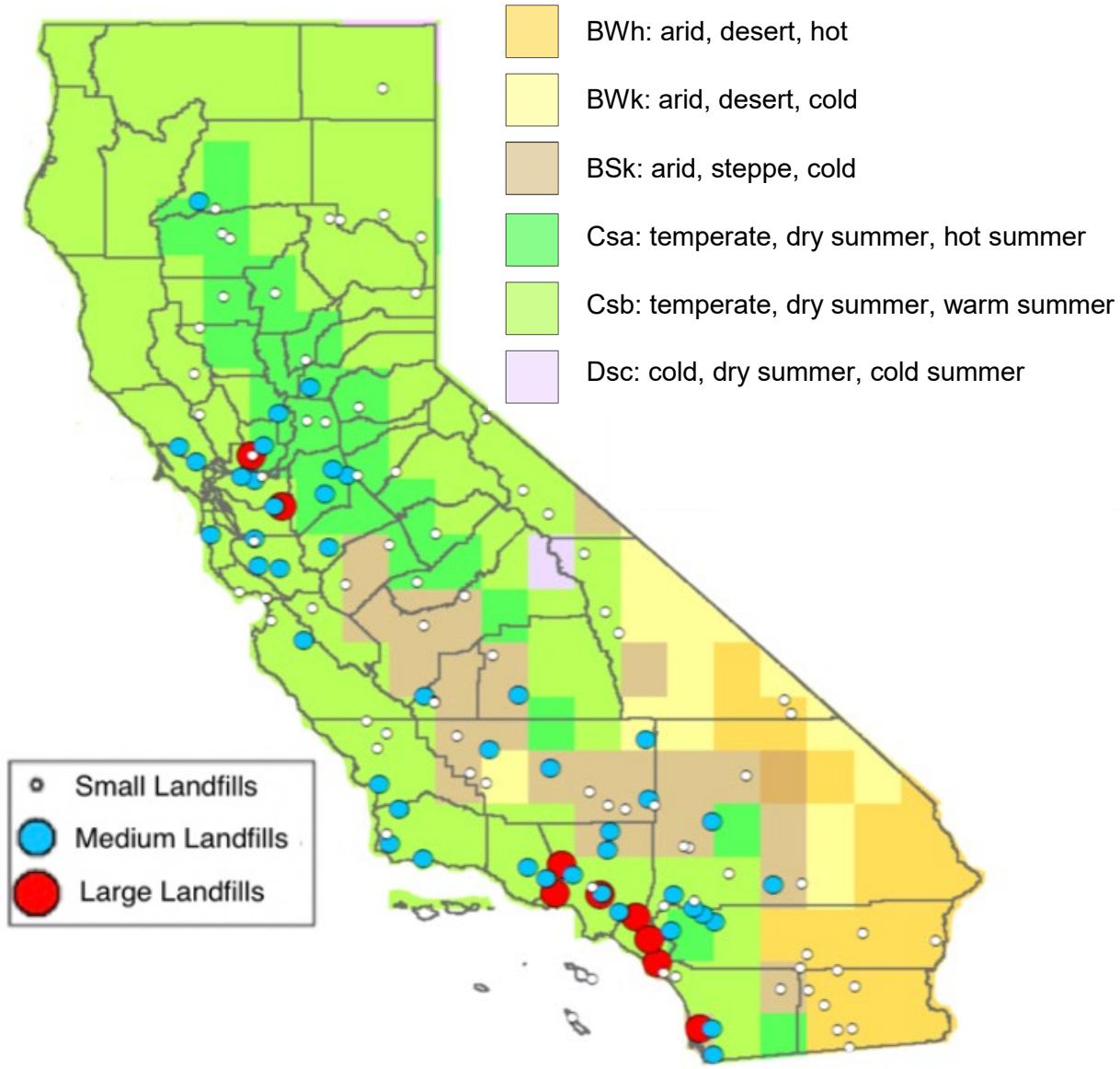

Figure 2.11 Histogram of Number of Landfills with Climate Zone

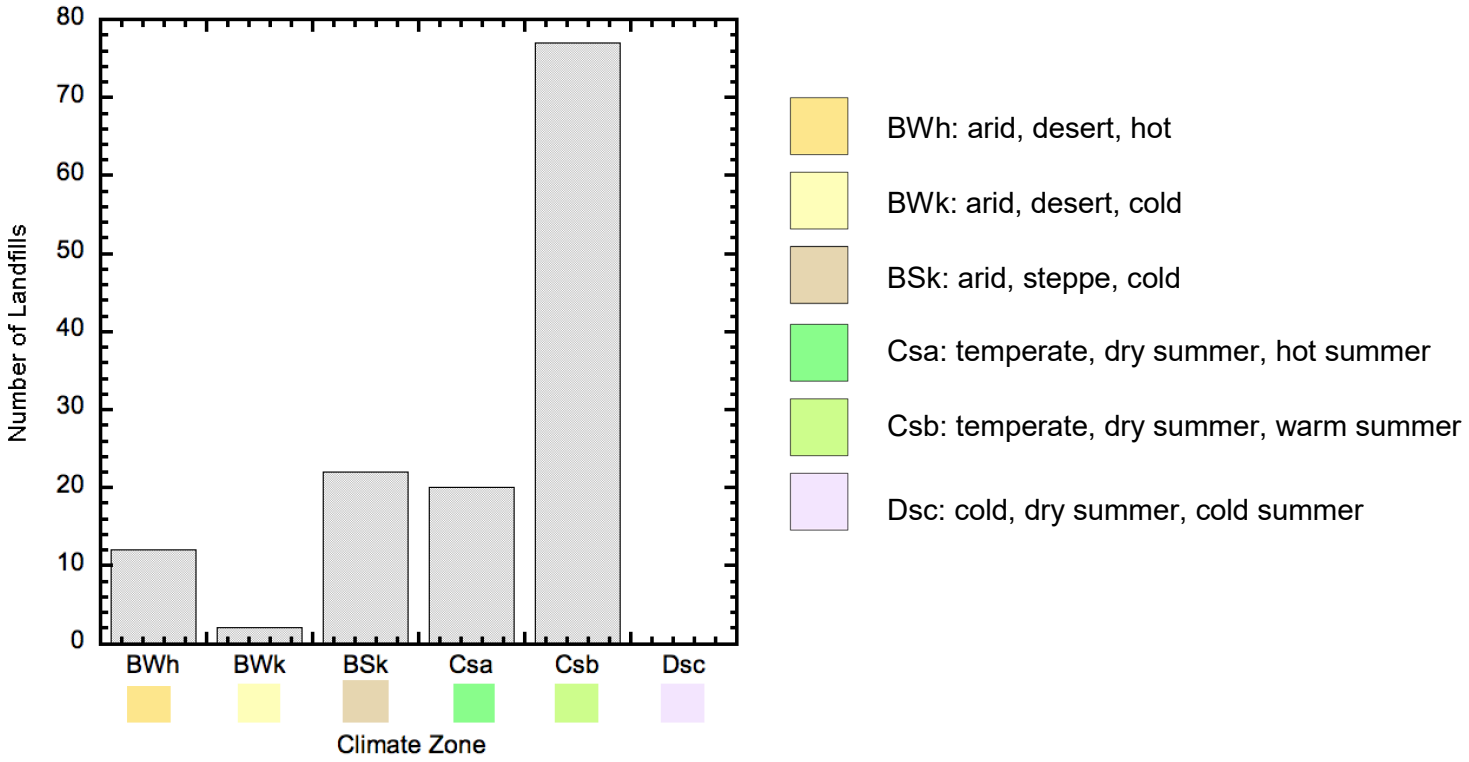

Figure 2.12 Relative Distribution of Number of California Landfills with Climate Zone

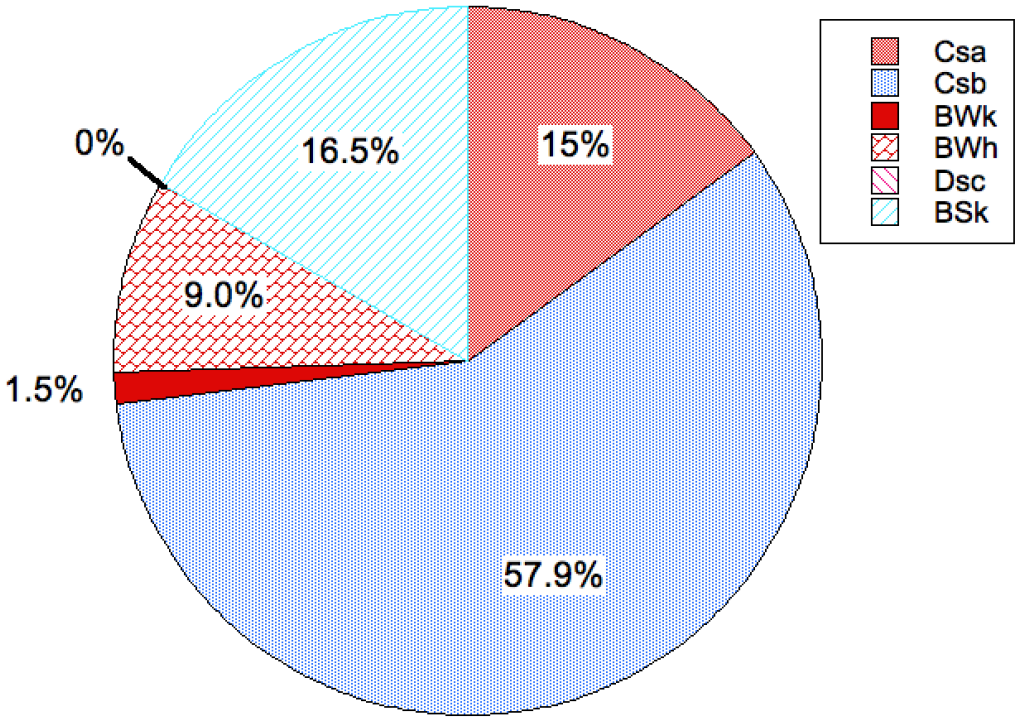

Figure 2.13 Histogram of Number of Landfills and WIP in the Landfills with Climate Zone

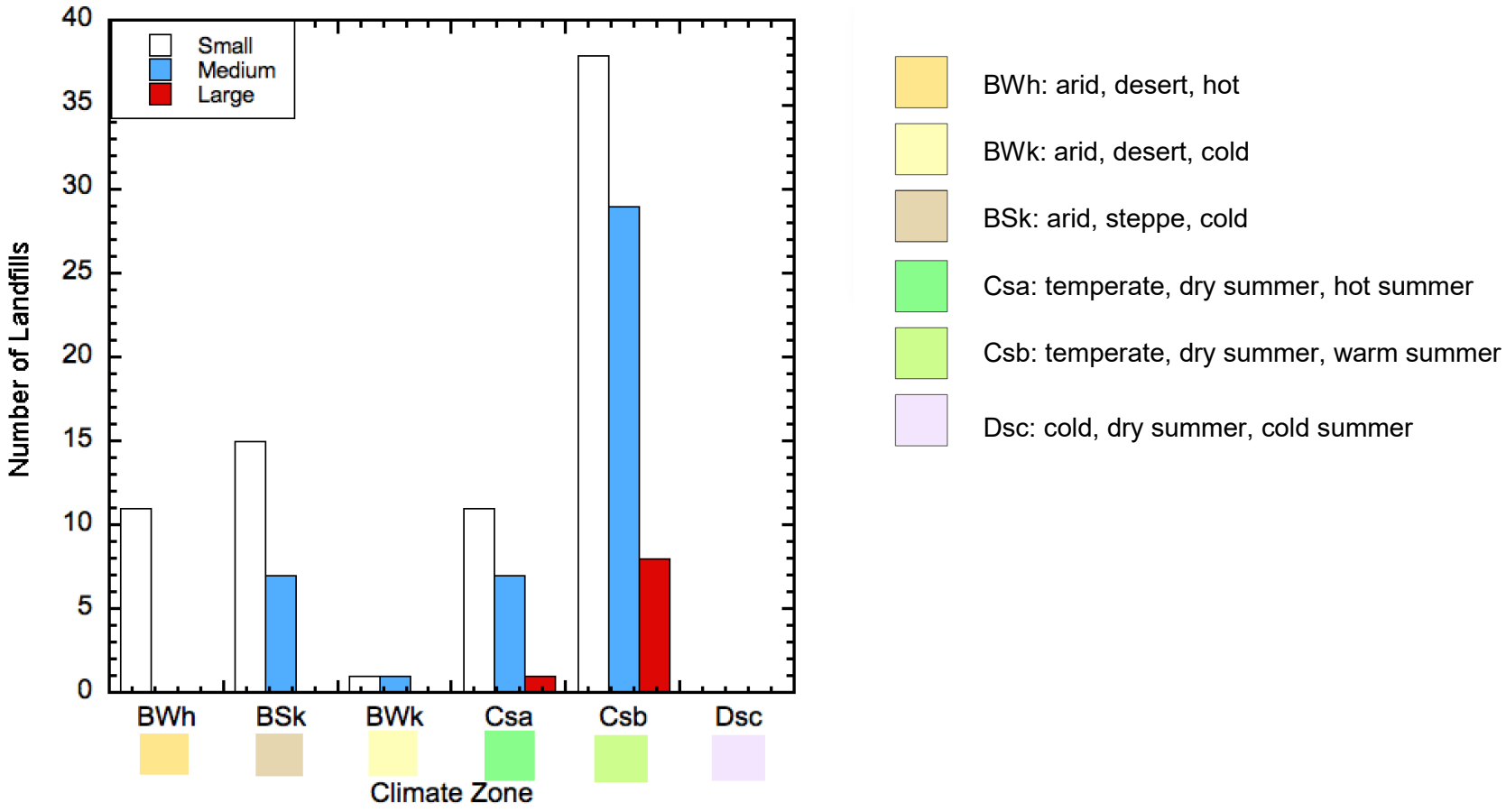

Figure 2.14 Relative Distribution of WIP with Climate Zone

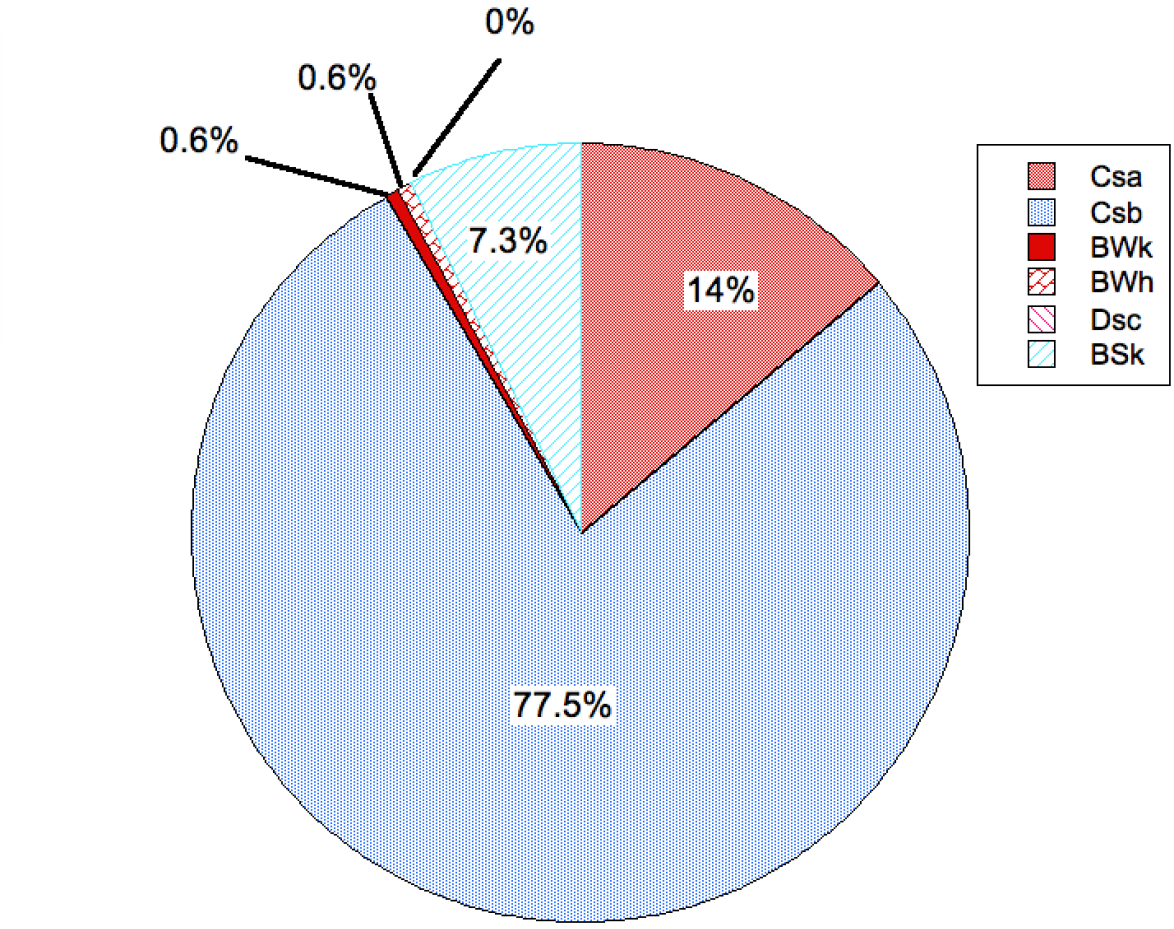

Landfill size classified in accordance with WIP and locations of oil and gas operations and fault lines in the state (that may have emissions/emissions pathways, which may affect landfill emissions measurements) are presented in Figures 2.15 and 2.16, respectively. A composite plot of landfill location, size, oil and gas operations, and fault lines is presented in Figure 2.17. The data in Figure 2.17 indicated that the majority of the landfill sites in California were in close proximity of oil and gas operations and fault lines. Oil and gas operations and landfills typically were located in central to western California. The extent of both oil and gas operations and landfill facilities were very low in eastern California. Fault lines are prevalent throughout the landmass of the state and also were in proximity of landfill facilities. Due to the prevalent extent of nearby oil and gas operations and fault lines, proximity to such features was not considered as a direct selection criterion.

Figure 2.15 Location of California Landfills in relation to Oil and Gas Operations

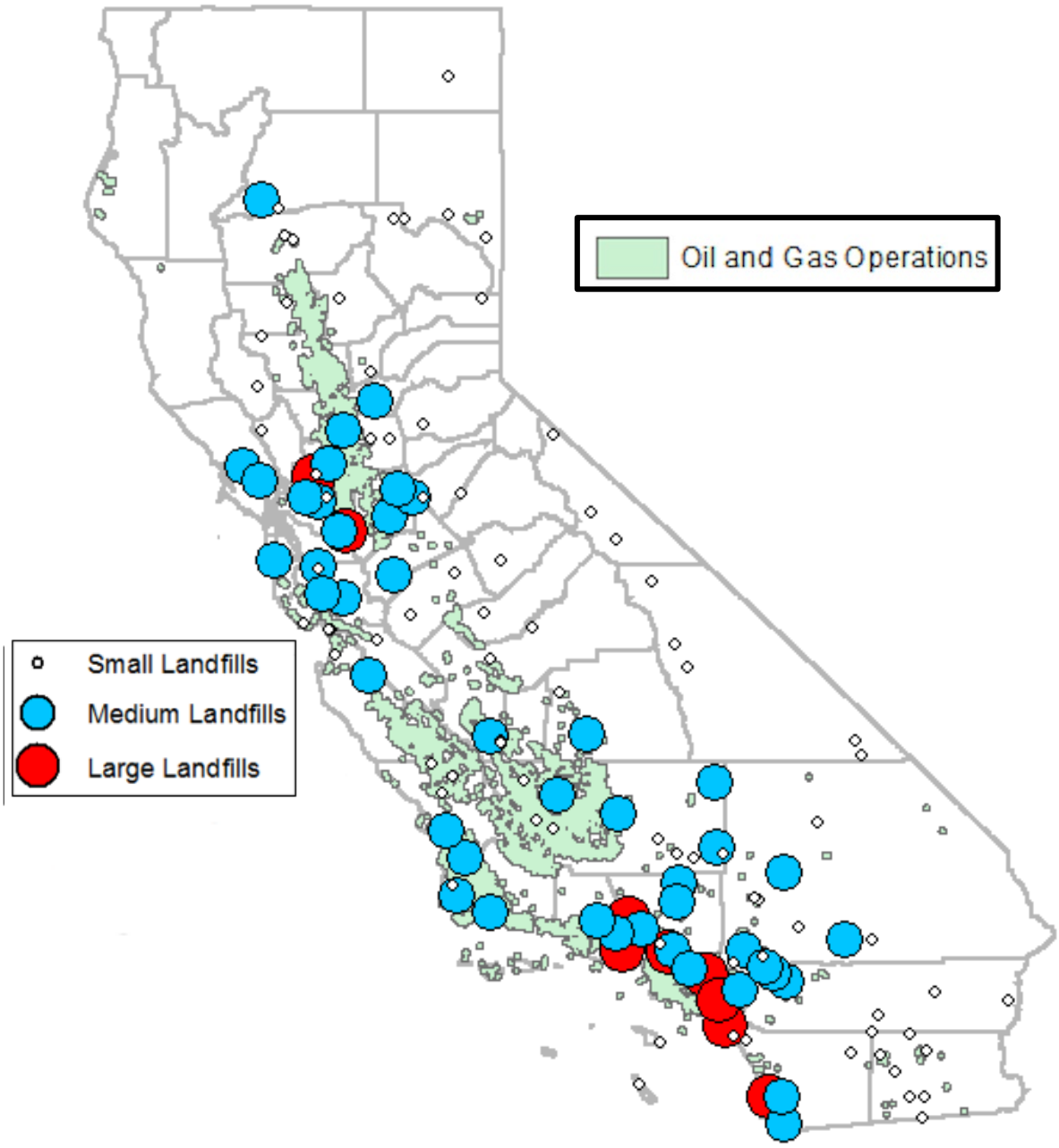

Figure 2.16 Location of California Landfills in relation to Fault Lines

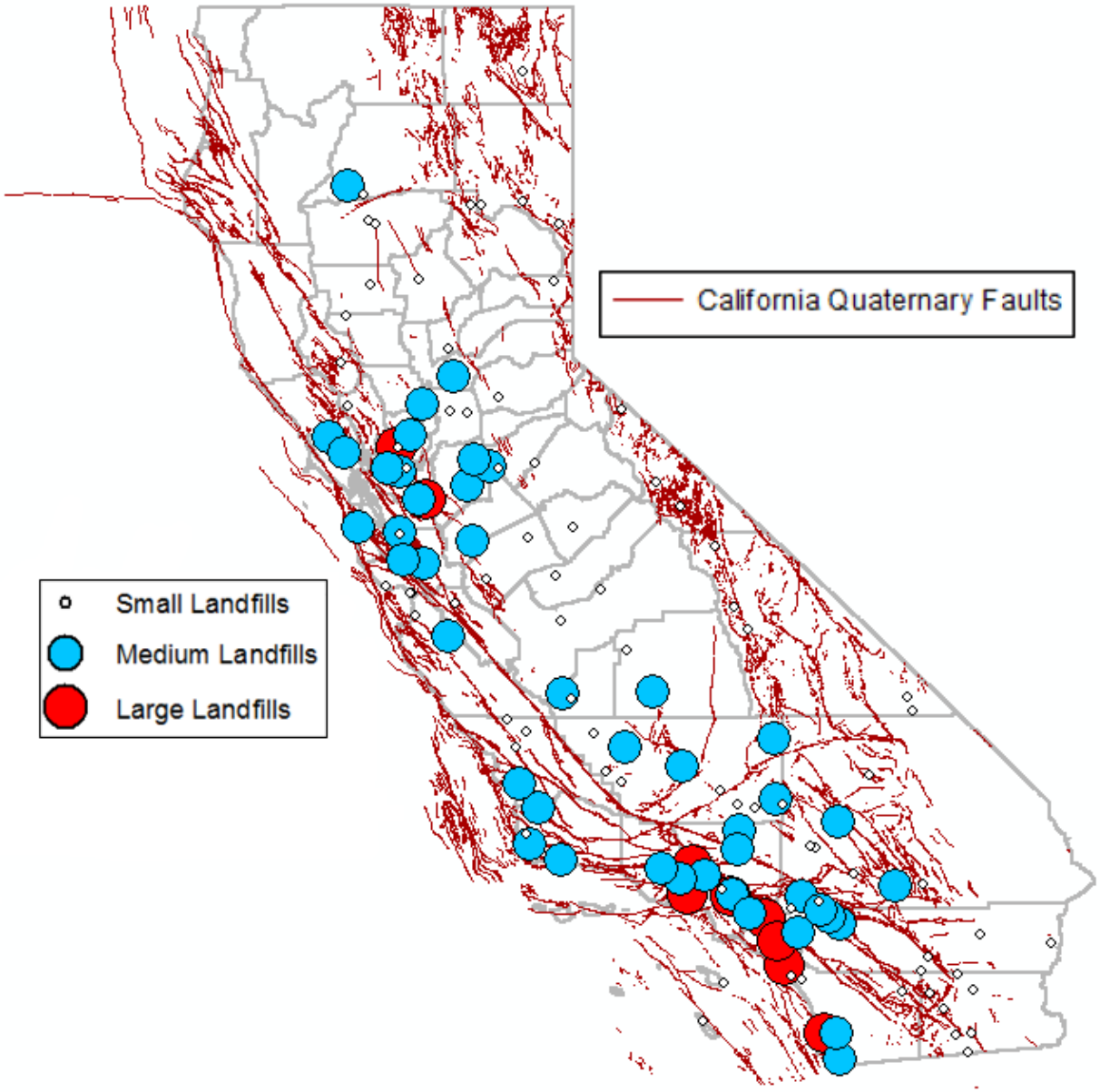

Figure 2.17 Location of California Landfills in relation to Oil and Gas Operations and Fault Lines

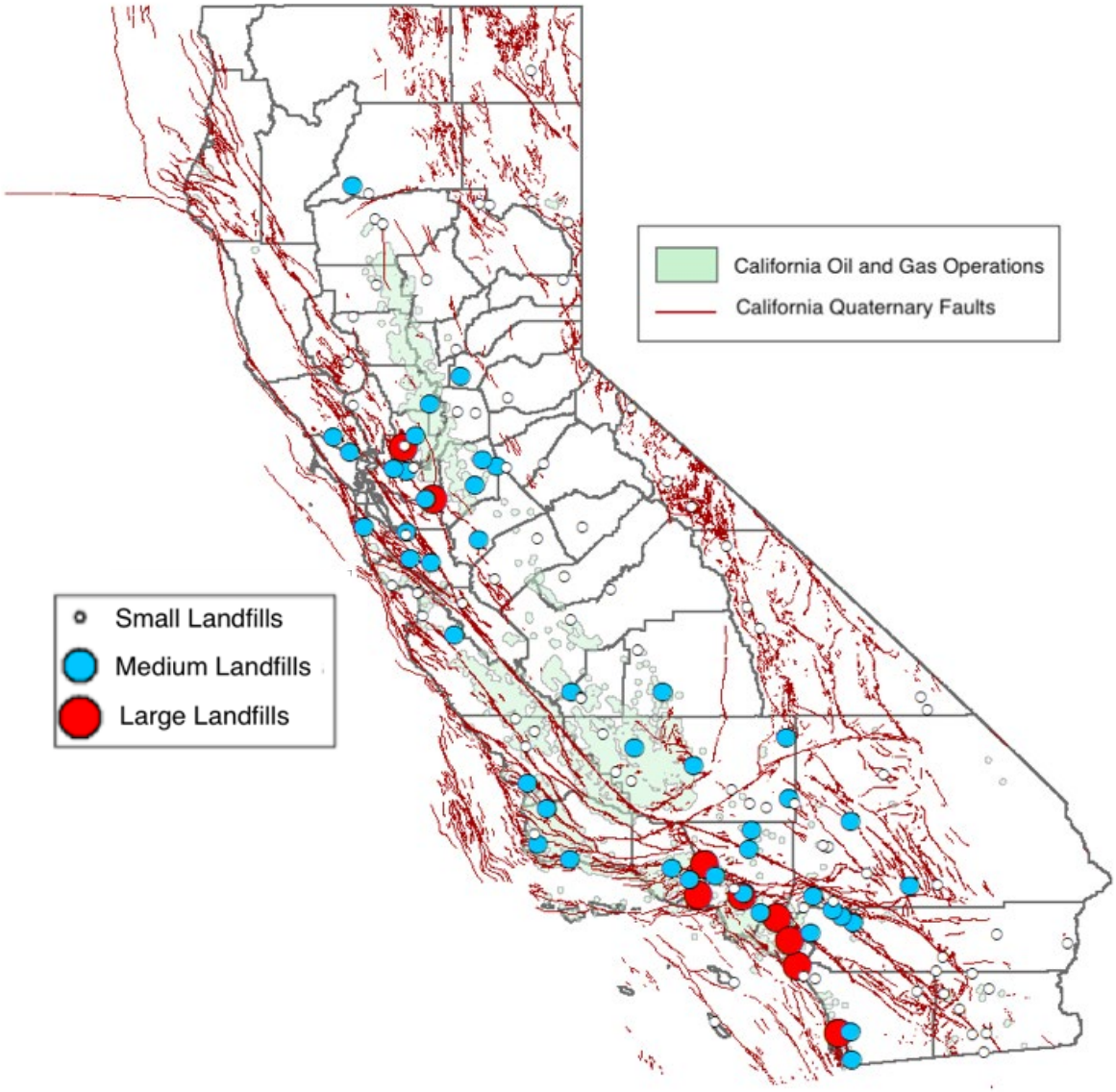

A map of California with population density is presented in Figure 2.18. Location of California landfills with WIP data and variation of population density in the state is presented in Figure 2.19. Landfills are typically located near population centers and were clustered around large metro areas including Bay Area and Sacramento in northern California and Los Angeles and San Diego in southern California.

Figure 2.18 Population Density in California

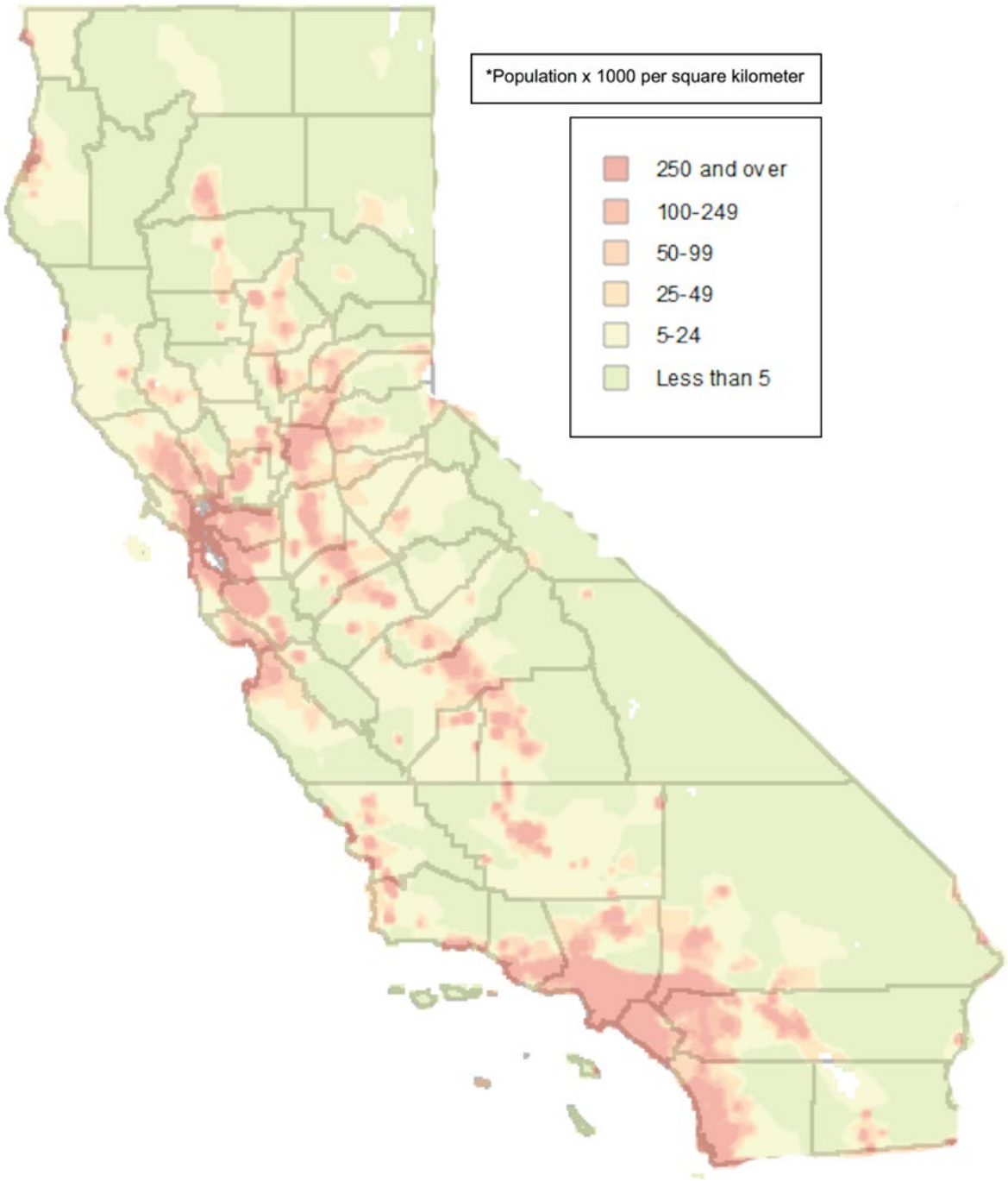

Figure 2.19 Location of California Landfills in relation to Population Density

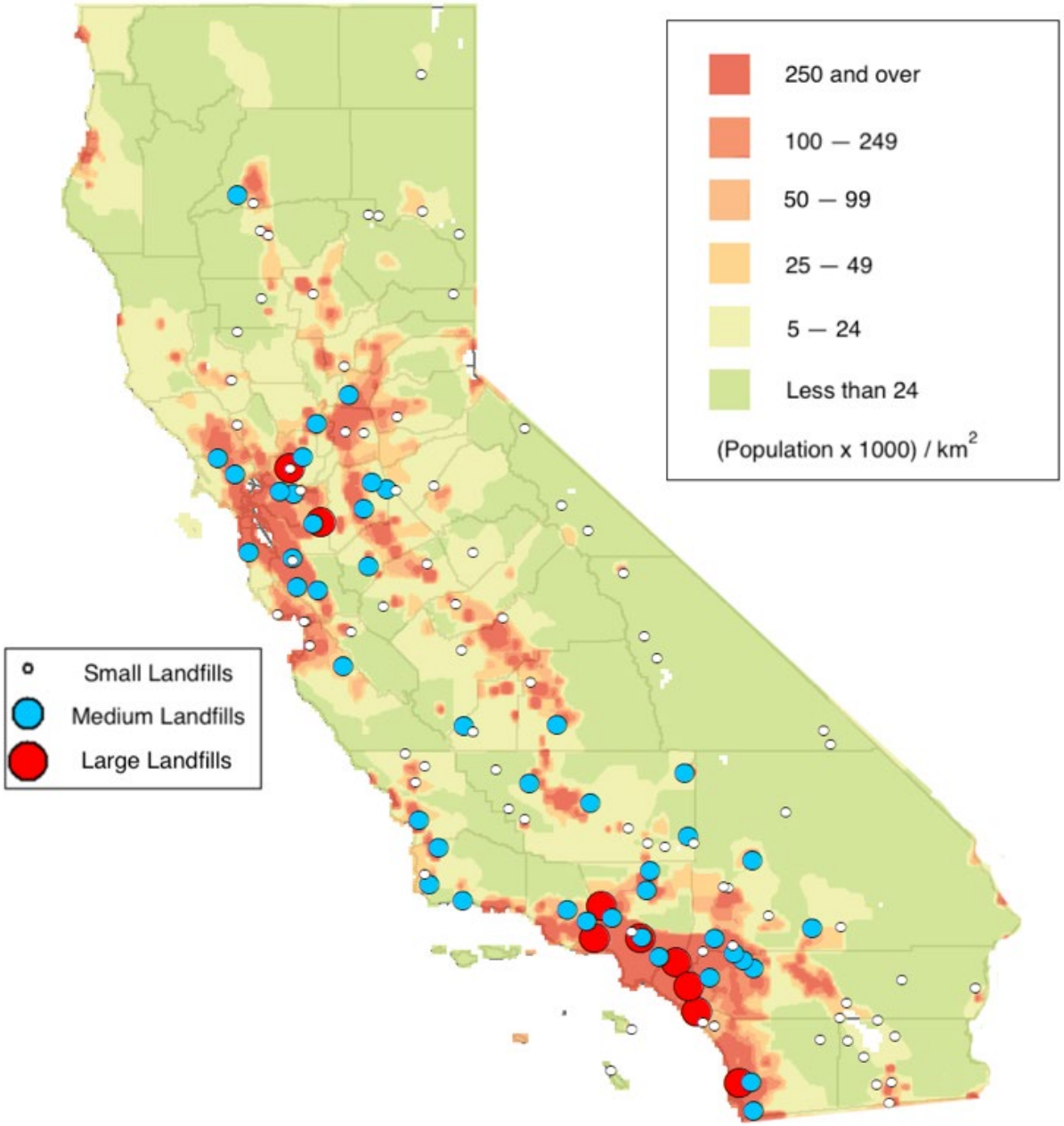

Landfills with active gas collection systems are presented in Figure 2.20. Gas collection systems were identified to have been installed at 74 landfills in the state. Landfills that accept tires are presented in Figure 2.21. A total of 63 landfills were identified as facilities with tires in the disposed waste stream. The landfills without gas collection systems and facilities that do not accept tires also are shown in the plots for reference.

Figure 2.20 California Landfills with Gas Collection Systems

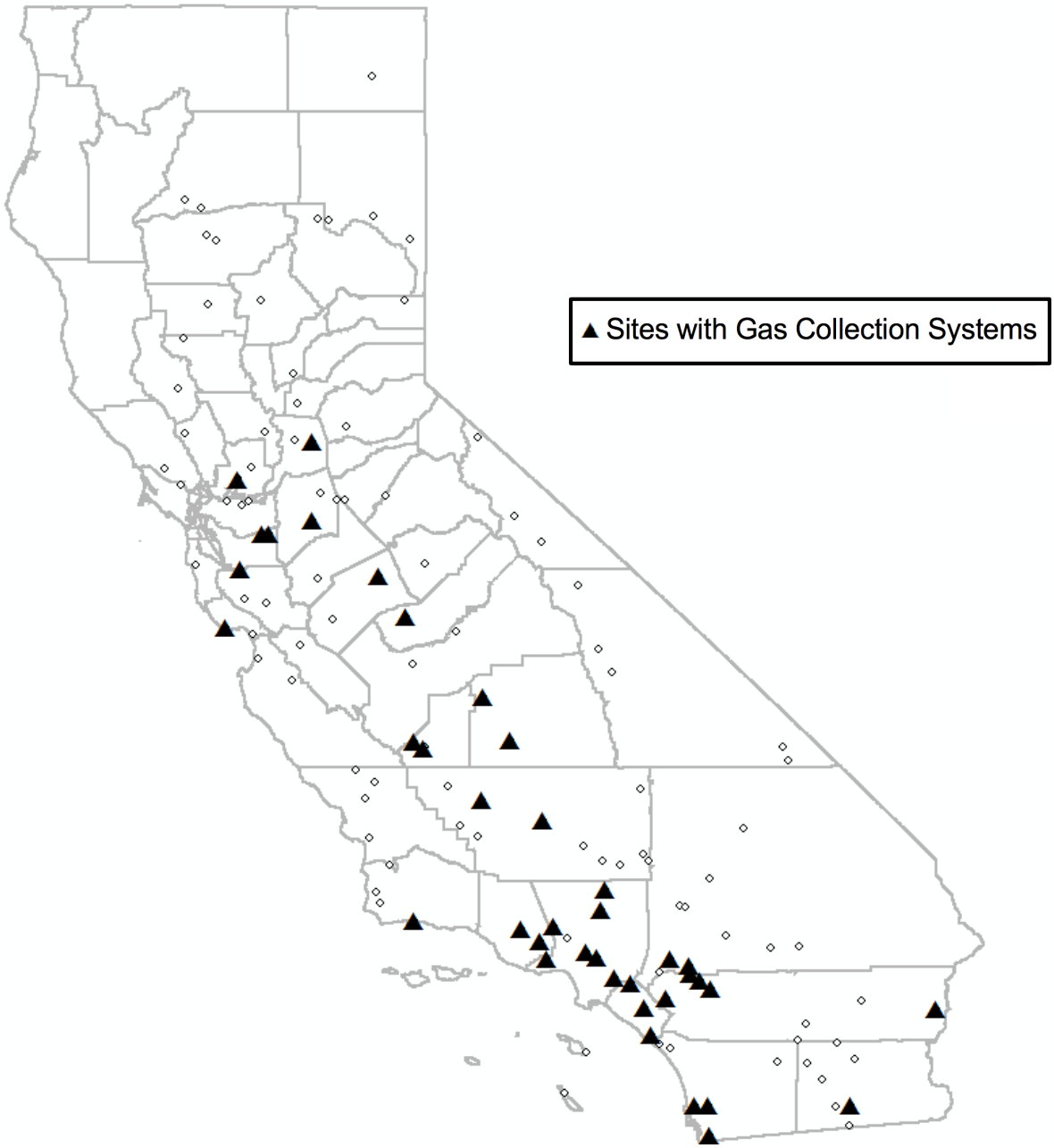

Figure 2.21 California Landfills that Accept Waste Tires

2.3 Landfill Site Selection

The landfill site selection protocol included a two-step process, first identifying a larger subset of landfills for aerial gas emissions measurements and then second identifying a smaller subset of the landfills included in the aerial measurements for land-based static flux chamber measurements. A total of 15 landfills was selected in the first step and then 5 of these landfills were further selected for chamber testing.

The majority of the criteria described in Table 2.2 was used for the first step of the selection process to identify the 15 landfill sites. The main facility size factor used in the analysis was waste in place. Facilities from all three WIP categories including small, medium, and large, were included in the analysis. Climatic conditions also were considered. Sites from all 5 climatic zones with landfills in California were targeted. Proximity to oil and gas operations and proximity to fault lines were not significant selection criteria as the landfill sites throughout the state was demonstrated to be in proximity to these sites (Figure 2.15) with no significant differences between the majority of the landfills in the state based on these criteria. Sites near population density centers and low-population rural areas were targeted. Sites with and without gas collection systems and with and without tire disposal was targeted. In general, sites with all three types of cover systems, including daily, intermediate, and final covers, were considered in the selection process. Relative fraction of the three cover categories and size of the working face at the landfill facilities also were included in the selection process. Landfills representing both areal and canyon facilities were selected. Landfills with wastes with different ages and varying operational conditions in particular in terms of waste types were included in the site identification process.

The 15 sites selected for the aerial measurements are presented in Table 2.3. The sites are listed in order of increasing WIP. The distribution of the sites across the state is presented in Figure 2.22. The small sites were selected to include all five climatic zones with landfills in California (Figure 2.10) in the aerial emissions analysis as medium- and large-size landfills are not located in all five climatic zones. The number of small sites selected for the analysis was higher than the number of medium landfills and also higher than the number of large landfills. The rationale for this choice was to include a high number of landfills without gas collection systems in the analysis recognizing the fact that the medium and large landfills have gas collection systems unless this is a facility that has become operational very recently and sufficient amount of waste placement that requires installation of a gas collection system has not yet occurred. The potential for high emissions from landfill facilities without gas collection systems was evaluated with the selection of these sites. The medium sites were selected in the three climatic zones with the highest amount of waste in place in the state including Csb, Csa, and Bsk climate zones (Figure 2.14). The large landfills are located in Csb and Csa climate zones and four landfills from these climate zones are included in the analysis. The small landfills are located in rural areas, the medium landfills also are located mainly in rural areas, whereas the large landfills are located in close proximity to major urban centers in northern and southern California (Figure 2.22). The active face at the facilities ranged from 65 to 12,100 m^2. The relative fractions of the daily, intermediate, and final covers were 0.1 to 20%, 25 to 99.8%, and 0 to 40.7%, respectively.

Table 2.3 – Landfills Selected for Aerial and Ground Testing (Bold Font for Ground Testing Sites)

No.	Landfill Name	Size	WIP* (m^3)	Permitted Throughput (tons/day)	Climate Zone	Gas Collection System	Tires	Active Face (m^2)	Cover Fraction[a] (%)		
									D	I	F
1	Stonyford Disposal Site	S	71,513	10	Csb	No	Yes	65	1.7	96.5	1.8
2	Salton City Solid Waste Site	S	152,082	6,000	BWh	No	No	NR	NR	NR	NR
3	Borrego Landfill	S	278,752	50	Bsk	No	Yes	NR	NR	NR	NR
4	Pumice Valley Landfill	S	292,496	110	Csb	No	No	1200	NA	25	0
5	Mariposa County Sanitary Landfill	S	594,757	100	Csa	No	Yes	200	20	80	0
6	Taft Recycling and Sanitary Landfill	S	2,767,148	800	BWk	No	Yes	NR	NR	NR	NR
7	**Teapot Dome Disposal Site**	M	5,369,126	800	BSk	Yes	No	1200	15.5	84.5	0
8	**Santa Maria Regional Landfill**	M	8,385,395	858	Csb	Yes	Yes	700	0.1	69.3	30.6
9	Redwood Landfill	M	17,643,577	2,300	Csb	Yes	Yes	2000	0.2	99.8	0
10	Simi Valley Landfill and Recycling Center	M	27,697,889	9,250	Csb	Yes	No	12100	0.7	99.3	0
11	Yolo County Central Landfill	M	37,490,107	1,800	Csa	Yes	Yes	11800	1.4	57.9	40.7
12	**Chiquita Canyon Sanitary Landfill**	L	42,266,798	6,000	Csb	Yes	No	5600	8.3	63.8	27.8
13	**Site A**	L	45,108,745	11,150	Csb	Yes	Yes	6100	0.6	89.5	9.9
14	Frank R. Bowerman Sanitary Landfill	L	46,637,855	11,500	Csb	Yes	No	NR	NR	NR	NR

No.	Landfill Name	Size	WIP* (m^3)	Permitted Throughput (tons/day)	Climate Zone	Gas Collection System	Tires	Active Face (m^2)	Cover Fraction[a] (%)		
									D	I	F
15	**Potrero Hills Landfill**	L	52,928,614	4,330	Csa	Yes	Yes	3000	3	91	6

*Sites listed in order of WIP; Data from SWIS database (2017)
NR – Not Reported
[a]D = daily, I = Intermediate, F = Final

Figure 2.22 Landfills Selected for Aerial and Flux Chamber Testing

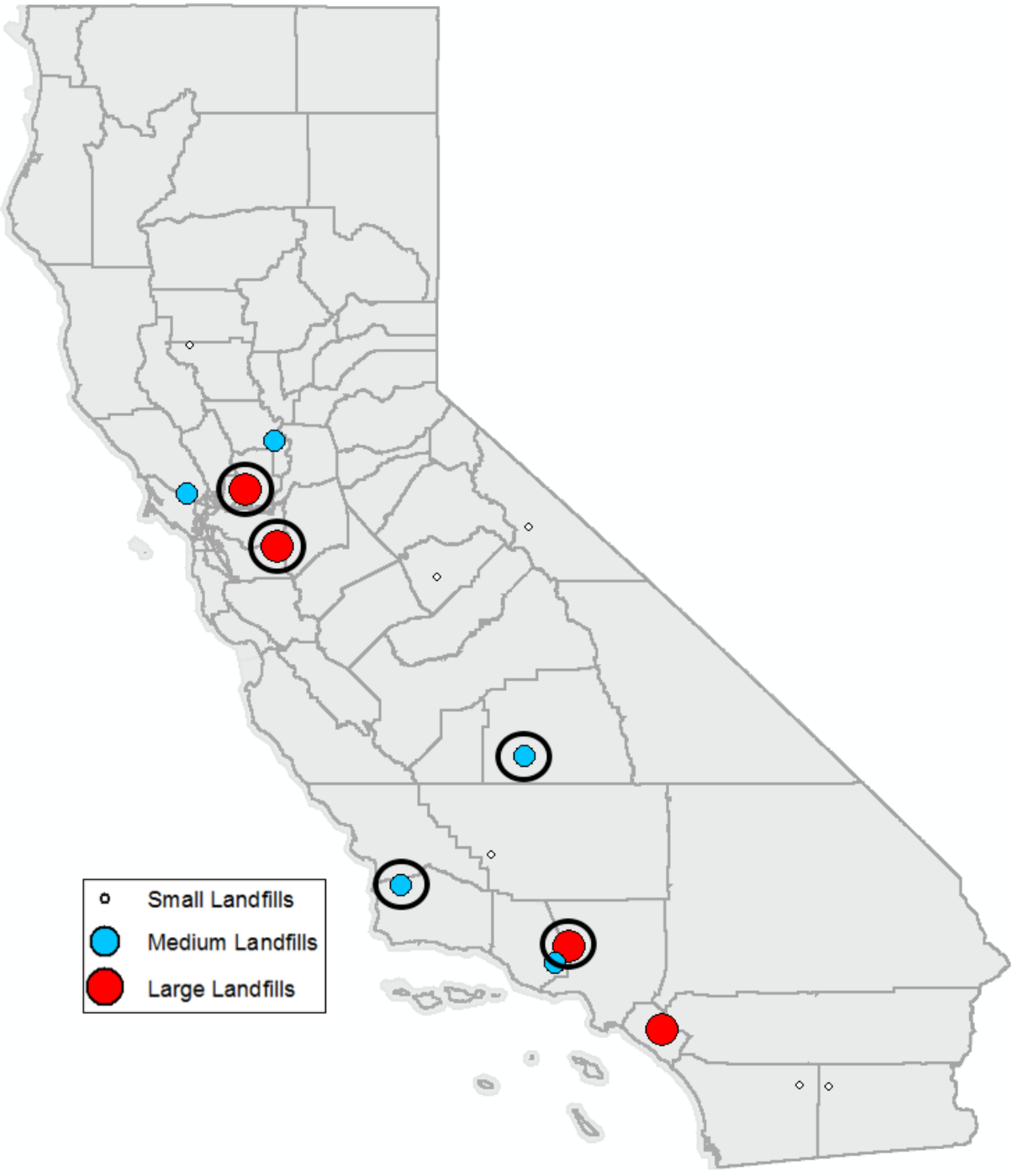

The five sites selected for static flux chamber testing are presented in bold in Table 2.3 and also marked in Figure 2.22. The emissions from the small landfills were low even though these sites did not have gas collection systems and thus small sites were not selected for further testing for static chamber analysis. The five selected sites included two medium-size facilities and three large landfills. The sites were located in the three climatic zones with the highest amount of waste in place in California including Csb, Csa, and Bsk climate zones (Figure 2.14). The total amount of waste in place at the five and fifteen selected sites was 154 million m^3 and 288 million m^3 and represented 13% and 24% of the total amount of WIP in California, respectively. All three large sites and one of the medium sites had all three cover systems, whereas the second medium site had only daily and intermediate covers (Table 2.3). The active face size and the relative areal extent of the three cover systems at the sites were variable and representative of the cover conditions in the state. The medium sites are areal landfills, whereas two of the large landfills (Altamont Landfill and Chiquita Canyon Landfill) are canyon landfills. The third large site (Potrero Hills Landfill) is located in a hilly area. Cooperation of sites was an essential component of selection for participation in the investigation.

PART 3 – FIELD INVESTIGATION, EXPERIMENTAL METHODOLOGY, AND NUMERICAL MODELING

3.1 Introduction

The field-testing program was designed with six specific objectives to obtain representative landfill surface gas flux and emissions data as a function of the main factors that control gas emissions from landfill sites:

- Obtain data and identify emissions trends for a large variety of landfill gas species ranging from the main landfill gases to various classes of trace gases with potential greenhouse gas, human health, and environmental impacts
- Obtain data from multiple landfills to assess the inter-landfill variability of gas emissions
- Obtain data over different seasons to assess effects of climatic conditions on inter- and intra-landfill gas emission variations
- Obtain data from all cover categories at a given landfill including daily, interim, and final covers to assess effects of cover category on intra-landfill gas emission variations
- Obtain data from locations underlain with wastes of varying ages to assess effects of waste age on intra-landfill gas emission variations
- Obtain data gas flux data at one landfill as a function of location away from a gas well, time of day of measurement, changes in gas extraction rates, and thickness of one soil cover material

The field testing included two types of measurement programs (October 2017 to November 2019): aerial measurements of methane and ethane at height above the landfill surfaces and measurements of all of the 82 landfill gas species included in the investigation directly on the landfill surfaces. Testing in the wet and dry seasons was conducted over the project period for both aerial measurements and ground-based measurements. Based on precipitation averages at the ground-based test sites, the wet season was defined as October 15 to April 30, and the dry season as May 1 to October 14.

3.2 Aerial Measurements of Gas Emissions

Aerial testing was completed at 16 sites during the project by Scientific Aviation to measure methane emissions. The test sites included the 15 landfills identified in Section 2 (Table 2.3) and one additional landfill (Sunshine Canyon Landfill) that provided opportunity for comparison of two similar, nearby landfills (Chiquita Canyon Landfill and Sunshine Canyon Landfill) that have different operational practices in regards to stripping of intermediate cover prior to placing overlying wastes (Chiquita Canyon Landfill strips the cover, Sunshine Canyon Landfill does not). When possible, ground testing and aerial testing were aligned to provide synchronous measurements of emissions.

Aerial surveys were conducted using a single engine Mooney aircraft that was instrumented with a Picarro G2401-m Analyzer (cavity ring down spectrometer). Ambient air is collected through tubes protruding from the right wing (Kynar, Teflon, and stainless steel). The Picarro instrumentation can analyze samples in-flight, allowing for almost instantaneous emissions results (Picarro, Inc. 2018). Methane and carbon

dioxide measurements are made with a Picarro 2301f cavity ring down spectrometer as described in Crosson (2008). Ethane measurements are made with an Aerodyne Methane/Ethane tunable diode infrared laser direct absorption spectrometer (Yacovitch et al. 2014). The plane flies in circles at various elevations around the site capturing both the up- and down-wind air concentrations. Assuming a Gaussian plume distribution, an emissions value can be determined in terms of mass per time (i.e., kg/hr). Emissions values have an accompanying uncertainty value, corresponding to a calculated uncertainty for each lap flown and then all uncertainties are summed, leading to generally higher values than expected for a typical standard deviation or similar value (Conley et al. 2017).

Aircraft have been used extensively to estimate surface emissions of pollutants and greenhouse gases (Karion et al. 2013, Caulton et al. 2014, Chang et al. 2014, Conley et al. 2016). Two sampling methods are routinely employed to estimate surface fluxes from aircraft, straight line transects and elliptical flight loops. All else being equal, the ellipse method is preferred because there are as many measurements of the upwind flux as there are the downwind. However, the ellipse method is not always practical, owing to complex terrain, air traffic restrictions, or other obstacles, which precludes creating a reasonable closed flight path around the site. Both methods have been demonstrated to be effective. Each of the methods has an uncertainty that can be determined from a theoretical analysis of the terms in the scalar budget of interest.

For the closed-path method (elliptical method) the flight path is chosen to build a virtual cylinder around the source, as presented in Figure 3.1. The flight path begins approximately 150 m above the ground level (AGL), depending on the site-specific terrain, which is aligned with the lowest safe flight level designated by the FAA, and ends at a higher altitude when enough laps have been conducted to reach a reliable measurement (Conley et al. 2017). At each point along the cylinder, the flux normal to the cylinder is calculated, thus providing the total amount of gas entering and leaving the cylinder. The difference between the two (assuming no other sources or sinks) is the surface emission rate.

Figure 3.1 Schematic of Flight Path around Unknown Source

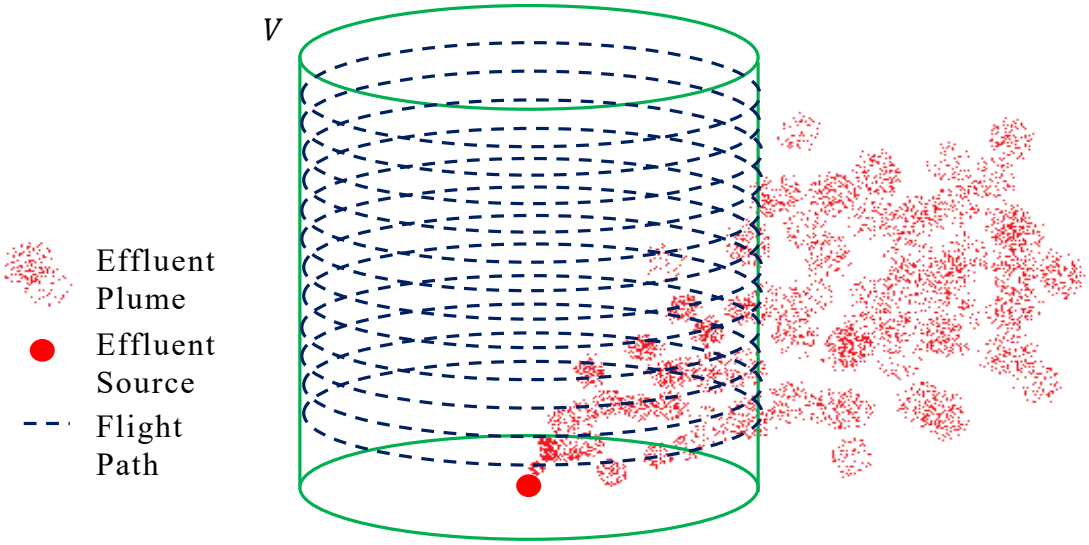

Mathematically, the method is straightforward and begins with the integrated form of the scalar continuity equation.

$$\langle \frac{\partial m}{\partial t} \rangle + \iiint \nabla \cdot \boldsymbol{F}_c dV = Q_c \tag{3.1}$$

Where, m is mass, t is time, F_c is flux, V is volume, Q_c is gas emission rate. The integrand in Equation 1 is the divergence of the flux and is summed (integrated) over the entire volume surrounding the source. The brackets in Equation 1 indicate a volumetrically averaged quantity, such as the time rate of change (or storage). Gauss's theorem is used to establish that the total divergence within a closed path is equal to the line integral (around the closed path) of the flux normal to the path.

$$Q_c = \langle \frac{\partial m}{\partial t} \rangle + \iiint \nabla \cdot \boldsymbol{F}_c dV = \left\langle \frac{\partial m}{\partial t} \right\rangle + \oint \boldsymbol{F}_c \cdot \hat{\boldsymbol{n}}\, dS \tag{3.2}$$

At any point along the path, the gas concentration is multiplied by the component of the wind vector normal to the path to yield the flux normal. Those fluxes are then summed over the closed path, and the result is the total divergence at that altitude. Next the divergences of all the circles at altitudes ranging from near the surface to the top of the plume are added together to yield the total surface source strength. The three main assumptions used in the analysis are: i) no vertical flux across the top of the virtual cylinder, ii) the virtual cylinder encompasses all of the plume from the ground source, and iii) all of the emissions are contributed by the ground source encompassed by the virtual cylinder formed by the flight path.

3.3 Ground-Based Measurements of Gas Emissions

Information for the landfills included in the ground-based testing program of the field investigation is summarized in Table 3.1. The table includes landfill name, landfill

location, size (provided in terms of waste in place), climate zone, annual precipitation, average daily temperature, and number of test locations at each landfill. A period of 30 years is commonly used for analyzing near-surface ground temperatures (e.g., Andersland and Ladanyi 1994) and was selected for this investigation of landfill cover systems. The climate zones for the selected landfills represented the zones with the highest amount of waste in place in the state (Figures 2.13 and 2.14).

Static flux chambers were used to directly evaluate the surface flux of all of the 82 gases included in the investigation. All of the available cover categories and all of the cover types under a given cover category were tested at the ground-testing sites. These locations also had different underlying waste ages, waste column heights, and waste characteristics. Subsequent to completion of the tests, cover temperatures at the test locations were obtained as well as densities of the covers were determined. When the flux tests were completed, cover material samples were collected to determine the geotechnical properties of the cover materials. Source gas (i.e., raw gas) from the landfill gas collection systems, was collected during each field campaign.

Table 3.1 – Ground Testing Landfill Sites

Landfill Name	Landfill Location	Waste in Place[a] (m^3)	Waste in Place[b] (m^3)	Landfill Climate Zone	Annual Ppt. (mm)[c]	Avg. Daily Temp (°C)[c]	Test Locations per Season
Santa Maria Regional Landfill	Santa Maria	1,360,577	8,385,395	Csb	462	14.9	5
Teapot Dome Disposal Site	Porterville	3,038,622	5,369,126	Bsk	278	17.4	5
Potrero Hills Landfill	Suisun City	26,454,935	52,928,614	Csa	462	18.2	7
Site A	Livermore	44,173,397	45,108,745	Csb	387	15.8	6
Chiquita Canyon Sanitary Landfill	Castaic	55,227,178	42,266,798	Csb	630	16.1	7

[a] WIP values reported by sites

[b] WIP values obtained from SWIS (2017)

[c] NOAA 30-year average for 1981-2010 (https://www.ncdc.noaa.gov/cdo-web/datasets)

3.4 Test Sites

Summaries of the ground testing sites are presented in the subsequent sections. The landfills are organized in order of smallest to largest WIP, as classified in SWIS. Thirty-year average weather data (1981 to 2010) for each site was obtained from NOAA (2019). All sites had active gas collection systems in place at the time of testing.

3.4.1 Teapot Dome Disposal Site

Teapot Dome Disposal Site (Teapot Dome Landfill) is a medium-size landfill (Section 2.2, Table 2.3) located in Porterville, California, approximately 115 km south of Fresno. The site is in an arid, steppe, and cold climate (Peel et al. 2007). Average weather data over a 30-year period indicate a daily average temperature of 17.4°C and average annual precipitation of 27.8 cm. The reported disposal area is 287,317 m^2 and the reported design capacity is 6,024,927 m^3 (SWIS 2017). The site is an areal site. The estimated closure date is 2022. The permitted throughput is 381 tonnes/day and the waste in place as of 2018 is 3,038,621 m^3 based on site records. Teapot Dome Landfill does not accept waste tires. The site has a specifically designated winter waste placement area used during the wet season. The site has daily and intermediate covers with no final cover present. Daily cover consists of processed green waste of approximately 4 cm (ranging from 2 to 8 cm) in thickness over 23 cm of soil at tested locations in the dry season, and a soil cover with a depth of 19 cm in the wet season at the tested locations. Intermediate cover consisted primarily of soils ranging in thickness from 34 to 78 cm at tested locations and in one case was 33 cm of soil overlying 9 cm of processed green waste. The cover types, designations, and thicknesses are presented in Table 3.2. A site map with testing locations is presented in Figure 3.2.

Table 3.2 – Teapot Dome Landfill Cover Characteristics

Cover Type Designation	Cover Type Description	Thickness (cm)
DC-GW	Daily Cover - Green Waste	27 (Dry Season)
DC-S	Daily Cover – Soil	19 (Wet Season)
IC-S+GW	Interim Cover - Soil + Green Waste	42
IC-N	Interim Cover - New (Waste)	35
IC-O	Interim Cover - Old (Waste)	78
IC-W	Interim Cover - Winter (Winter Waste Placement Area)	34

Figure 3.2 Teapot Dome Landfill with Test Locations (Google Maps 2019)

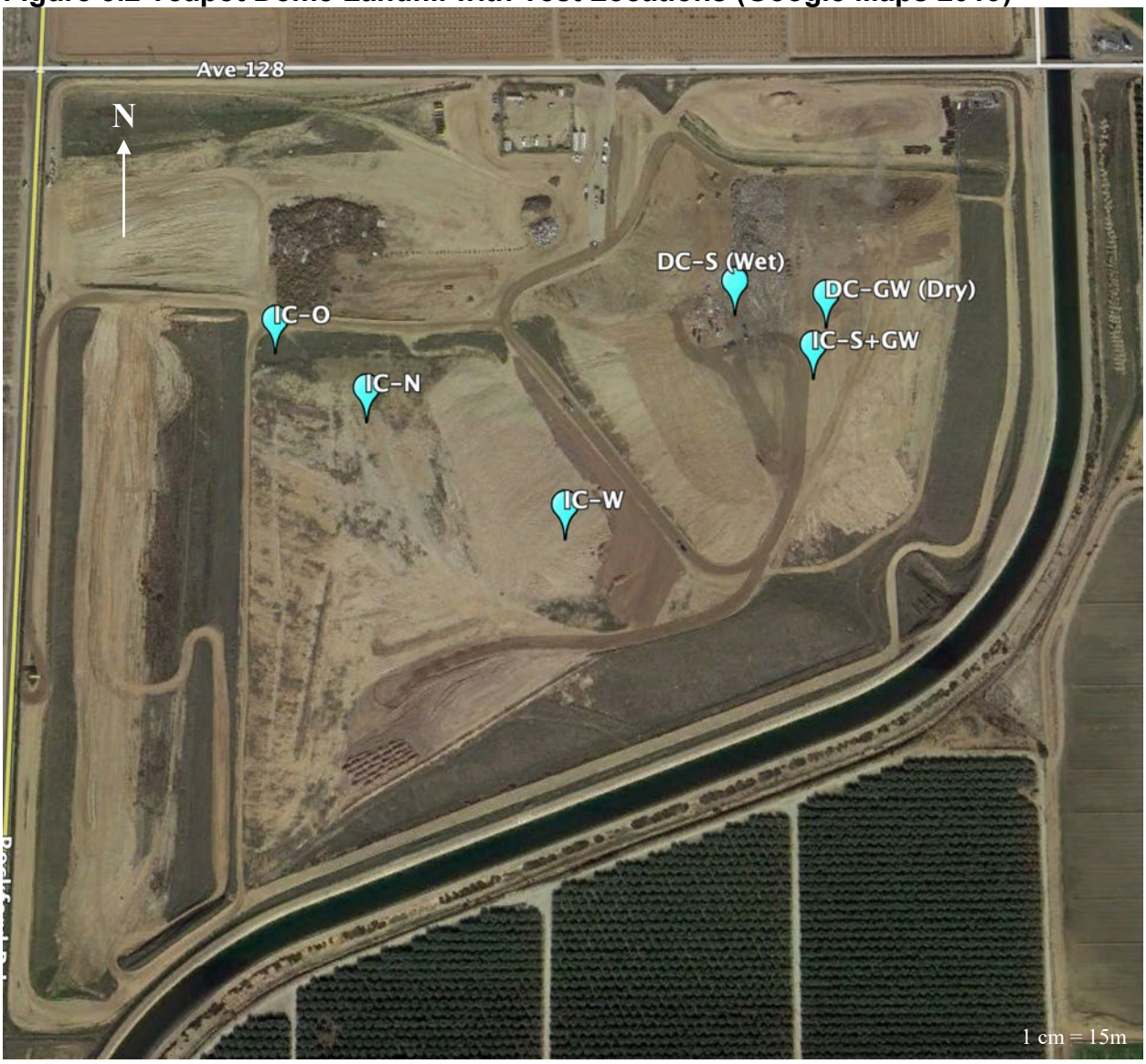

3.4.2 Santa Maria Regional Landfill

Santa Maria Regional Landfill is a medium-size landfill (Section 2.2, Table 2.3) located in Santa Maria, California. The site is in a temperate, dry summer and warm summer climate (Peel et al. 2007). Average weather data over a 30-year period indicate a daily average temperature of 14.9°C and average annual precipitation of 46.2 cm. The reported disposal area is 999,946 m^2 and the reported design capacity is 10,702,545 m^3 (SWIS 2017). The site is an areal site. The estimated closure date is 2020. The permitted throughput is 778 tonnes/day and the waste in place as of 2018 is 1,360,577 m^3, based on site records. Santa Maria Regional Landfill does not accept waste tires. The site has daily, intermediate, and final cover areas. Daily cover consists of wood waste received at the site with an approximate depth of 28 cm at tested locations. This daily cover is overlain with concrete fines with an approximate depth of 50 cm to

construct an interim cover. Other tested locations for interim cover consisted of soil with a thickness of approximately 68 cm. Final cover is present over an older cell of the site and consists of 100 cm of soil underlain by a GCL and 61 cm of interim cover material below the GCL over the waste mass. The landfill's gas-to-energy system is connected to a nearby hospital facility. The site operators indicated that large fluctuation in the gas draw from the landfill occurs due to the variations in hospital electricity use. During the field investigation, the gas-to-energy system was temporarily shut down to simulate of the high and low demand gas draw periods at the hospital. The cover types, designations, and thicknesses are presented in Table 3.3. A site map with testing locations is presented in Figure 3.3.

Table 3.3 – Santa Maria Regional Landfill Cover Characteristics

Cover Type Designation	Cover Type Description	Thickness (cm)
DC-WW	Daily Cover - Wood Waste	28
DC+IC	Daily Cover + Interim Cover	79
IC-H	Interim Cover - High Draw	68
IC-L	Interim Cover - Low Draw	68
FC	Final Cover	100

Figure 3.3 Santa Maria Regional Landfill with Test Locations (Google Maps 2019)

3.4.3 Chiquita Canyon Sanitary Landfill

Chiquita Canyon Sanitary Landfill (Chiquita Canyon Landfill) is a large-size landfill (Section 2.2, Table 2.3) located in Castaic, California, approximately 65 miles northwest of Los Angeles, California. The site is in a temperate, dry summer and warm summer climate (Peel et al. 2007). Average weather data over a 30-year period indicate a daily average temperature of 18.2°C and average annual precipitation of 46.2 cm. The reported disposal area is 1,040,008 m^2 and the reported design capacity is 48,885,055 m^3 (SWIS 2017). The site is a canyon site. The estimated closure date is 2019. The permitted throughput is 5443 tonnes/day and the waste in place as of 2018 is 55,227,178 m^3, based on site records. Chiquita Canyon Landfill accepts waste tires. The site has a specifically designated winter waste placement area used during the wet season. The site has daily, intermediate, and final cover areas. Daily cover consists of soil material disposed of at the site, with both uncontaminated (i.e., clean) and contaminated soils used, with thicknesses ranging from 34-50 cm at tested locations. Intermediate cover consists of soils ranging in thickness between 30 and 68 cm at tested locations. An overlying layer of green waste was used on slopes to aid with erosion control, ranging in thickness from 10 cm (old green waste, approximately 1-2 years old, visibly degraded, and gray) to 30 cm (new green waste, approximately 6 months old, and brown) at tested locations. Final cover consists of soil cover approximately 150 cm in thickness including 60 cm of foundation soil, 30 cm of compacted low hydraulic conductivity soil, and 60 cm of vegetative soil layer. The cover types, designations, and thicknesses are presented in Table 3.4. A site map with testing locations is presented in Figure 3.4.

Table 3.4 – Chiquita Canyon Landfill Cover Characteristics

Cover Type Abbreviation	Cover Type Description	Thickness (cm)
DC-Cl	Daily Cover - Clean Soil	34
DC-Co	Daily Cover - Contaminated Soil	50
IC-S	Interim Cover - Soil	30
IC-W	Interim Cover - Winter (Placement of Waste)	40
IC-OGW	Interim Cover - Old Green Waste	65
IC-NGW	Interim Cover - New Green Waste	98
FC	Final Cover	150

Figure 3.4 Chiquita Canyon Landfill with Test Locations (Google Maps 2019)

3.4.4 Site A

Site A is a large-size landfill (Section 2.2, Table 2.3) located in Livermore, California, approximately 55 km northeast of San Jose, California. The site is in a temperate, dry summer and warm summer climate (Peel et al. 2007). Average weather data over a 30-year period indicate a daily average temperature of 15.8°C and average annual precipitation of 38.7 cm. The reported disposal area is 1,910,054 m^2 and the reported design capacity is 95,110,624 m^3 (SWIS 2017). The site is a canyon site. The estimated closure date is 2025. The permitted throughput is 10,115 tonnes/day and the waste in place as of 2018 is 44,173,397 m^3, based on site records. Site A accepts waste tires. The site accepts both Class II (designated waste) (only site included in the analysis with Class II waste) and Class III (nonhazardous solid waste) waste. These wastes are disposed of at different areas at the landfill. Surface flux tests were conducted at both areas of the landfill to capture potential variations in surface gas flux between due to the different waste types. The site has daily, intermediate, and final cover areas. Daily cover consists of auto shredder waste that is covered with soil, ranging in thickness from

approximately 32 to100 cm at tested locations. Intermediate cover consists of different soils ranging in thickness from 40-150 cm at tested locations. Final cover at the site consists of two different types: a traditional final cover and an alternative final cover. The traditional final cover consists of a foundation soil layer, compacted clay layer, and a vegetative soil layer totaling 210 cm thickness. The alternative cover consists of a monolithic evapotranspirative (ET) cover system with an approximate thickness of 90 cm overlying existing interim cover of at least 30 cm. The cover types, designations, and thicknesses are presented in Table 3.5. A site map with testing locations is presented in Figure 3.5.

Table 3.5 – Site A Cover Characteristics

Cover Type Designation	Cover Type Description	Thickness (cm)
ED-II	Extended Daily - Class II (Waste)	100 (Dry Season); 230 (Wet Season)
ED-III	Extended Daily - Class III (Waste)	32 (Dry Season); 139 (Wet Season)
IC-II	Interim Cover - Class II (Waste)	39
IC-III	Interim Cover - Class III (Waste)	151
FC	Final Cover – Class III (Waste)	210
AFC	Alternative Final Cover – Class III (Waste)	120

Figure 3.5 Site A with Test Locations (Google Maps 2019)

3.4.5 Potrero Hills Landfill

Potrero Hills Landfill is a large-size landfill (Section 2.2, Table 2.3) located in Suisun City, California, approximately 72 km southwest of Sacramento, California. The site is in a temperate, dry summer and hot summer climate (Peel et al. 2007). Average weather data over a 30-year period indicate a daily average temperature of 16.1°C and average annual precipitation of 63.0 cm. The reported disposal area is 1,375,886 m^2 and the reported design capacity is 63,534,509 m^3 (SWIS 2017). The site is a canyon site. The estimated closure date is 2048. The permitted throughput is 3,928 tonnes/day and the waste in place as of 2018 is 26,454,935 m^3, based on site records. Potrero Hills Landfill accepts waste tires. In addition to regular daytime testing, nighttime testing was conducted at the site to capture diurnal differences in surface flux. The site has daily, intermediate, and final covers. The daily cover consists of auto shredder and green waste disposed of at the site, ranging in thickness from 31-76 cm at the tested locations. In the wet season, an additional daily cover of construction and demolition waste was tested, with a thickness of 21 cm at the tested location. The nighttime testing

was conducted at the auto fluff daily cover location during the dry season. The intermediate cover consists of different types of soil disposed of at the site, ranging in thickness from 84-290 cm. The high thickness (i.e., 290 cm) location for the upper bound of the interim covers was associated with soil material left in place from a former stockpile area at the site tested during the dry season. The final cover consists of 30 cm of topsoil overlying 60 cm of compacted clay overlying 30 cm of foundation soil overlying existing interim cover. The cover types, designations, and thicknesses are presented in Table 3.6. A site map with testing locations is presented in Figure 3.6.

Table 3.6 – Potrero Hills Landfill Cover Characteristics

Cover Type Designation	Cover Type Description	Thickness (cm)
DC-AF	Daily Cover - Auto Fluff	76 (Dry Season); 44 (Wet Season)
DC-GW	Daily Cover - Green Waste	31 (Dry Season); 52 (Wet Season)
DC-C+D	Daily Cover - Construction and Demolition Waste	21
IC-S	Interim Cover - Soil	290 (Dry Season)
IC-BM	Interim Cover - Bay Mud	130
IC-C1	Interim Cover - Cell 1	84
FC	Final Cover	120

Figure 3.6 Potrero Hills Landfill with Test Locations

3.5 Static Flux Chamber Testing

Surface gas emissions from landfills can be determined using small to large-scale direct and indirect measurement approaches applied on a continuous or discrete basis. Point, line, and areal measurements can be made. The test methods can be used to estimate flux and/or concentration of target gases. The majority of the testing techniques provide direct measurement of or estimation of concentration data and require the use of analytical or numerical models to estimate flux. The only method that can be used to directly determine concentrations and thereby flux (negative or positive) is the flux chamber method (Rolston 1986, Livingston and Hutchinson 1995). The static chamber technique is based on establishing a sealed volume above the measurement surface where gas is emitted through (or gas is absorbed through) such that the gas cannot escape and its accumulation (or depletion) in the volume can be monitored. The method allows for determination of flux from specific individual cover materials and types and has long been used for methane as well as trace gases at landfills to identify variability of surface flux across cover types and conditions (e.g., Bogner et al. 1995, Bogner et al. 1997c, Borjesson and Svensson 1997, Scheutz and Kjeldsen 2003, Barlaz et al. 2004, Scheutz et al. 2003, Abichou et al. 2006a). This method was selected for the project to obtain representative estimates of the gas emissions.

3.5.1 Static Flux Chamber Specifications

For this test program, custom-built large-scale stainless-steel chambers with lateral dimensions of 1 x 1 m (1 m^2 measurement area) and 0.4 m height were used. At each test location, two chamber tests were conducted to provide duplicate testing using nearby chamber placements. This provides measurement of variability and increases statistical significance of data obtained. Two different sampling intervals were used for the static flux chamber measurements. These were selected to provide different sampling rates. The sampling intervals, including logarithmic and linear time increments, were selected to account for different types of gas accumulation. Some gases accumulate and volatilize quickly, whereas other gas species accumulate more slowly and constantly, requiring the different sampling intervals for each chamber. The testing schedules are summarized in Table 3.7. At each cover type location, a total of 10 gas samples were collected consisting of 5 samples collected from Chamber A and 5 samples collected from Chamber B. The two chambers were placed at randomly selected locations within a given cover type ensuring safe distance from operations, level ground, and proximity of the two chambers.

Table 3.7 – Flux Chamber Testing Schedules

Sample Number	Chamber A Elapsed Time (min)	Chamber B Elapsed Time (min)
1	0	0
2	7	30
3	15	60
4	30	90
5	60	120

3.5.2 Protocol for Testing

For conducting a measurement: first the collar was inserted into the landfill surface to a depth of approximately 50 to 100 mm (Figure 3.7). Then a bentonite-water paste was applied around the perimeter of the collar at the soil-collar interface to seal the interface against gas leakage (Figure 3.8). Next the lid was placed and secured over the collar to form an air-tight seal. Finally, a fan installed on the underside of the lid, installed to circulate the gas collected to ensure uniform distribution prior to sampling, was turned on to start mixing the gas accumulating in the chamber. A generator, which was placed 30 m downwind from the chambers, was used to power the fan. A photograph of an assembled flux chamber is presented in Figure 3.9.

Figure 3.7 Installation of Chamber Collar

Figure 3.8 Placement of Bentonite around Perimeter of Collar

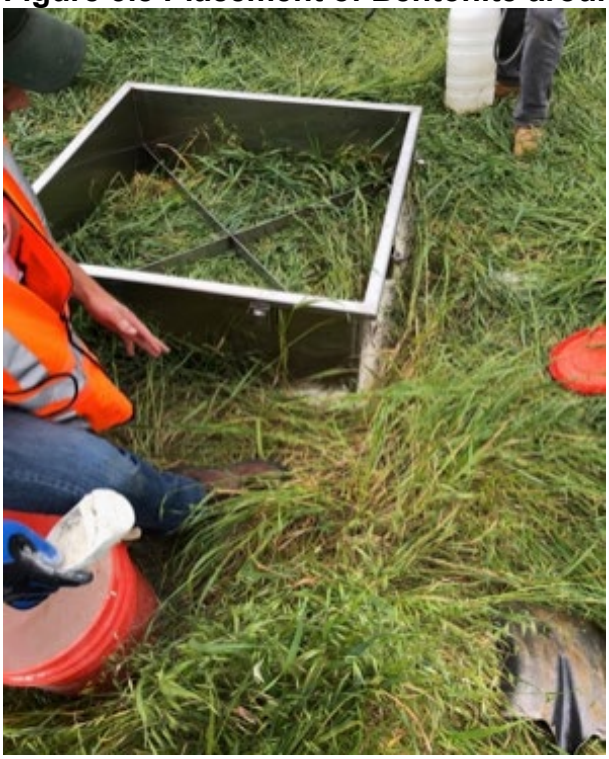

Figure 3.9 Assembled Flux Chamber

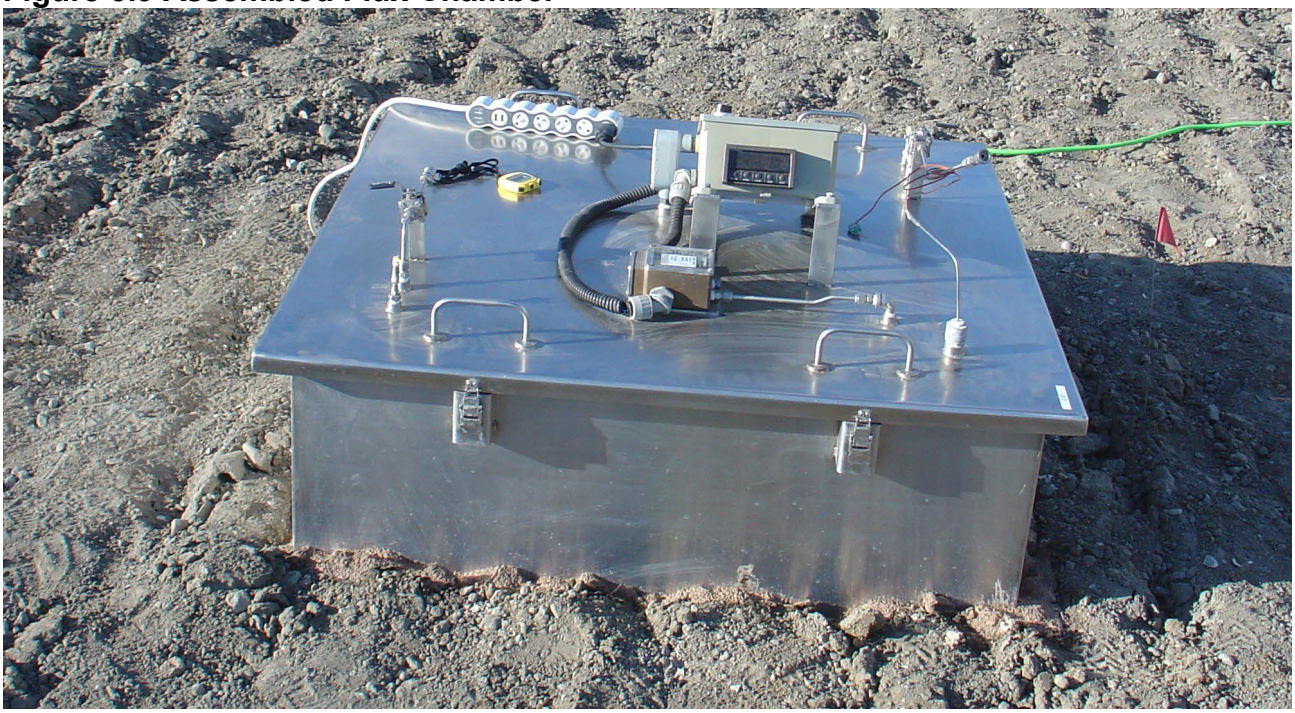

To prepare for the flux chamber testing, the Swagelok hardware on the chamber (Figure 3.10a) is baked at 225°C in an oven in the laboratory to volatilize any chemical residue

from previous use or storage. The hardware is installed on the chamber prior to each field campaign. Gas samples were obtained from the chamber during a sampling event by connecting gas canisters to sampling ports installed on the lid of the chambers (Figure 3.10b). The gas samples were obtained using 2-L evacuated stainless steel canisters equipped with bellow valves. The sampling ports consisted of ball valves, stainless steel tubing, and a Swagelok stainless steel Ultra-Torr vacuum fitting. For sampling, the valves were opened in the following order: the ball valve then the bellow valve. The valves were left open for approximately 10 seconds until the canister was full. The Rowland Blake Laboratory recommends opening the bellow valve on the canister a quarter turn only to ensure the canister is completely closed upon collection of the sample. Then, the valves were closed in the reverse order they were opened. This order was followed for opening and closing the valves to minimize contamination of the gas samples. The canister was then removed from the sampling port and was stored in a weather-proof box. The gas samples were collected using the pre-established schedule of sampling intervals (Table 3.7). The start time of an individual sampling event was established as the time of the sealing of the lid/starting of the fan on the lid.

Figure 3.10 Gas Sample Collection

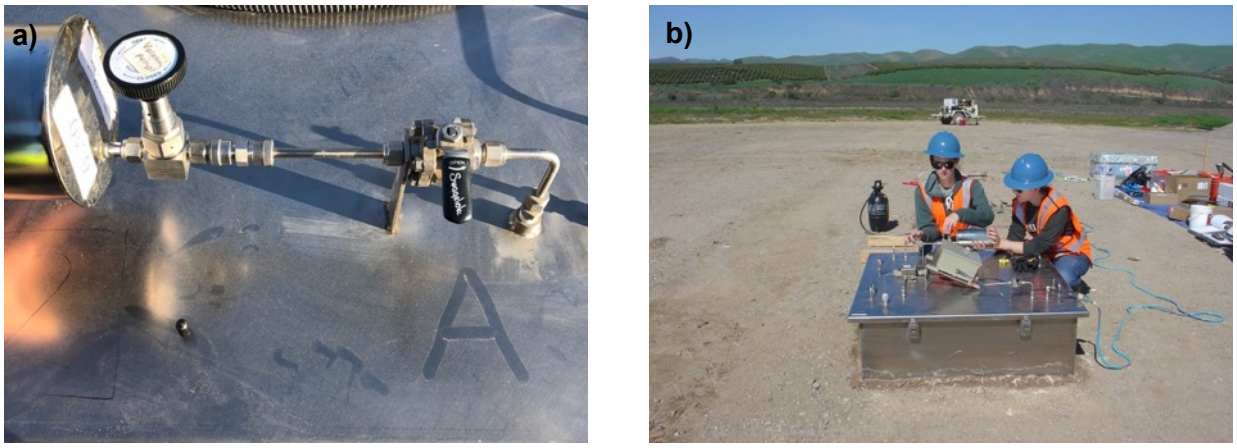

3.6 Complementary Field Tests

Field tests, in addition to surface flux tests were conducted to supplement interpretation of the results of the main test program and provide mechanistic explanations for the observed behavior. These additional tests included gas management system sampling, determination of cover temperatures, determination of in-situ cover properties, and collection of cover material samples for laboratory analysis.

Raw gas, which is the gas collected from the site prior to inflowing to the gas management system (flare or gas-to-energy facility) was sampled during each individual field campaign at a given site. This gas provides a composite gas concentration distribution for the given site at the time of sampling. Raw LFG samples were obtained from the flare system or gas-to-energy facility header at a location near the inlet to the system. The raw gas samples also were collected using the 2-L capacity, custom-built evacuated stainless steel canisters. The canister was directly connected to the sampling

port using a flexible PVC tube of minimal length. When all the connections were secured, the ball valve on the sampling port was opened to purge any ambient air present in the sampling connection. Subsequently, the bellow valve on the canister was opened for only 3-4 seconds until the canister was full to minimize the potential for gas escaping the canister back into the flare system. A total of two raw LFG samples was taken during each field campaign. An example of raw gas sampling is presented in Figure 3.11.

Figure 3.11 Raw Gas Sampling

After the last scheduled sample was retrieved from a given chamber, the lid was removed and the height of the collars was measured at midpoint along each side for use in calculation of the chamber volume (Figure 3.12a). In addition, the temperature of the tested cover material was measured at three different points within the perimeter of the chamber using a rigid thermocouple probe that was inserted approximately 50-150 mm into the cover material (Figure 3.12b). An attempt was made to insert the thermocouple probe to the maximum depth of 150 mm for each temperature measurement. However, this was not possible when the cover materials were exceedingly hard and stiff, in particular during the dry season.

Figure 3.12 Post-Flux Tests Prior to Removal of Chamber Collar

Further cover temperature analysis was conducted by using permanently installed thermocouple arrays. Temperature measurement arrays were installed within the intermediate covers at each of the five landfill sites at positions near the flux chamber test locations. The temperatures were measured using Type K thermocouples. The arrays each contained 4 thermocouple sensors that extended between 10 and 100 cm beneath the ground surface into the covers. Photographs of power augering to install a temperature array and retrieval of temperature data from datalogger are presented in Figure 3.13.

Figure 3.13 Installation of Thermocouple Array and Field Temperature Measurement

In addition, sand cone tests in accordance with ASTM D1556 were conducted at each chamber location to determine density of the cover materials (Figure 3.14). Certain cover systems, such as green waste, were not conducive to sand cone testing due to large particle size and void space. Finally, cover samples were obtained from each chamber location for laboratory analysis with the mass of samples ranging from 100 to 2000 g depending on the cover material. A surface sample was taken from each chamber (A and B). A sample also was taken as part of the sand cone test. Therefore, a total of 4 samples were collected per cover type.

Figure 3.14 Sand Cone Testing

Furthermore, the cover thickness was evaluated at each test location. A backhoe or excavator was typically provided by the landfill personnel and the cover material was excavated to determine the cover thickness after all of the measurements (i.e., flux chamber, collar depth, cover temperature, cover sample collection, and sand cone) were made at a test location. The excavation was made until the boundary between the cover system and underlying waste layers was delineated and the thickness of the cover system was measured using a measuring tape. If heavy construction equipment were not available, a shovel was used in relatively loose covers or thin covers. The cover thicknesses were measured experimentally in daily and intermediate cover systems. Excavations were not conducted in final covers in order not to disturb the integrity of these cover systems. Examples of cover thickness characterization is presented in Figure 3.15.

Figure 3.15 Cover Thickness Characterization

3.7 Laboratory Investigation

The main categories of laboratory analyses conducted in the investigation were analytical testing and geotechnical testing. The analytical testing was conducted to determine the concentrations of the chemical species included in the study. The geotechnical testing was conducted to determine index properties and engineering behavior of the cover materials.

Laboratory investigations were conducted to determine the concentrations of methane and nitrous oxide and to characterize the cover materials at each landfill. The gas concentrations were determined by the Rowland-Blake Laboratory at the University of California at Irvine. Geotechnical characterizations tests, including moisture content and density, particle size distribution and specific gravity were conducted at California Polytechnic University at San Luis Obispo to enable interpretation of the gas flux data.

3.7.1 Analytical Testing

The gas samples obtained in the field tests were analyzed at Rowland-Blake Laboratory in the Chemistry Department at the University of California-Irvine. The laboratory has high-resolution analysis systems capable of identifying and quantifying over 100 non-methane hydrocarbons and halocarbons including the (hydro)chlorofluorocarbons investigated in the current study. The laboratory is equipped with two VOC analytical systems, each of which consists of 3 Agilent 6890 gas chromatographs that house 2 electron capture detectors, 3 flame ionization detectors, and a quadrupole mass spectrometer.

For analysis of gas samples obtained in the study for VOCs, the amount of gas trapped from the canisters ranged between 10-1000 cm^3 (at standard temperature and pressure). This gas was introduced into the analytical system's manifold and then passed over glass beads contained in a loop and maintained at liquid nitrogen temperature. The flow was regulated by a Brooks Instrument mass flow controller (model 5850E), and was kept below 500 cm^3/min to ensure complete trapping of the

relevant components. This procedure pre-concentrated the relatively less volatile components of the sample (such as halocarbons and hydrocarbons) while allowing more volatile components (such as N_2, O_2, and Ar) to be pumped away. The less volatile compounds were next re-volatilized by immersing the loop containing the beads in hot water (80°C), and then flushed into a helium carrier flow (head pressure 330 kPa). This sample flow was then split into six streams. Each stream was chromatographically separated on an individual column and sensed by a single detector. Three GCs (each HP 6890) form the core of the analytical system. The research group uses two ECDs (sensitive to halocarbons and alkyl nitrates), two FIDs (sensitive to hydrocarbons), and one quadrupole MSD (for unambiguous compound identification and selected ion monitoring). The output signal was captured using Dionex software. Each resulting chromatogram was inspected, and each peak shape individually checked. This type of quality control is very important for datasets of large sizes, because a slight change in retention time or peak shape can cause problems for automated quantification.

Calibration and measurement intercomparisons are conducted on a continuous basis. Calibration is an ongoing process, whereby new standards are referenced to older certified standards, with appropriate checks for stability, and also with occasional inter-laboratory comparisons. Multiple standards are employed, including working standards that are analyzed every four samples and absolute standards that are analyzed twice daily. The UCI research group regularly collects and calibrates pressurized cylinders of air from different environments for use as working standards. The primary reference standard for halocarbons was previously calibrated from static dilutions of standards prepared in the laboratory. Its absolute accuracy is tied to a manometer measurement and how accurately the appropriate volume ratios for the dilution line used are known. For hydrocarbons, the research group uses a National Bureau of Standards propane standard (SRM 1660A) to calculate a Per-Carbon-Response-Factor (PCRF) for the FIDs. This is compared to PCRFs calculated from more readily available commercial standards to check the absolute accuracy of the commercial standard, as well as the appropriateness of using the same PCRF for different compounds. The research group had cross-checked their calibration scheme against absolute standards from other groups for both hydrocarbons and halocarbons. In addition, the group has participated in the Non-Methane Hydrocarbon Intercomparison Experiment (NOMHICE). The results of this experiment demonstrate that the group's analytical procedures consistently yield accurate identification of a wide range of unknown hydrocarbons and produce excellent quantitative results. The typical absolute accuracy is estimated to be 2-10%, and up to 30% for some compounds, increasing as the detection limits are approached (Colman et al. 2001). The researchers impose a conservative limit of detection (LOD) of 3 pptv on the NMHCs. The halocarbon LOD varies by compound, from 0.01 pptv for chlorobrominated species (e.g., $CHBrCl_2$, $CHBr_2Cl$, CH_2BrCl) to 10 pptv for CFC-12. Once the samples are assayed, the stored chromatograms are individually inspected and the reports from these are then summarized in spreadsheet format and checked for inconsistencies. A summary of the LODs for all chemicals included in this study is presented in Appendix B (Table B2).

3.7.2 Geotechnical Testing

The cover material index properties and engineering behavior were determined at the geotechnical/geoenvironmental testing laboratories in the Civil and Environmental Engineering Department at Cal Poly. Geotechnical tests were conducted to determine moisture content, specific gravity, particle size distribution, and Atterberg limits of the cover materials to supplement the interpretation of the surface flux data.

A total of 232 samples were collected from the five landfill sites during the course of dry and wet season testing, consisting of daily, intermediate and final covers from both the surface and the sand cone depth, when applicable. Moisture content tests were conducted on all samples, and specific gravity tests were conducted on samples from each cover type. Particle size analysis was only conducted on soil samples. Atterberg limits were performed only on plastic soils when applicable. If a sand cone test could not be conducted in the field, a density range estimate was made in the laboratory to complete phase relations for each cover type.

The moisture contents of the cover materials were determined using procedures described in ASTM D2216. For each material, samples with masses in the range of 200 to 600 g were used. Larger quantities of samples were required for materials with larger particle sizes to obtain representative measurements.

The specific gravity of the landfill covers composed of soil was determined using the standardized procedure described in ASTM D854. A modified version of the same test was used for non-soil cover materials with relatively large particle sizes based on the methodology outlined in Yesiller et al. (2014). A 1900-mL mason jar was used to accommodate larger particle diameters of materials such as green waste or auto-shredder waste. To avoid floating particles, the samples were placed in a mesh bag (191 x 356 mm) with a lead weight. An example specific gravity test setup is presented in Figure 3.16.

Figure 3.16 Modified Specific Gravity Testing for Large Particle Cover Materials

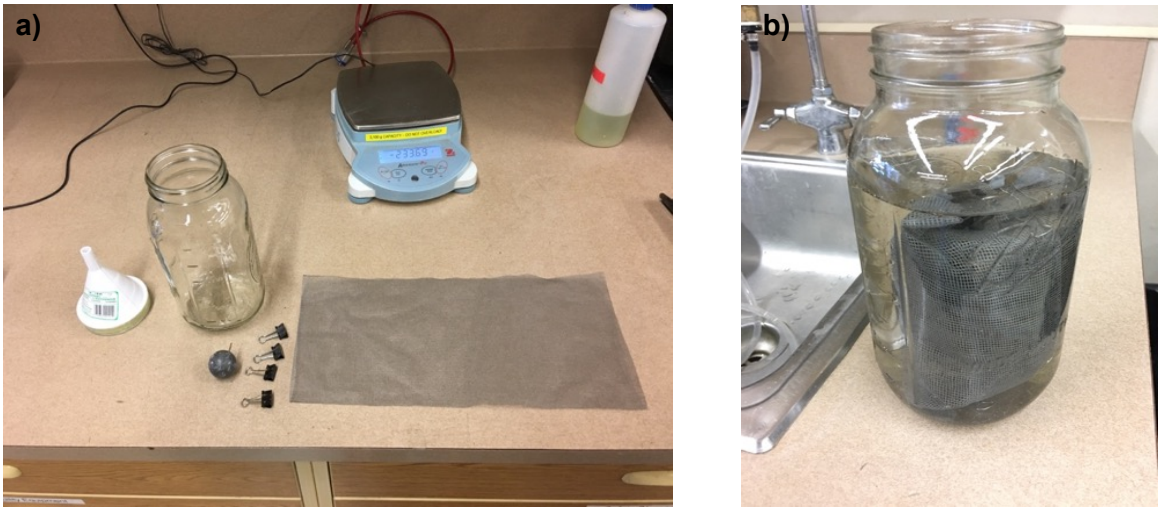

The particle size distribution tests for the soil samples were conducted using ASTM D422. The analysis consisted of first a hydrometer test to determine the distribution of fine-grained particles, followed by a dry sieve to determine the composition of the coarse-grained fraction. The particle size analysis results were used to classify the soils based on the United Soil Classification System (USCS) and also the United States Department of Agriculture (USDA) Method. On fine-grained soils with plastic characteristics, Atterberg Limits tests were performed according to ASTM 4318.

Density was estimated in the laboratory for cover materials where sand cone tests could not be determined in the field. The density was obtained either using a vessel of known volume filled to an approximated representative field density and then determining the mass of the material in the vessel or using a water submersion method similar to the bulk density method (ASTM D7263).

3.8 Determination of Surface Flux

In order to quantify gas emissions from the numerous cover materials, surface flux specific to each location and constituent was determined. The surface flux of the 82 chemicals was determined by converting the concentration datasets obtained from the field investigation to surface flux using Equation 3.3.

$$F = \frac{dC}{dt} * \frac{V}{A} \tag{3.3}$$

Where, F is the surface flux (expressed in units of mass per area-time.), dC/dt is the concentration gradient, (the rate of change of concentration over time within the flux chamber), V is the volume within the static flux chamber (units of volume), and A is the area of the landfill surface enclosed by the chamber (units of area). To determine the concentration gradient, plots of the concentration versus sampling time were constructed for each location, constituent, and chamber. Prior to calculating the surface flux, a linear regression analysis was performed to evaluate the fit of each concentration versus time dataset to obtain gradient data.

The fit of each linear regression model was evaluated using coefficient of determination (R^2), which indicates how well the regression models the data (Devore 2008). The analysis started with generating the concentration versus time data for each chamber measurement. R^2 acceptance and rejection criteria were used to determine the number of points that may need to be removed to potentially reach a predetermined threshold. Point removals were performed from data points obtained later in time to earlier points in order to give higher weight to the earlier points. The earlier data points were assigned higher weight in the analysis due to the potential decrease in the concentration gradient over the duration of the sampling event, which can be caused by the accumulation of the chemical that may occur after extended run time of the chamber. The target threshold R^2 value was established as 0.9.

For determination of flux, first, a regression line was fit to all five datapoints from a given chamber. If the fit resulted in a linear relationship with R^2>0.9, all data points were used. If R^2<0.9, data points were systematically removed from the curve fit starting with the last point until a fit with R^2>0.9 was attained (Yeşiller et al. 2018). Up to 2 data points are removed from a given chamber test, leaving three data points for determining the R^2 value. (An example of the regression evaluation process is presented in Figure 3.17.

Figure 3.17 Regression Evaluation Process with 3, 4, and 5 Points

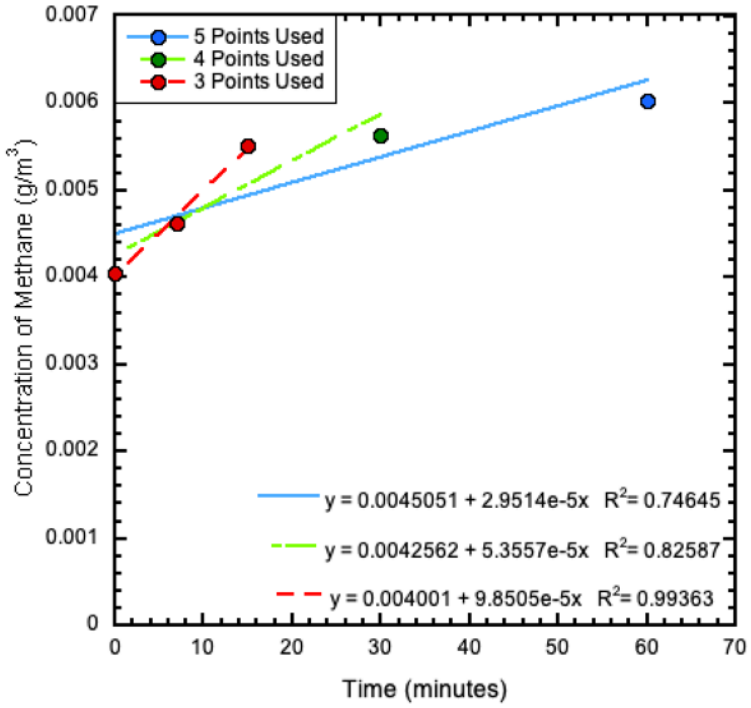

For cases when R^2 was not greater than or equal to 0.9 for both chambers at a given test location, a secondary threshold of R^2 greater than or equal to 0.7 was used and for these cases based on engineering judgement, the R^2 value is reported in parentheses after the calculated flux value to indicate the relative confidence in the regression fit. When the alternate method to determine flux was used, only one value per cover type was calculated. For tests conducted during excessively windy conditions and for some highly porous covers (i.e., auto fluff) with R^2<0.7, the first two data points were used in the analysis when flux could not be calculated otherwise for either chamber. In these cases, the data points indicated concentrations increasing with time and then quickly decreasing starting with the third data point. This trend indicated that dilution of the accumulated chemicals in the chamber was present.

The concentration values for the gases included in the analysis were provided in units of ppmv and ppbv, respectively by the Rowland Blake Laboratory. Using temperature and barometric pressure data recorded during the field campaigns, the concentration was converted from volumetric-based to mass-based units, as shown in Equation 3.4.

$$C_{(\frac{g}{m^3})} = \frac{C_{(ppmv)} * P * MM * 1e3}{1e6 * R * T} \quad (3.4)$$

Where, C (g/m^3) is the concentration expressed in mass-based units, C (ppmv) is the concentration expressed in volume-based units, P is atmospheric pressure in kPa, MM is molar mass in g/mol, R is the ideal gas constant expressed in units of J/mol*K, and T is soil temperature in Kelvin.

3.9 Methane Generation and Gas Collection Efficiency

Moisture content, temperature, pH, presence of oxygen, and waste age/composition significantly affect methane generation. In general, high methane generation is associated with fresh, high moisture content MSW in a warm environment under anaerobic conditions and a stable, slightly acidic pH ((Tchobanoglous et al. 1993, Christensen et al. 1996).). MSW with a high fraction of biodegradable organic matter has high methane generation potential. Site specific climatic conditions (i.e., precipitation/average temperatures) and operational practices (i.e., waste depth, degree of compaction, waste in place) affect the MSW state and associated LFG generation rate.

Given that in-situ methane generation rates in full scale, MSW landfills are difficult to measure, various kinetic models have been developed to estimate generation rates. USEPA's Landfill Gas Emissions Model (LandGEM) is the most widely applied kinetic model to estimate LFG generation rates from MSW landfills. LandGEM is based on a first order MSW decomposition rate analysis for quantifying methane generation rates (Equation 3.5). The site-specific inputs to the LandGEM model include the landfill open and expected closure dates (or waste design capacity) and the past and projected annual waste acceptance rates (Mg or short tons/year). The first order decomposition rate and methane generation potential are singular values for a given site at a given climatic region using LandGEM analysis, whereas variations in these parameters occur potentially over time, space, and between sites at a given climatic region.

$$Q_n = kL_0 \sum_{i=0}^{n} \sum_{j=0}^{0.9} \frac{M_i}{10} e^{-kt_{i,j}} \quad (3.5)$$

Where, Q_n is the methane generation rate in year n (m^3/year), M_i is the waste mass placement in the ith year, j is an intra-annual time increment, t is time (years), k is the first order decay rate (year^{-1}), and L_0 is the methane generation potential (m^3/Mg wet waste).

LandGEM predictions are based on two parameters: first order MSW decay rate (k, year^{-1}) and methane generation potential (L_0). The first order decomposition rate k is a site-specific parameter that depends on the moisture content, availability of nutrients, pH, and temperature of the waste mass, among many potential factors. Higher k values used in LandGEM simulations result in both a faster increase in methane generation and a faster decay in methane generation over time (USEPA 2005). First order decomposition rates have been reported to range from 0.003 to 0.21 year^{-1}, where

higher values have been determined for bioreactor landfills up to 2.2 $year^{-1}$ (Tolaymat et al. 2010, Kim and Townsend 2012). L_0 represents the maximum volume of methane that can be generated per unit input of MSW and is based on the composition of the incoming and previously placed MSW (Krause et al. 2016). High L_0 values are associated with wastes with high cellulose content, equivalent to a high fraction of biodegradable organic carbon. L_0 values typically range between 6.2 to 270 m^3/Mg wet waste, where higher and lower values have been reported for individual waste components (i.e., paper or food waste alone) (US EPA 2005, Krause et al. 2016). Based on field data collected in the early 1990's, the USEPA recommends several default parameter sets of both k and L_0 based on the climatic conditions (i.e., precipitation) at a given landfill site.

As input, LandGEM requires waste acceptance data for the entire operational lifespan of a landfill. Insufficient records for multiple study landfills and unknown waste generation rates in the future required both a back and forward projection in the waste acceptance rates over time. Various mathematical models were tested and compared to fit the trends in overall waste generation data from open to closure.

Waste generation data used as the basis for curve fitting was obtained from two sources including CARB compiled data (1996 to 2019) and data (1991 to 2012) compiled by Scott Walker (2012). The generation data from these sources were combined, where Walker's data was used pre-2012 and CARB's data was used for 2013-2019 resulting in final datasets for each landfill for the period 1991-2019. Open and closure dates for each landfill were obtained from the Walker (2012) and SWIS databases, respectively.

MATLAB's (r2017a) built in curve fitting toolbox (i.e., the "fit" function) was used for computing back and forward trends in waste generation rates. The trust region algorithm (based on non-linear minimization of sum of squared residuals) and all default optimization settings were used for each curve fit. Values of the parameters were routinely initialized at the same starting points for each curve fitting run (at 0.01). Each of the curve fits were passed through the origin (i.e., zero WIP in the first year) by modifying the mathematical functions and/or corresponding optimization routine. Waste in place as a function of time was used as the dependent variable for curve fitting. For each landfill, time dependent WIP values from 1990 to 2019 were obtained from the 2012 WIP estimate from the Walker dataset and by adding or subtracting the respective generation values. The mathematical model functions investigated for curve fitting ranged from exponential, to polynomial and power functions of different orders (Table 3.8). In addition, hyperbolic and single and double logistic equations were investigated as they replicated the trends in WIP for multiple landfills. Model performance was assessed using two quantitative criteria: coefficient of determination (R^2) and the root mean squared error. Qualitative performance of each model was evaluated by assessing whether the curve fits over or underpredicted past or future WIP values. Based on these performance criteria, an acceptable mathematical model was selected for each site. For Santa Maria Regional Landfill, all curve fits led to equally poor

predictions; therefore, linear interpolation was used to estimate back and forward trends in waste generation rates over time.

Table 3.8 – Mathematical Models Used to Predict Back/Forward Trends in Waste Generation Over Time (*t* represents time)

Model Name	Mathematical Formulation	Model Parameters
Exponential-1	$WIP = Ae^{Bt}$	A, B
Exponetnial-2	$WIP = Ae^{Bt} + Ce^{Dt}$	A, B, C, D
Polynomial-1	$WIP = At^2 + Bt$	A, B
Polynomial-2	$WIP = At^3 + Bt^2 + Ct$	A, B, C
Polynomial-3	$WIP = At^4 + Bt^3 + Ct^2 + Dt$	A, B, C, D
Power-1	$WIP = At^B$	A, B
Power-2	$WIP = At^B + C$	A, B, C
Hyperbolic	$WIP = \frac{At}{(B+t)}$	A, B
Logistic	$WIP = \frac{A}{(1+e^{(-Bt+C)})}$	A, B, C
Double Logistic	$WIP = \frac{A}{(1+e^{(-Bt+C)})} + \frac{D}{(1+e^{(-Et+F)})}$	A, B, C, D, E, F

Full methane mass balance in a landfill (Equation 3.6) has the methane generated for the *n*th year (Q_n) equivalent to the summation of that collected by the gas extraction system ($Q_{co,n}$), emitted through the cover ($Q_{em,n}$), oxidized in the cover ($Q_{ox,n}$), stored in the landfill ($Q_{st,n}$), or migrated through the sides or bottom of the landfill ($Q_{mi,n}$) (Barlaz et al. 2009).

$$Q_n = Q_{co,n} + Q_{em,n} + Q_{ox,n} + Q_{st,n} + Q_{mi,n} \quad (3.6)$$

While gas collection efficiency can be determined using the full mass balance, the efficiency typically is calculated considering the emissions and collection data (e.g., Barlaz et al. 2009) (Equation 3.7) due to the lack of specific data for gas oxidation in covers, gas stored in the waste mass or migrated through the liner systems. The gas emissions measured in the field campaigns and gas extraction data obtained from the landfills as reported to CARB were used to estimate the collection efficiencies in this study.

$$\alpha_n = \frac{Q_{co,n}}{Q_{co,n} + Q_{em,n}} \quad (3.7)$$

A baseline analysis using default LandGEM parameters and a more refined approach using modeled parameters were included to provide a potential range of values for gas generation. The refined approach included data from studies more recent than the 1990s. A methane mass balance was used to assess the effectiveness of the refined approach.

3.9.1 Default LandGEM Analysis

Baseline estimates of methane generation were obtained by varying the LandGEM default parameter values. LandGEM includes two default parameter sets (Table 3.9). The first set is used to determine the applicability of the Clean Air Act (CAA) regulations for MSW emissions, relating to New Source Performance Standards for new MSW landfills and Emissions Guidelines for existing MSW landfills (US EPA 2005). The second set is based on emissions factors from the USEPA's AP-42 report summarizing air pollutant emissions factors for MSW landfills and is used in the absence of site-specific data for methane or NMVOC concentrations (US EPA 2005, 2008).

Table 3.9 – Default LandGEM Parameters

Default Parameter Set	Landfill Type	L_0 (m^3/Mg wet waste)	k ($year^{-1}$)
CAA	Conventional	170	0.05
	Arid Area	170	0.02
Inventory	Conventional	100	0.04
	Arid Area	100	0.02

Conventional and arid are used for landfills in areas with rainfall exceeding or less than 635 mm/year, respectively (Wang et al. 2013, 2015). The landfills in the study were located in areas with 278 to 630 mm/year precipitation. Four simulations, as listed above in Table 3.9, were run for each landfill and then averaged to determine the baseline methane generation and corresponding collection efficiency values for 2018. To assess uncertainty in these predictions, 95% prediction intervals were calculated assuming the error residuals were normally distributed with a mean of 0 and standard deviation equal to the standard deviation of methane generation for 2018-2019.

3.9.2 Refined LandGEM Analysis

The refined analysis was based on the improved determination of both L_0 and k using two novel, yet independent approaches.

3.9.2.1 Determination of Waste-Specific L_0 Parameter

A waste component specific methane generation potential model, similar to that proposed by Machado et al. (2009) and Cho et al. (2012), was adopted to predict overall L_0 values for each landfill. This model assumes that methane is generated from the biodegradable MSW components only and that an aggregate, whole-site methane generation potential can be calculated based on the weighted average of the individual methane generation potentials ($L_{0,i}$) of the n waste components. The individual methane generation potentials are multiplied by the weight fraction of the ith component in the waste stream and summed to determine the overall L_0 value (Equation 3.8). In the model, F is a correction factor (ranging from 0 to 1) that scales down the L_0 values predicted in the laboratory assays to that expected under field conditions. Typically, the specific methane generation potential for each waste component is measured independently in the laboratory using biochemical methane potential assays which are representative of the maximum methane that can be generated under optimal conditions.

$$L_0 = F * \sum_{i=1}^{n} L_{0,i} * WF_i \quad (3.8)$$

A comprehensive Monte Carlo analysis was conducted to provide whole-site methane generation potentials for each landfill. Monte Carlo analyses evaluate the uncertainty of model predictions due to the uncertainty in methane generation potentials and the correction factor. First, probability distributions of uncertain model inputs are assigned or developed, based on prior knowledge or expert judgement. Next, the model is run for thousands of iterations, where each model run randomly samples the input probability distributions, and the model predictions are stored. After a large number of iterations has been reached, the distribution of model predictions (and hence the predictive certainty) was analyzed and compared with a parametric statistical model.

To develop the sampling distributions, a large number of waste component specific methane generation potentials were obtained from the literature for a variety of biodegradable wastes: food, paper, green (yard), wood, and textiles. All other constituents of MSW were considered inert and non-biodegradable. Only studies that had explicitly stated that a laboratory BMP assay was conducted were included. Based on the pervasiveness of certain components within these general categories, specific sampling distributions of $L_{0,i}$ values were developed for cardboard, office paper, newspaper, magazines/coated paper/junk mail, other miscellaneous paper, mixed food waste, mixed yard waste, manure, mixed textile, and mixed wood waste. The cardboard component comprised $L_{0,i}$ values ranging from un-corrugated/corrugated cardboard to paperboard products. The office paper component comprised $L_{0,i}$ values ranging from printer paper to recycled office paper of varying degrees. The coated paper component comprised $L_{0,i}$ values ranging from magazines, brochures, phone books, to junk mail products. The miscellaneous paper component comprised remaining paper materials, including soiled paper. Food waste components included $L_{0,i}$ values calculated for mixed food wastes separated to individual fruits and vegetables. Similarly, green waste components included $L_{0,i}$ values calculated for mixed yard wastes separated to individual branches, grasses, and leaves/stems. Textile waste components included $L_{0,i}$ values calculated for mixed textile wastes separated to individual products containing leather, rubber, cotton, and cloth diapers. Finally, wood waste components included $L_{0,i}$ values ranging from mixed wood wastes (C&D materials) to individual wood obtained from different tree specimens. The values for each of these distributions are presented in Appendix B (Table B3).

Non-parametric statistical distributions were developed for waste components with a sufficient number of samples (N > 20). A non-parametric kernel density estimator (KDE) tool based on the kd-trees algorithm (MATLAB version) was used to develop the non-parametric probability distributions for sampling. A Gaussian kernel was used along with a rule of thumb estimator for determining the bandwidth of each kernel center. An example KDE distribution is developed for the cardboard waste component (Figure 3.18). The probability density estimate of the KDE model is overlain on an empirical histogram of the $L_{0,i}$ values obtained from the literature. The KDE model matched the general trend in the empirical probability density estimates of the data obtained from the

literature. Methane generation potential values around 230 m^3/Mg have a higher probability of selection in the MC simulations, based on the bell shape of the KDE curve. Similar bell-shaped KDE distributions were obtained for office paper, newspaper, coated paper, miscellaneous paper, food wastes, yard wastes, textile wastes, and wood wastes.

Figure 3.18 Empirical (Blue Histogram) and Modeled (Red Line, KDE) Probability Density Estimates for the Methane Generation Potential of Cardboard Waste

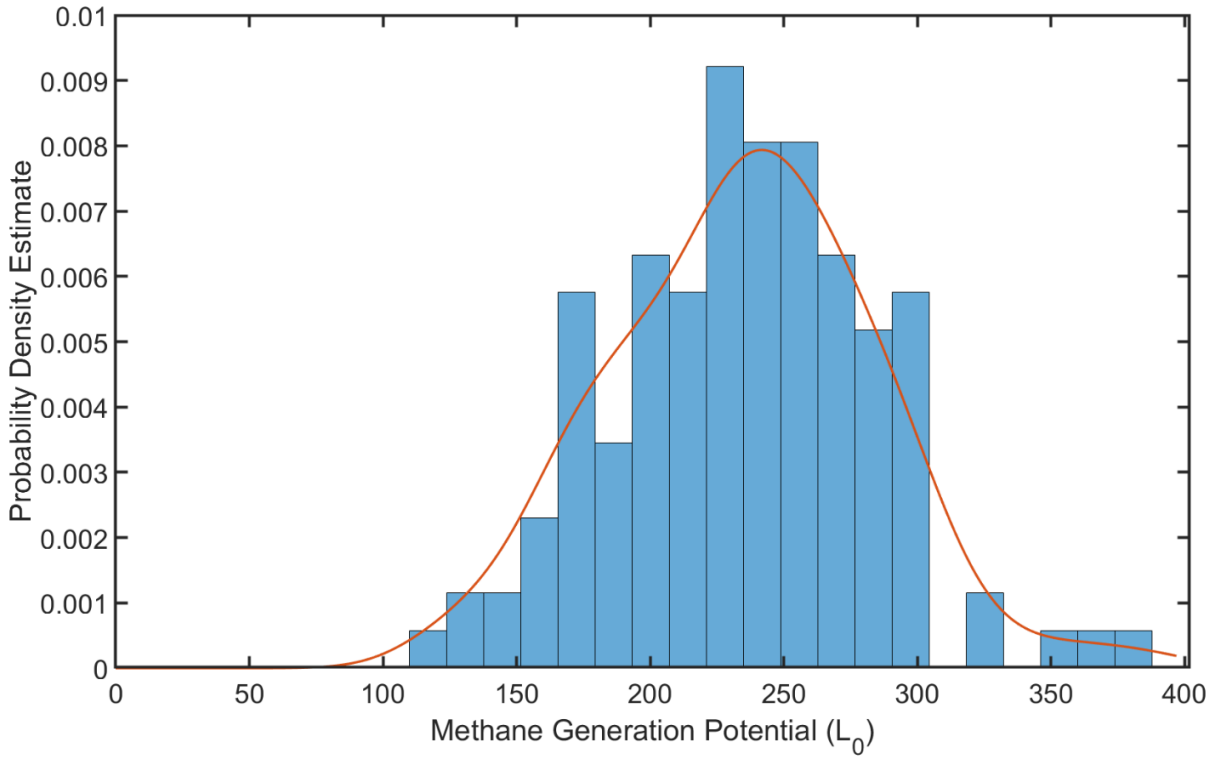

Model inputs that lacked sufficient data (N <20) to estimate kernel density distributions were assigned uniform probability densities. The ranges of the uniform distributions covered the minimum and maximum values expected based on the values obtained from the literature. $L_{0,i}$ values for manure and values of the correction factor (F) were designated as uniform input distributions.

Table 3.10 summarizes all input sampling distributions for the MC analysis and the corresponding references from which the values of $L_{0,i}$ were obtained. A majority of the input distributions was developed using the KDE tool. The number of data points used in the construction of each kernel distribution ranged from 31-125. Office paper had the highest methane generation potential. Food wastes had the highest range in $L_{0,i}$ values, based on the median of the $L_{0,i}$ values obtained from the literature. $L_{0,i}$ values were low for both wood waste and green waste, which contain higher amounts of lignin (non-biodegradable) compared to cellulosic matter (biodegradable).

Table 3.10 – Input Sampling Distributions Constructed for the MC Analysis

Model Input	Distribution Type	N	Min.	Median	Max.	Reference
Cardboard	KDE	125	119	236	387	1-8
Office Paper	KDE	49	115	293	369	1-3, 5-10
News-Paper	KDE	39	18	75	322	1,2,3,7,8
Coated Paper	KDE	38	84.4	289	366	1,2,3,8
Misc. Paper	KDE	43	106	279	367	1,2,8,13
Food Wastes	KDE	68	11	272	538	6, 8-11, 12-20
Green(Yard) Wastes	KDE	31	30.6	124	345	3, 6, 8, 13, 16, 21
Manure	Uniform	-	2	-	99	20
Textile Wastes	KDE	43	3	207	365	4, 6-8,10, 11, 13
Wood Wastes	KDE	49	0	41.2	310	6-8, 10, 11, 19, 22
Correction Factor, F	Uniform	-	0	-	1	12
Weight Fractions (WF)	Point	-	0	-	100	-

[1]Vermuelen et al. 1993, [2]Owens and Chynoweth 1993, [3]Eleazer et al. 1997, [4]Jokela et al. 2005, [5]Qu et al. 2009, [6]Machado et al. 2009, [7]Krause et al. 2018a, [8]Krause et al. 2018b, Chickering et al. 2018, [9]Ishii and Furuichi 2013, [10]Wangyao et al. 2010, [11]Jeon et al. 2007, [12]Cho et al. 2012, [13]Karanjekar et al. 2015, [14]Zhang et al. 2007, [15]Lee et al. 2009, [16]Buffiere et al. 2006, [17]Cho et al. 1995, [18]Nieto et al. 2012, [19]Manfredi et al. 2010, [20]Moody et al. 2011, [21]Yazdani et al. 2012, [22]Wang et al. 2011

Site specific waste characterization data was obtained from CalRecycle (2019b). The web tool integrates the 2016 Statewide Waste Characterization study data with local employment and population data to provide both commercial and residential waste disposal estimates and composition for different counties and specific jurisdictions. For each landfill, commercial and residential disposal and composition data from the nearest jurisdiction was downloaded and used to determine the weights required in Equation 3.8. The data from the commercial and residential sectors were filtered to only include biodegradable waste components resulting in 22 distinct material types: various types of cardboard, paper waste, food waste, yard waste, textile waste, manure, and other wood wastes such as clean dimensional lumber. The commercial and residential sectors for each material type were then summed, and a general weight fraction for each material type was determined using the total amount of disposed biodegradable waste.

For each landfill, L_0 values were predicted a high number of times using Equation 3.8 and random sampling of the model inputs/distributions presented in Table 3.10. Preliminary analysis varying the number of simulations from 10K to 50K indicated that 50,000 model simulations was sufficient to reach a stable output parametric distribution. A logarithmic (base 10) transformation of the predicted L_0 values was required to improve the parametric distribution model fit. The empirical histogram of the output L_0 values predicted for Santa Maria Regional Landfill overlain with the parametric model fit

is presented in Figure 3.19. The extreme value parametric distribution demonstrated the best fit to the histograms summarizing the empirical probability density estimate for all L_0 predictions. This result was confirmed by comparing the maximum likelihood estimate of all parametric model fits from the parametric models available in MATLAB's statistics toolbox. The uncertainty of L_0 values was summarized using the 95% confidence intervals derived from the 5% and 97.5% quantiles of the fitted extreme value distribution. For this particular output distribution, the mean value of L_0 was 79.3 m^3/Mg with a variance of 1.43 m^3/Mg.

Figure 3.19 Empirical (Blue Histogram) and Modeled (Red Dash Line, Using a Parametric Model) Probability Density Estimates for the Methane Generation Potential of Santa Maria Regional Landfill

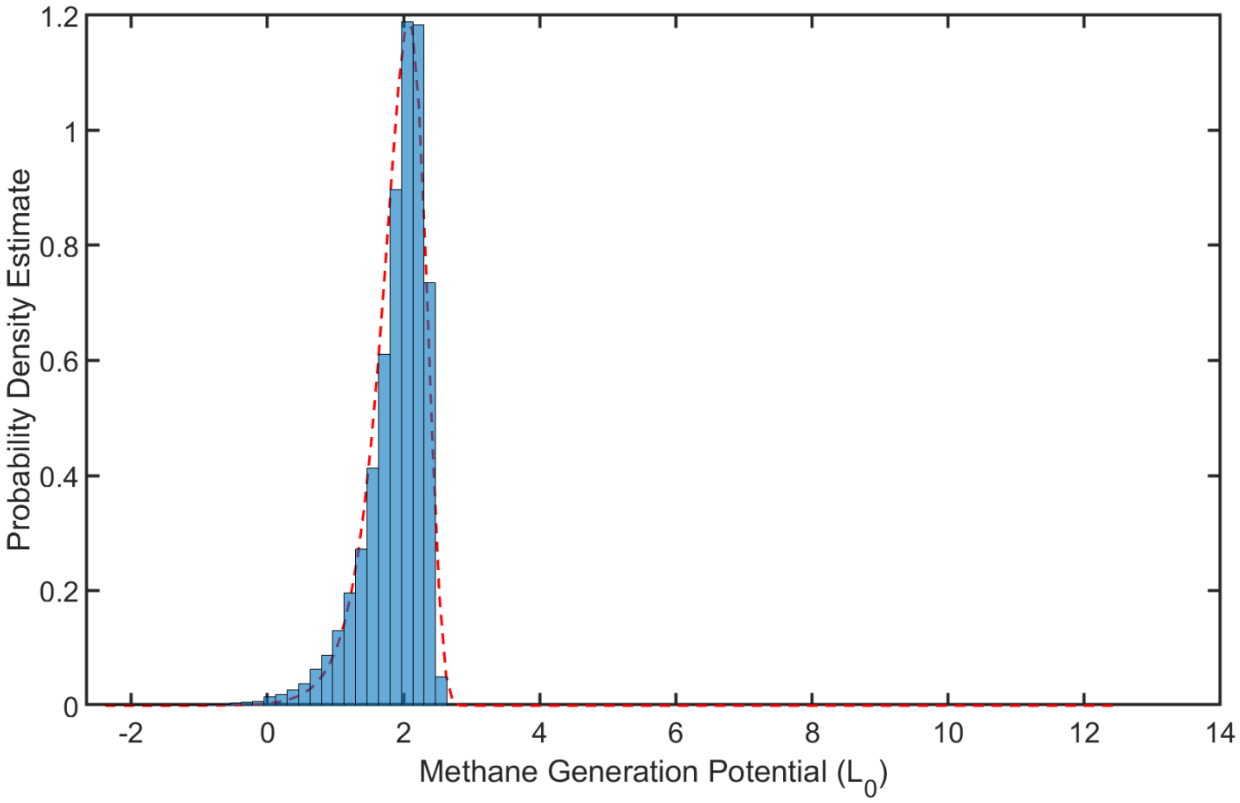

3.9.2.2 Determination of Site-Specific *k* Parameter

Site-specific *k*-values conventionally have been determined through fitting LandGEM against time-variable gas recovery data (not representative of gas generation). While this approach is effective, large datasets (time and recovery rate) are required to obtain reliable statistically significant results. For the sites investigated in this study, extensive historical data were not available for an effective model calibration. Thus, a regression analysis was used herein. Several previous studies indicated that correlations exist between site-specific climatic/ operational conditions and field calibrated first order decay values and simple linear regression models were developed for predicting site-specific values of the first order decay rate (Garg et al. 2006, Thompson et al. 2009, Fei et al. 2016). Garg et al. (2006) identified four key parameters for predicting k-values using a fuzzy synthetic evaluation methodology including annual precipitation rates,

average daily temperature, biodegradable fraction of the MSW, and landfill depth. Through a multiple-linear regression analysis using site specific data from 57 landfills, Fei et al. (2014) indicated that waste in place, the fraction of biodegradable waste, and waste temperature, were correlated to *k*-values. Thompson et al. (2009) developed a linear regression between annual precipitation rates and *k*-values for Canadian landfills. For predicting *k*-values, a major limitation of previously developed regression models is that these are unable to describe potential complex, non-linear relationships between the model inputs and outputs. Moreover, uncertainty in the model predictions typically were not assessed in the previous studies. An artificial neural network (ANN) model was developed in this study to predict k-values for all landfill sites.

In baseline analysis, the architecture of a neural network contains 3 layers: an input, hidden, and output layer (Figure 3.19). Within each layer are nodes (also termed neurons) that connect the input layer to the output layer. In general, the number of nodes in the input and output layers is equal to the number of input and output variables, respectively. The number of nodes in the hidden layer is set to vary. The mathematical connection between the input and hidden layers is similar to a multiple linear regression model (Equation 3.9). As input, the ANN model receives the independent variables used for prediction (i.e., precipitation, daily average temperature, etc.) and the necessary parameters required to run the model (i.e., weights and biases) and outputs a prediction ($\hat{Y}$) that is different than the true target output (Y) by some error (e). The n values in Figure 3.20 are a linear combination of the input weights (IW) multiplied by the inputs themselves with an added bias (b^1) value to account for noise.

Figure 3.20 Architecture of an Artificial Neural Network (adapted from MATLAB 2019)

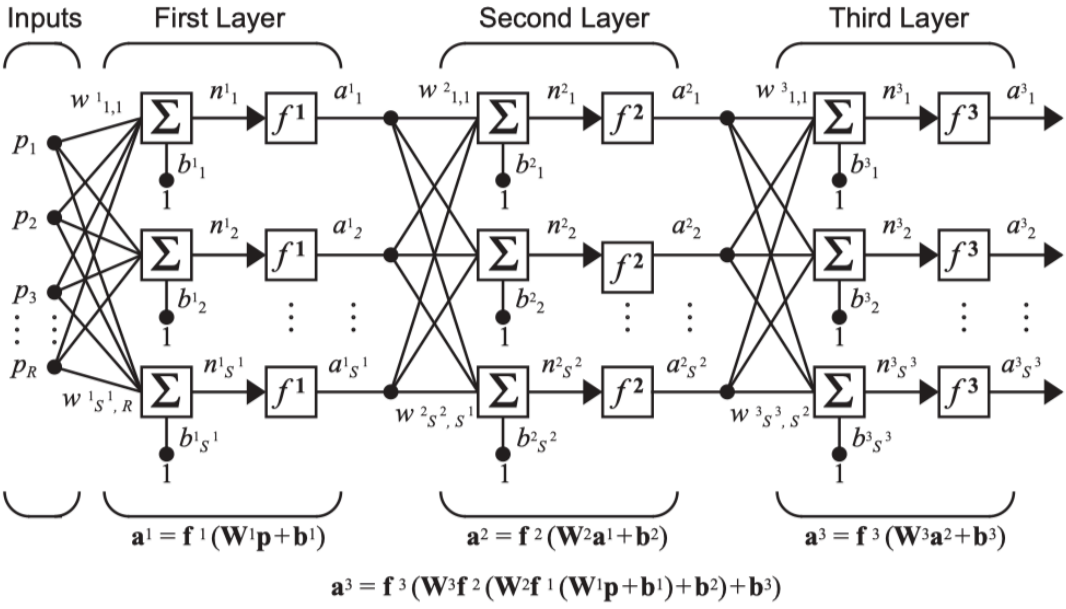

Optimization of the input/output layer weights and biases was performed backpropagation. A loss function (Equation 3.10) that measures the discrepancy

between the input and output target values from the model (the mean squared error, *MSE*) is minimized by iteratively running the forward model using a random initialization of the weights and biases. This process continues until an optimal value of the loss function is reached.

$$Y = f(X_i, IW, b^1, LW, b^2) + e \tag{3.9}$$

$$MSE = \frac{1}{N} \sum_{k=1}^{N} (Y - \hat{Y})^2 \tag{3.10}$$

The overall fit and predictive accuracy of a neural network is highly dependent on the quality of the input data and the potential relationships linking the input and output variables. The eight inputs selected in this study included annual precipitation (mm), daily average temperature (°C), waste in place (tons), waste throughput (tons/day), landfill depth (m), landfill areal coverage (m^2), fraction of biodegradable waste (%), and relative waste age (years) (the difference between the year in which the landfill opened and the year of analysis). Studies with the inputs identified above and k-values that had been predicted using calibration of landfill gas collection data with modeled generation data from LandGEM. A total of 23 studies from MSW landfills worldwide (Finland, Netherlands, Mexico, U.S., Canada) were found in the literature with the necessary data to populate the regression model (Garg et al. 2006, Barlaz e al. 2010a, Zhao et al. 2013, El-Fadel et al. 1996, Faour et al. 2007, Tolaymat et al. 2010, Wang et al. 2013, 2015, Bentley et al. 2005, Karanjekar et al. 2015, Sormunen et al. 2013, Oonk et al. 2013, Wangyao et al. 2010, Machado et al. 2009, Lamborn et al. 2012, Vu et al. 2017, Nwaokorie et al. 2018, Willumsen and Terraza 2007, Amini et al. 2012, 2013, Lagos et al. 2017, Budka et al. 2007). Individual values are presented in Appendix B, Table B4. While the majority of the landfills were located in cold, wet regions, landfill data also were used from dry temperate regions including California, Mexico, and South America.

The ANN models were configured, trained, and tested using MATLAB's built in neural network toolbox. A feed forward neural network with one hidden layer was used for the primary ANN architecture (similar to Figure 3.20). The ANN was trained using the standard Levenberg Marquart backpropagation technique, with all of the default settings for learning of the weights and biases applied. These settings included normalization of the input data and minimization of *MSE* during training. The dataset of 53 individual data points was randomly divided into training, testing, and validation data sets at a set ratio of 70%, 15%, and 15%. One of the most critical parameters of any ANN architecture is the number of hidden layers and number of nodes within the hidden layer(s). In general, one layer is sufficient for learning low dimensional problems and was adopted herein (Hagan et al. 2014). The number of nodes within the hidden layer was optimized using a novel evolutionary, global single objective optimizer (detailed settings of the optimization runs are similar to those described in Awad et al. 2016). The objective function of this optimization routine was set to equally weigh the errors obtained from the training, test, and validation sets to avoid overfitting of the network. The *MSE* of the training, test, and validation sets were normalized by the total expected variance of the model (*VAR*) (Equation 3.11, where $\bar{Y}$ is the mean of the *j* measured values of the target variable, *Y*). The optimizer was set to run for a limited number of

generations and was run for ten independent realizations. The best run (lowest objective function) from these realizations was used as the final ANN architecture for the prediction of *k*-values based on site specific climatic/ operational conditions. The uncertainty of *k* values (95% confidence interval) was calculated assuming the residuals from the ANN model were normally distributed with zero mean and standard deviation equal to the square root of the overall *MSE* of the ANN model.

$$VAR = \frac{1}{N} \sum_{j=1}^{N} (Y_j - \bar{Y})^2 \tag{3.11}$$

3.9.3 Methane Mass Balance Model

According to Equation 3.6, the methane generation predicted by LandGEM should be equal to the sum of the methane outputs, transformations, and inputs from, within, and to the landfill, respectively. In Equation 3.6, the methane mass balance outputs include emissions, gas collection, storage, and migration. Transformations in the methane mass balance model include methane oxidation in the soil covers, resulting in a net loss of methane. Potential inputs to the mass balance model included negative emissions, or net uptake of methane from the atmosphere. Predicted methane generation was subtracted from the sum of the methane collected and emitted to determine net surplus or deficit of methane, which were indications of the importance of transformation or output/input pathways other than collection/emission pathways measured herein. In this model, outputs/transformations and inputs are designated as positive and negative values, respectively.

The time frame considered (2018-2019) for the mass balance was associated with the field campaigns and was the most recent year from which methane collection data was available. Mass balances were conducted using the refined LandGEM predictions. Results are presented for both the mean and 95% confidence intervals of methane flows expected for each pathway to capture the full variation expected at each site.

Gas collection typically is calculated using the sum of the average daily flows recorded at the entrance to the flare or main header of the gas collection system. To estimate total methane volume, the net LFG collection is multiplied by the average inlet volumetric methane composition. To investigate the potential uncertainty in methane collection measurements resulting from these two steps, LFG flow and methane composition data were analyzed from four landfills in the U.S. (Santa Maria Regional and Crazy Horse Landfills in California; Loudoun County Solid Waste Management Facility in Virginia; and Franklin County Landfill in Ohio) from which data were available. These landfills represent a range in operational scale (small to large) and climate (dry, temperate to cold, wet). An MC prediction framework was run to simulate the total methane collection volume (m^3) at each of these sites for the time periods in which data was available. Similar to the L_0 MC predictive framework, non-parametric KDE distributions were fitted to the time varying LFG flow rate and, if available, the time varying volumetric methane composition. If the volumetric methane composition was not available, it was assumed that this input distribution to the MC simulations was uniform, ranging from 40 to 60% (vol/vol). Predictions of methane composition were made for the same time periods/intervals. To arrive at a stable output distribution in total methane

volume, 50,000 simulations were conducted. The resulting distributions in total methane volume predicted from these simulations appeared normal (Figure 3.21). After fitting a normal distribution to each output distribution, the mean and standard deviation were used to build 95% confidence intervals representing the overall uncertainty in gas collection measurements.

To extrapolate the estimated uncertainty in gas collection from the four landfills to the landfill sites in this study, several assumptions were made. First, it was assumed that the percent difference between the mean value and the lower or upper tail of the 95% confidence interval was representative of the overall measurement uncertainty in gas collection. This calculation was performed using the log (base 10) values of the mean and 95% confidence bound to reduce potential scaling effects of total methane collection between landfills of different size. Next, as a conservative measure, the median of the overall uncertainty calculated for the four representative landfills (44.1%) was applied to each of the landfill sites in this study to arrive at an overall 95% confidence interval.

Figure 3.21 Total Methane Collection Predicted for the Loudoun County Solid Waste Management Facility in Virginia using the New MC Simulation Framework

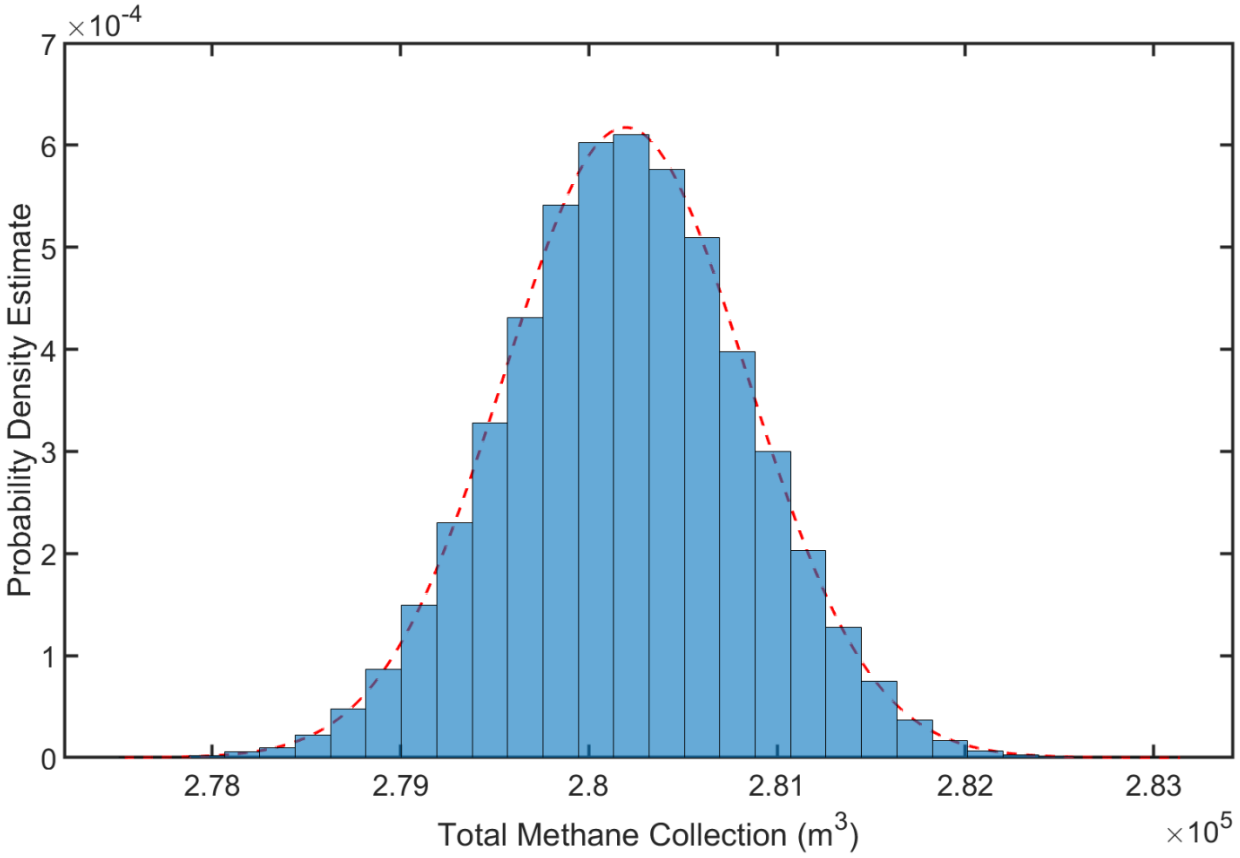

The uncertainty in the LandGEM methane generation predictions was assessed using the refined parameter approach. For ground-based measurements, the distribution in methane whole-site emissions from daily, intermediate, and final covers was assumed

to be normal (for each season). These normal distributions were then combined across cover categories and then across seasons, resulting in a composite normal distribution, with mean, standard deviation, and associated 95% confidence intervals. For aerial-based measurements, the reported uncertainty was not assumed to be the overall standard deviation, as recommended by Bromley (2017). Instead, the uncertainty was assumed to be representative of the 95% confidence bounds of the reported mean in emissions estimates obtained from the aerial testing investigations.

3.10 Calculation of the Indirect Effects of LFG Emissions

The metrics applied to assess the indirect effects of LFG emissions on public health, air quality, and climate change included tropospheric ozone formation, secondary aerosol formation, indirect/direct global warming, and stratospheric ozone depletion potentials. HAP classification was also used to further evaluate to what extent a chemical emitted from a landfill site impacted human health. Tropospheric ozone formation potentials (OFPs) for each site were quantified using the MIR scale, which is determined through modeling of the change in peak ozone concentration when an individual chemical species is released into the troposphere, assuming high concentrations of NOx (i.e., in an urban environment) (Carter 2009). The OFP (g O_3/yr) for the *i*th NMVOC species was calculated using Equation 3.12 below, using the MIR_i (g O_3/g NMVOC) value in Table 1.1:

$$OFP_i = E_{LF,i} * MIR_i \quad (3.12)$$

Where, $E_{LF,i}$ represents the annual net surface emissions of the *i*th NMVOC for a given landfill (g/yr). In this report, whole site, annual emissions were calculated using the fluxes measured for the different cover categories at a given landfill. For each landfill, the relative areas of the different cover categories and the area of the landfill are used together with the specific fluxes for the covers to calculate annual emissions for the entire landfill site, where calculated fluxes for each NMVOC species were averaged from both chamber estimates.

Secondary organic aerosol formation potentials (SOAFPs) were calculated through application of the FAC, which represents the fraction of a given NMVOC that is converted into an organic aerosol, as measured through laboratory-based smog chamber experiments (Grosjean and Seinfeld 1989, Grosjean 1992). The SOAFP for the *i*th NMVOC is simply the product of the net surface emissions from a given landfill site and the given FAC_i value presented in Table 1.1 (Equation 3.13):

$$SOAFP_i = E_{LF,i} * FAC_i \quad (3.13)$$

Other than carbon tetrachloride (CCl_4, which is a high GWP gas), certain NMVOC species surveyed in this study also exert an indirect and direct effect on global climate change. Indirect effects on global climate change associated with NMVOCs can be attributed to formation of secondary organic aerosols (thereby increasing cloud albedo), increase in O_3 formation and depletion of hydroxyl radicals (thereby increasing the atmospheric lifetime of CH_4), where indirect GWP values have been previously reported

and are summarized in Table 1.2 (Collins et al. 2002). In this way, the indirect effect on global climate change (in terms of carbon dioxide equivalents, CO_2-eq) was calculated for the *i*th NMVOC as the product of the indirect GWP_i and the net surface emissions from a given landfill site (Equation 3.14). Direct effects of NMVOC degradation products on climate change (i.e., an increase in carbon dioxide from NMVOC oxidation) were calculated based on the molecular weight (MW_i) and number of carbon atoms ($N_{c,i}$) for the *i*th NMVOC, based on a simple molar conversion (Equation 3.14) (IPCC). Thus, the total combined CO_2-eqs was calculated in this study by summing the indirect (IGW_i, Eq. 3) and direct radiative forcing effects (DGW_i, Equation 3.15) (Majumdar and Srivastava 2012, Majumdar et al. 2014).

$$IGW_i = E_{LF,i} * GWP_i \tag{3.14}$$

$$DGW_i = \frac{E_{LF,i}}{MW_i} * N_{c,i} * (44) \tag{3.15}$$

The stratospheric ozone depletion potential (ODP) weighted emissions was further computed to compare the effect of NMVOC emissions on air quality across different landfill sites. This metric was relevant for the halogenated hydrocarbons chemical family as well as the CFCs and HCFCs belonging to the F-gas classification, where, depending on the extent of vertical mixing in the atmosphere, the presence of chlorine or bromine atoms significantly contributes to a reduction in the stratospheric ozone layer. The ODP weighted emissions for the *i*th NMVOC was calculated as the product of the ODP value (Table 1.1) and the net surface emissions for a given landfill site (Equation 3.16).

$$WODP_i = E_{LF,i} * ODP_i \tag{3.16}$$

Finally, the cumulative surface emissions from all HAPs identified in Table 1.1 were obtained to compare the human health impacts of net NMVOC surface emissions on surrounding communities and workers present at each site.

3.11 Additional Static Flux Chamber Investigations

Additional tests were conducted in the dry season at Santa Maria Regional Landfill and Teapot Dome Landfill. The tests at SMRL were conducted to investigate the influence of various landfill operational conditions on flux. The testing program at Teapot Dome Landfill was conducted to evaluate the effects of the specific operational practice of designated winter waste placement at California landfills on LFG surface flux.

3.11.1 Radial Gas Extraction Well Testing at SMRL

Additional static flux chamber testing was conducted at Santa Maria Regional Landfill to experimentally ascertain the radius of influence of a typical gas extraction well. A well located at a central location of the waste mass away from other gas extraction wells was selected to minimize the potential influence of nearby gas extraction wells on the flux tests. The tests were conducted on the interim cover composed of native soil materials near testing locations that were previously investigated (e.g., the same cell of

the landfill). Flux chamber testing was conducted on two separate days (1 week apart) during the dry weather season to obtain replicate results (October 4, 2019 and October 11, 2019). The gas well investigated had had two nested casings with shallow and deep active extraction zones, where each zone was representative of younger and older waste conditions, respectively. The waste depths contributing LFG to each screened zone was 6.1-9.1 m and 21.3 m for the shallow and deep casings, respectively. During both testing periods, flux chambers were placed at logarithmically spaced intervals (i.e., 0.5, 1, 2, 4, 8, 16, and 32 m) to capture both the magnitude and variation in fluxes extending radially from the gas extraction well (Figure 3.22). The number on the chamber locations depicted in Figure 3.22 corresponds with the raw concentration and flux chamber data tabulated in the spreadsheets provided as supplemental information to this report. Photographs of the tests are presented in Figure 3.23. The chamber testing locations were selected to avoid interference between tests (Figure 3.23b). For the second day of testing, it was difficult to find a location placed 1 m away from the extraction well that was not infringing on existing or upcoming chamber footprints; therefore, this location was offset by approximately 0.5 m.

Figure 3.22 Flux Chamber Locations at SMRL: a) Testing Day 1, b) Testing Day 2.

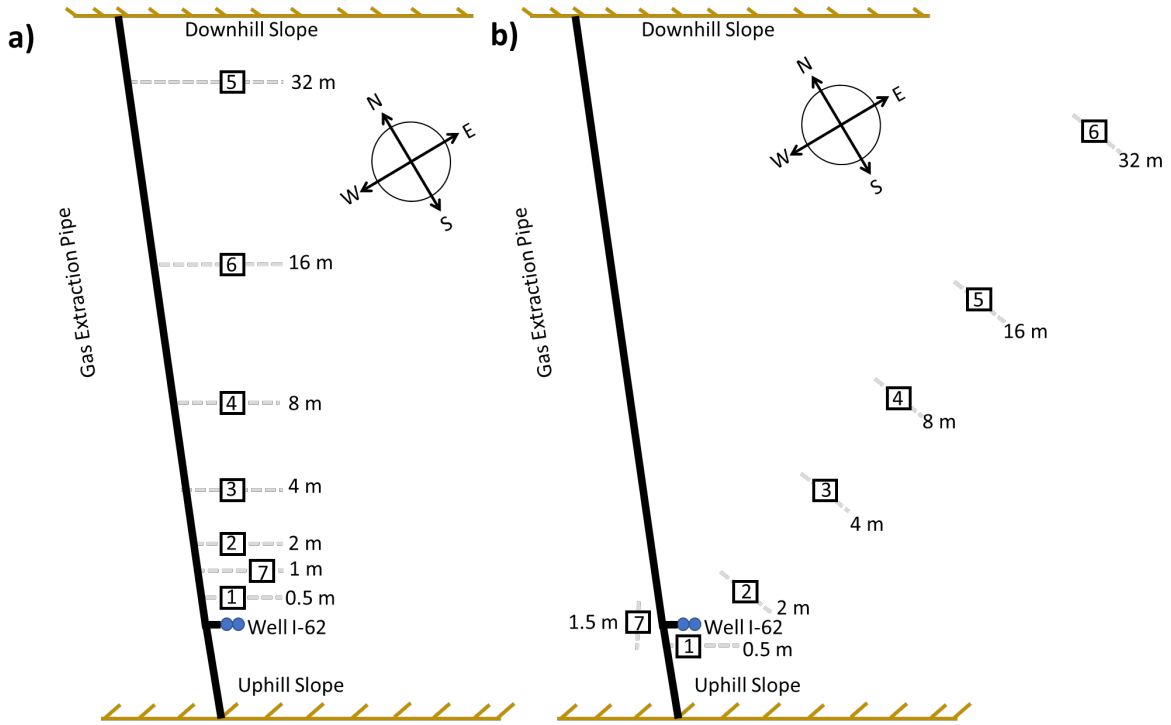

Gas extraction vacuum pressures and LFG composition were monitored throughout the entire duration of both field-testing days using a GEM5000. At least one GEM measurement was made at each extraction casing (shallow and deep) during each individual flux chamber test. The flux tests were conducted using logarithmic sampling (1 hr total duration) to be able to finish all of the radial testing in a given test day and not have any influence from potential variations in weather conditions. The 1-hr test

duration was determined to be effective for obtaining reliable flux measurements in terms of tests passing the R^2 threshold based on the previous flux chamber tests at the landfill.

After the flux chamber measurements, the cover was excavated near the vicinity of the specific testing locations to determine the thickness of the interim covers as a function of radial distance from the well. A photograph of determination of cover thickness is presented in Figure 3.24.

Figure 3.23 a) Radial Gas Well Static Flux Chamber Testing at SMRL (0.5 and 2 m distance) and b) Chamber Footprints and Spacing from the Gas Extraction Well.

Figure 3.24 Excavation Results adjacent to Chambers Placed at a) 32 m versus b) 1 m from the Gas Collection Well.

3.11.2 Cover Thickness Testing at SMRL

To ascertain the effects of cover thickness on GHG and NMVOC fluxes, an experimental test program was carried out on October 18, 2019 at Santa Maria Regional Landfill. A rectangular testing plot with dimensions of 4.7 m width, 4 m length, and 1.1 m height was constructed by the landfill operators over the existing intermediate cover with an approximate thickness of 0.45 m (Figure 3.25a). The test plot was constructed over the same intermediate cover as the cover investigated in the radial gas extraction well tests. The test plot was constructed at a central location in the cell to minimize the potential effects of the gas wells on the landfill gas emissions. Flux measurements were made at approximately 0.31 m depth intervals over the course of the one-day testing campaign, where an excavator was used to carefully remove each layer of the test plot to progressively reduce the thickness of the cover (Figure 3.25b). Overall, a total of 6 flux chamber measurements were made at varying heights above or below the existing intermediate cover level including: 1.12 m, 0.90 m, 0.61 m, 0.32 m, 0.02 m, and -0.31 m (i.e., below the top of the existing intermediate cover). Gas extraction vacuum pressures and LFG composition were monitored during each test using a GEM5000. Similar to the radial well testing experiments, the flux tests were conducted using a logarithmic sampling frequency (i.e., Chamber A, sampling at 0, 7, 15, 30, and 60 minutes) as this method resulted in reliable results at this landfill as verified using the results from previous tests.

Figure 3.25 a) Static Flux Chamber Testing on the Test Plot Constructed at SMRL, b) Removal of 0.3 m-thick Soil Layer for Testing the Next Cover Thickness.

3.11.3 Temporal Surface Flux Testing at SMRL

Testing was conducted at Santa Maria Regional Landfill to evaluate the temporal variability in landfill gas flux. As flux chamber tests represent a single snapshot in time, conducting chamber measurements over a weeklong period provides variation expected as a function of time. For the temporal tests, a was placed at a central location within the well-field at the same landfill cell used for both the radial testing and cover thickness testing (soil intermediate cover). This chamber was not moved or disturbed in any way throughout the duration of this field-testing program. A series of flux tests were conducted on October 21, 2019, October 25, 2019, and October 26, 2019 at different times throughout each testing day. On October 21, 2019, one flux chamber test was conducted at 1:13 PM. On October 25, 2019 and October 26, 2019, 4 consecutive flux

chamber tests were conducted at 8:00 AM, 1:30 PM, 6:30 PM, and 1:15 AM. For each of these chamber tests, a logarithmic sampling frequency was selected, similar to the testing programs for radial well distance and cover thickness tests. A final sampling time of 2 hours was added to improve the resolution of the flux measurements. Gas extraction vacuum pressures and LFG composition were monitored during each test using a GEM5000. After each test was performed, both the air and soil temperatures (in triplicate locations) were measured in the vicinity of the chamber location.

3.11.4 Contaminated, Non-Hazardous Soils Testing at SMRL

The fourth additional field-testing program conducted at SMRL focused on quantification of both GHG and NMVOC fluxes from an inactive cell and an active cell containing non-hazardous hydrocarbon impacted soil (NHIS). Even though NHIS is deemed non-hazardous by state and federal regulations (due to concentrations below regulatory limits), NHIS still contains detectable amounts of crude oil, where the variety of chemical compounds composing crude oil is generally referred to as total petroleum hydrocarbons (TPH). All of the chemicals within the aromatic family under investigation in this study (i.e., BTEX), as well as longer chain alkanes, alkenes, and alkynes are expected to constitute some fraction of TPH in the contaminated soil. These compounds are expected to be readily volatilized from the contaminated sediment or easily dissolved/transported via the aqueous phase during precipitation events, which may pose a significant threat to the environment as these materials are generally left uncovered during filling of the NHIS cells at SMRL.

The NHIS facility at the SMRL contains two active cells: one that has portions of final cover and been filled (Cell 2) and the other that does not yet have final cover in place (Cell 1). Historically, the landfill has accepted contaminated soils from large and small projects. Both cells were constructed over 15-21-m-thick MSW that was placed prior to 1970 through to 2001. A bottom geomembrane liner system was placed over the existing MSW at both cells prior to placement of the NHIS wastes. In addition, Cell 2 has a final cover in place that consists of either GCL or geomembrane liner system overlain by 0.9 m of vegetative soil cover. NHIS Cell 2 has an active gas recovery system in place that extends into both shallow and deep MSW layers at the cell. NHIS Cell 1 has an active gas recovery system in place that extends into the deep MSW layers at the cell. Cell 1 was filled in various stages and includes an active face (which remains uncovered from day to day operations) and an extended daily cover area where clean soil is placed over the contaminated soil until filling restarts.

For the NHIS field-testing campaign, two distinct testing locations were selected for flux chamber measurements. The first site was selected and tested in Cell 2 to represent final cover conditions. The cover topsoil at the first testing location was sandy, not well compacted, and highly vegetated. The second site was selected at an extended daily cover area in Cell 1, where clean soil had been placed to a relatively shallow thickness for an extended period of time. The cover soil was sandy, not well vegetated, and very dry compared to the final cover testing location. At both sites, flux chamber tests were conducted using the two primary sampling frequencies (logarithmic and linear) to

ensure that a broad spectrum of fluxes could be reliably predicted for the NMVOCs surveyed. The field campaign was conducted on October 7, 2019.

3.11.5 Wet Waste Placement Testing at Teapot Dome Landfill

Wet and dry season field campaigns ascertained that the interim cover location at Teapot Dome landfill that was designated as a wet waste placement area was associated with some of the highest fluxes of GHGs and NMVOCs measured throughout the entire field-testing program in this investigation. An additional field-testing program was conducted at this landfill to further investigate the effects of dedicated wet waste placement on LFG flux. The tests were conducted on November 18, 2019. While the tests were conducted at the same cell and approximate location in November 2019 as the previous wet and dry season tests, the cell had been filled with 3 to 4.5 m of fresh wastes. The wastes were covered with an intermediate cover (thickness of approximately 0.45 m) similar to the cover that was present during the previous wet and dry season tests. Similar to previous field-testing methodology, two chambers with different sampling frequencies (logarithmic and linear) were placed and tested at the same site that was associated with wet waste placement that was identified during previous campaigns. Raw gas samples were also collected to determine the LFG composition and concentration during the site visit.